2017

Historical reconstructions of water quality in the Kimberley using sediment records. Report of 2.2.9 prepared for the Kimberley Marine Research Program

John Keesing

Dongyan Liu

Zineng Yuan

Yajun Peng

Yujue Wang

See next page for additional authors

Keesing J, Liu D, Yuan Z, Peng Y, Wang Y, Richard P, Masque P, Chen Y, Fang Y (2017) Historical reconstructions of water quality in the Kimberley using sediment records. Report of 2.2.9 prepared for the Kimberley Marine Research Program, Western Australian Marine Science Institution, Perth, Western Australia, 91 pp.
https://wamsi.org.au/project/sediments/

Authors

John Keesing, Dongyan Liu, Zineng Yuan, Yajun Peng, Yujue Wang, Pierre Richard, Pere Masque´, Yingjun Chen, and Yin Fang

Historical resconstructions of water quality in the Kimberley

John Keesing[1,7], Dongyan Liu[2], Zineng Yuan[3], Yajun Peng[3], Yujue Wang[3], Pierre Richard[4], Pere Masque[5,7], Yingjun Chen[6] Yin Fang[6]

[1]*CSIRO Oceans & Atmosphere, IOMRC, Australia*

[2]*East China Normal University, Shanghai, China*

[3]*Yantai Institute of Coastal Zone Research, Chinese Academy of Science, China*

[4]*CNRS-Universite de La Rochelle, France*

[5]*Centre for Marine Ecosystems Research, Edith Cowan University, Australia*

[6]*Tongji University, Shanghai, China*

[7]Western Australian Marine Science Institution, Perth, Australia

WAMSI Kimberley Marine Research Program

Final Report

Project 2.2.9

December 2017

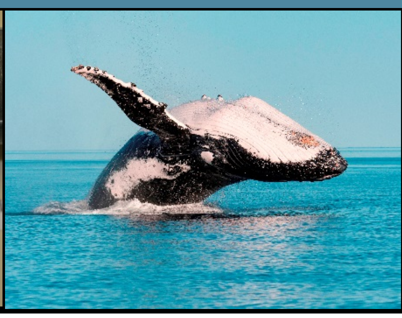

WAMSI Kimberley Marine Research Program

Initiated with the support of the State Government, the Kimberley Marine Research Program is co-invested by the WAMSI partners to provide regional understanding and baseline knowledge about the Kimberley marine environment. The program has been created in response to the extraordinary, unspoilt wilderness value of the Kimberley and increasing pressure for development in this region. The purpose is to provide science based information to support decision making in relation to the Kimberley marine park network, other conservation activities and future development proposals.

Front cover images (L-R)

Image 1: Satellite image of the Kimberley coastline (Image: Landgate)

Image 2: Sediment Core. (Image: CSIRO)

Image 3: Humpback Whale (Image: Pam Osborn)

Image 4: Collecting sediment cores at Cygnet Bay (Image: CSIRO)

Year of publication: August 2017

Metadata: http://catalogue.aodn.org.au/geonetwork/srv/eng/metadata.show?uuid=03675b95-2f38-761e-e053-08114f8cbf86

Citation: Keesing J, Liu D, Yuan Z, Peng Y, Wang Y, Richard P, Masque P, Chen Y, Fang Y (2017) Historical reconstructions of water quality in the Kimberley using sediment records. Report of 2.2.9 prepared for the Kimberley Marine Research Program, Western Australian Marine Science Institution, Perth, Western Australia, 91 pp.

Author Contributions: JK and LD conceived and designed the study and wrote the report. All authors analysed data and wrote sections of the report. All authors have read and approved the final manuscript.

Corresponding author and Institution: John Keesing (CSIRO, Crawley, Western Australia).

Funding Sources: This project was funded (commissioned) by the Western Australian Marine Science Institution as part of the WAMSI Kimberley Marine Research Program, a $30M program with seed funding of $12M provided by State government as part of the Kimberley Science and Conservation Strategy. The Program has been made possible through co-investment from the WAMSI Joint Venture partners and further enabled by data and information provided by Woodside Energy Ltd.

Competing Interests: The commercial investors and data providers had no role in the data analysis, data interpretation, the decision to publish or in the preparation of the manuscript. The authors have declared that no competing interests exist.

Acknowledgements: This project was undertaken by a project team spread across five organisations in three countries all of which made considerable financial contributions to the projects. In addition, the research was sponsored by the Western Australian Marine Science Institution (WAMSI) and the Natural Science Foundation of China (41376121), the Strategic Priority Research Program of the Chinese Academy of Sciences (XDA11020405) and Natural Science Foundation of Shandong Province (JQ201414). We also wish to thank and acknowledge the assistance of James Brown and Ali McCarthy of Cygnet Bay Pearls with field work and for sharing their knowledge of the history of pearl farming in Cygnet Bay. Janine Kinloch and Georgina Pitt from the WA Department of Parks and Wildlife provided data on the river catchments and bush fire scar statistics. We also thank Dr Andrew Revill (CSIRO) for undertaking a thorough review of the report. A summary of our response to his main criticisms and how they have been addressed is given at the end of the Executive Summary.

Collection permits/ethics approval: Permission to take cores in area controlled by Kimberley Ports was obtained.

Contents

Executive Summary

Overview

The Kimberley Marine Research Project 2.2.9 made use of a suite of palaeoecological approaches to reconstruct a chronology of change in coastal water quality over the last approximately 100 years. The biogeochemical proxies addressed phytoplankton composition and biomass, temperature and terrestrial influences. Where possible these were matched to historical land/water use, meteorological or hydrological observational records. The project examined sediment cores from three coastal locations in the Kimberley Region of Western Australia, Koolama Bay (King George River), Cygnet Bay and Roebuck Bay. Each sampling location provided a contrast with which to evaluate changes over either a spatial or temporal gradient of human or natural influences.

Cygnet Bay: impacts of pearl farming on water and sediment quality

Pearl oyster aquaculture, with a 50-year history in Australia, has been regarded as an anthropogenic activity with low environmental risk. To assess the long-term environmental effects of pearl oyster farming, sediment cores taken in Cygnet Bay, Western Australia, were used to reconstruct environmental processes covering an approximately 90-year period.

Biogeochemical parameters in sediment cores from inside and outside a pearl farming area displayed contrasting characteristics over time. The spatial comparison of multiple proxies (grain size, TOC, TN and BSi, C/N ratio, δ13C and δ15N) in sediment cores revealed localised, decadal environmental effects of pearl farming, including alteration of sediment texture and increases in organic matter and diatom biomass.

Total organic carbon (TOC), total nitrogen, biogenic silica (BSi), and fine-grained sediment at the pearl farming site displayed significant increases with phases of expansion of oyster stocking. In contrast, only small variations in response to climatic signals (rainfall and temperature) over time occurred in the cores outside the pearl farm. The variation in C/N, δ13C and δ15N ranges over time suggested that increased organic matter was mainly contributed by autochthonous sources, rather than terrestrial input. The sequential t-test for a regime shift detected approximately two to three-fold increases in organic matter, one to five-fold increases in silt proportion and two to five-fold increases in BSi concentrations after pearl oyster farming, in contrast to the control site. The rapid development of modern long-line culture since the late 1980s was presumed to be the dominant driver of environmental changes in sediments. The results provide insight to the magnitude of environmental change, which can occur over decades resulting from even minimal anthropogenic activity. Although sediment quality in King Sound did not reach a eutrophic level, the study showed that small environmental disturbances accumulating over a long period of time may cause detectable changes in marine ecosystems, particularly in sensitive oligotrophic waters.

One possible option to manage the rate of environmental change could be to dispose of the waste from cleaning the culture apparatus on land. This was recently recommended to enhance ecosystem sustainability of bivalve culture in the USA (for high density mussel and edible oyster culture). This measure was also recommended as a way of reducing the potential of invasive species becoming established in bivalve farming areas. However, given the very slow rate of environmental change detected in this study, it is not recommended as a management intervention in the Kimberley pearl farming situation unless a risk assessment proved there was an existing and unacceptable risk to invasive species becoming established, and it was demonstrated that the implementation of the measure would not have unintended consequences on the water column productivity on which the oyster culture depends.

Cygnet Bay: impact of climate change on phytoplankton biomass

Ocean warming can modify the biomass and geographic distribution of phytoplankton on decadal scales. Significant increases in sea surface temperature (SST) and rainfall in the northwest of Australia over recent decades is attributed to climate change. Four biomarker proxies were used (TEX_{86} index, long chain *n*-alkanes, brassicasterol and dinosterol) to reconstruct approximately 60-year variations of SST, terrestrial input, and diatom and dinoflagellate biomass in the coastal waters of the remote Kimberley region. The results suggested that the most significant increases in SST and terrestrial input have occurred since the mid-1990s, accompanied by an abrupt increase in diatom and dinoflagellate biomasses. Compared with the results before that time, the average TEX_{86}^{H} temperature increased approximately 1°C until 2011, rainfall increased in about 250 mm, and brassicasterol and dinosterol contents increased 8.5 and 1.7 times, respectively. Principal component analysis indicated that the warming SST played a more important role on the phytoplankton increase than increased rainfall and river discharge. A series of recent high-profile publications have explained how climate change has impacted on physical processes to cause a warming influence in the Kimberley over the last two decades but this study is the first to show the consequences in terms of an ecological response.

Koolama Bay (King George River): impact of riverine inputs and climate change

The King George River area was chosen as part of this study as it is significantly influenced by the seasonal wet season (December – March) dry season (April – November) rainfall cycle. The large freshwater output into Koolama Bay from the King George River offered the opportunity to compare sediment cores from two embayments; one influenced by the river catchment and large freshwater outflows and an adjacent embayment without direct riverine input. Contrary to expectation we found no evidence that the two sites differed greatly, at least not in ways attributable to differential freshwater flows. There was little evidence that the contribution of carbon from land based plant material had changed over time. This is consistent with long term rainfall patterns in the area. Unlike Broome, where rainfall has increased by 40% of its long-term average since the mid-1990s, rainfall at Kalumburu (the closest site we could obtain rainfall data from, but noted to be outside the King George River catchment) has been relatively stable since 1940 averaging 1212 mm annually with only a 6.8% increase since 1997. The cores appeared not to be strongly influenced by freshwater flows but did show significant evidence of an increasing contribution of marine organic matter over time and a coincident increase in diatom and dinoflagellate biomarkers which we interpret as indicating an increasing biomass of marine phytoplankton. These increases occurred over the same period as increases in sea temperature indicating that, consistent with what we found at both Cygnet Bay and at Broome, that increased phytoplankton biomass has occurred over the same period as anthropogenic ocean warming. No evidence of an increase in anthropogenic nitrogen in the cores over time was found.

Koolama Bay (King George River): detection of black carbon from bushfires in the catchment

"Black carbon (BC)" or elemental carbon is produced exclusively from incomplete combustion of biomass and fossil fuels, and is ubiquitous in the environment. BC from bushfires can make its way into marine sediments by two pathways; it can settle from the atmosphere and it can be transported from the site of the fire through river runoff. The preliminary results presented here are from a pilot study to examine the potential for using BC analyses of coastal marine sediment archives to reconstruct the time course of, or at least reflect the temporal variability, in bushfires in the Kimberley. It was expected that the amount of black carbon (BC) in coastal sediments will be influenced by the extent of fires in the relevant catchment, rainfall and/or river discharge. The results of analyses of BC in our cores was matched to the very recent record (2000 to 2013) of area burnt in the catchment. Additional information about rainfall and river discharge is also considered, although for this study, the nearest rainfall data we were able to obtain was from Kalumburu which is the King Edward River Catchment and the only river discharge data was from the Drysdale River. These types of data are only sparsely collected in the Kimberley and records are often incomplete or discontinuous. BC in the cores showed peaks in the (approximate) years of 1974, 1980, 1996, 1999, 2010 and 2012 and lows in 1986, 2002 and 2006. We found that a model incorporating early season area burnt (with a one-year lag, i.e. the year before) and rainfall explained a significant amount of the variability in BC in the core (R^2=0.812, p=0.035). This result is intuitive but needs to be regarded with caution as the sample size is small (bush fire data matched to BC from 2002-2013) and the rainfall record is from an adjacent catchment. Nevertheless, the result is encouraging and suggests that a study which sought to optimize the spatial and temporal matching of good time series of explanatory data (area burnt and rainfall) and a sediment core location with a good sedimentation rate and good age preservation would yield results which can be regarded with greater confidence. In determining a potential site for more work, we consider the King Edward River catchment as offering high potential. This catchment has a good rainfall record at Kalumburu (since 1940), it has a very large catchment area (84,000 km^2) and a much larger area burnt each year (> 600,000 ha compared to <250,000 ha in King George River). In addition, the King Edward River flows into a semi enclosed embayment (Napier Broome Bay) which will offer the likelihood of a higher sedimentation rate and less sediment disturbance. Cambridge Gulf is also another location with characteristics that offer the likelihood of a successful application of these techniques.

Broome – influence of outflow from Dampier Creek on water and sediment quality

Broome is located on Roebuck Bay adjacent to Dampier Creek and offered the opportunity for a Kimberley site potentially influenced by human activity signals typical of a coastal city. In this case we focused on a comparison of two sites, the first potentially influenced by Broome's historical and recent anthropogenic inputs via Dampier Creek which carries urban runoff into the bay as well as direct intentional or accidental inputs from other sources (such as the wastewater treatment plant, the old abattoir and the golf course) and another to the south-east which was to serve as a reference site. Enrichment of levels of ^{15}Nitrogen is an indicator of anthropogenic nitrogen and this increased gradually to the present, but significantly at sites closest to Broome from about 1960 (20 cm core depth) although it should be noted that the highest levels reached near the surface in about 2010 had occurred previously much deeper in the core (56-71 cm and 97-110 cm), well beyond the extent to which we were able to age the core. Nevertheless, the trend of more enriched $\delta^{15}N$ values since 1960 is very significant and when compared with the reference site are highly suggestive of a real increase in anthropogenic nitrogen discharges from Broome. Coprostanol, a biomarker of sewage was at levels close to the limit of detection in the samples and thus there was no evidence of significant sewage pollution. Concerns of pollution affecting the ecology of Roebuck Bay have been highlighted since the annual (wet season) blooms of the blue green algae *Lyngbya cf. majuscula* began in 2005. *Lyngbya* is a nitrogen-fixing cyanobacteria and is not limited by nitrogen but is known to respond to phosphorus and iron enrichment. We did not measure these nutrients in our cores. Cores taken within the intertidal area closer to Broome Town Beach may be more instructive as to both the time course of nutrient pollution and the history and spread of *Lyngbya* through the use of specific biomarkers for cyanobacteria.

Broome - climate change impacts on terrestrial inputs and phytoplankton patterns

Climate change has had a significant impact on rainfall and temperature in the Kimberley and Broome. Rainfall shows a 41% increase since 1997 with average rainfall of 780 mm compared with 554 mm between 1940 and 1996. In addition, ocean temperatures in the northwest of Australia have also risen, especially in the last two decades with an increase in anomalous warm events superimposed on an overall trend of increasing water temperature. The coincidence of temperature and rainfall increases since the late 1990s makes it difficult to determine which of these factors may have had the greatest influence on water quality indicators as represented in the sediment. In addition, Tropical Cyclone (TC) Rosita passed just 15 km south of Broome in April 2000 causing significant erosion and loss of coastal vegetation along the eastern side of Roebuck Bay, and this may have also influenced our results. Biomarkers indicative of material derived from land plants such as long chain alkenones showed increases that could be associated with either increased rainfall and/or tropical cyclone Rosita. Biomarkers of diatoms (brassicasterol), dinoflagellates (dinosterol) and haptophytes (alkenones) along with Total Organic Carbon (TOC) and Total Nitrogen (TN) showed significant increases after the late 1990s coincident with both temperature and rainfall increases. However statistical analyses suggested that temperature increases had had a stronger influence on these parameters. In summary, the results from the Broome cores indicate that while increased rainfall since the late 1990s and the passing of TC Rosita in 2000 is likely to have had an influence on the amount of land based plant material incorporated into sediments, that increased temperature rather than increased rainfall had the greatest influence on phytoplankton biomass, total organic carbon and total nitrogen. It is likely that ocean warming in this region has led to a significant increase in primary production in the region based on these results. Examination of microfossils in sediments compared with phytoplankton in the water column would reveal whether there has been a change in species composition associated with the biomass increases.

1.1 Implications for management

- For the Kimberley generally: climate change, especially temperature increases have had and may continue to have a significant influence on phytoplankton biomass. This may be of benefit to pearl farming but may have other, as yet unrealised impacts on ecosystem dynamics;
- Broome: Our study provides general support to other studies which have shown increased nutrient pollution in Roebuck Bay. The impacts of this are unclear and warrants further monitoring associated with some impact and cause and effect studies; and
- For pearl farming: it is evident that small changes in the environment accumulated over the long term are detectable even from minimal anthropogenic activity. Options for reducing the rate of environmental change are discussed but at this stage there is no evidence, from ours or previous studies in the area, that management intervention is warranted.

1.2 Key residual knowledge gaps

For the Kimberley generally:

- the limited coverage of rainfall measurements and the sparse and incomplete records of river discharge in the Kimberley hampers linking hydrological and meteorological forcing with ecological data sets. These observations are neither difficult nor expensive to obtain using modern technology;
- Examination of microfossils in sediments compared with phytoplankton in the water column would reveal whether there has been a change in species composition associated with the biomass increases;

Northeastern Kimberley:

- the use of sediment cores targeted at questions about bush fire history would be worthwhile. Napier Broome Bay and Cambridge Sound are the preferred targets for this work based on hydrological and sedimentological considerations but management considerations may dictate looking at other areas; and

Broome:

- Further examination of the source and time course of nutrient pollution and spread of *Lyngbya* using sediment cores for nutrient analyses and cyanobacterial and sewage biomarkers could be considered. A larger number of shorter cores over a larger area of the intertidal areas would be instructive about the time course of pollution and first appearance and spread of *Lyngbya*.

Clarifications on methodology and interpretation of biogeochemical proxies

Peer review of this report raised four main concerns about methodology and interpretation. As these criticisms apply throughout each of the chapters it is best to address them here, rather than to do so repeatedly throughout the report.

Firstly, that the sterol biomarkers used as proxies for phytoplankton biomass degrade over time in sediments and that our data showing significant increases since the mid-1990s (which we attribute to anthropogenic climate change) may have been exaggerated by biomarker degradation prior to this time. While it is true that biomarkers can degrade in sediments, they are remarkably stable (Rousseau et al. 1995; Volkman et al. 1998) although degradation might be expected to be more rapid in warm tropical temperatures and well oxygenated coastal surface sediments. We have addressed this concern by taking on the reviewer's suggestion to examine the concentration of biomarkers relative to organic carbon content instead of just concentration per gram of sediment. This confirms our interpretation that the biomarkers remain well preserved in our samples. In addition as we show in several places, biomarker levels track other geochemical parameters and in particular in figure 3.20 we show that at one of our sites (Cygnet Bay), high levels of biomarkers associated with a concomitant pattern of sediment enrichment (which we attribute to pearl oyster culture) are present well before the 1990's, i.e. into the early 1980s, indicating that (at least in Cygnet Bay) the phytoplankton biomarkers are well preserved.

Secondly, that the use of TEX_{86}^H as a proxy in shallow coastal waters may not be a reliable proxy for SST, and at best it is a proxy of depth integrated temperature. Schouten *et al.* (2002) proposed TEX_{86} (TetraEther indeX of tetraethers consisting of 86 carbon atoms) as a proxy for SST, based on the relative distribution of marine archaea isoprenoid glycerol dialkyl glycerol tetraethers (GDGTs). The selected GDGTs are membrane lipids synthesized by Thaumarchaeota, which contain different numbers of cyclopentane and cyclohexane rings. It has been demonstrated that the addition of rings into GDGTs enables archaea to adjust membrane stability in response to temperature changes (Chong, 2010; Uda *et al.*, 2001). However, knowledge of the ecology of Thaumarchaeota remains scant and their occurrence throughout the top 200 m of water depth (but to a greater extent at the deeper end of this range Richey and Tierney (2016)) means the GDGTs we measure in sediments from 15m of water might represent production over a bigger area and greater range of depths and thus TEX_{86}^H might be better regarded as a proxy of depth integrated temperature. However, a number of regional studies also have shown that TEX_{86} temperature corresponds well with annual mean SST. For example, Zhu et al. (2011) found a good correspondence between TEX_{86}^H temperature and SST in surface sediments (water depth < 120 m) from the Yangtze River fan. In the tropical eastern Indian Ocean, Chen et al. (2014) found a good correspondence between TEX_{86}^H temperature and annual mean SST for surface sediments in the non-upwelling area. Smith et al. (2013) looked at the correlation between TEX_{86} and SST in south eastern Australia and while they found that this ratio performed the best compared to other indicators, the signal was a depth integrated one. The TEX_{86}^H temperatures in our three sites including six sediment records all show consistent trends with the instrumental SST. Thus, despite lack of direct validation in the Kimberley, we tend to interpret the TEX_{86}^H as annual SST at our sites. However, there are still many uncertainties around the ecology of these organisms and the mechanisms by which the lipids become incorporated into sediments which means there is still significant work to be done to understand the interpretation of this ratio. For example, we cannot entirely rule out the possible influence from other non-temperature factors such as GDGTs transported from terrestrial soils (Hopmans et al. 2004), incorporation of methanotrophic archaea (Zhang et al. 2011), growth phase and species variability (Elling et al. 2014; Elling et al. 2015) and dissolved O_2 (Qin et al. 2015). But, the good agreement between TEX_{86}^H temperature and instrumental SST suggests that at least temperature is the main factor for the TEX_{86} index and the warming trend in our study area is real. Despite any uncertainty over this matter we point out we have not relied heavily on this proxy and whether it is more a proxy of depth integrated temperature than SST is not important to our study. We have compared our measurements of TEX_{86}^H to SST (extended reconstruction of SST, ERSST) because this is the most widely available temperature time series for the Kimberley, and as we acknowledge in this report ERSST is not without its own accuracy concerns (Kennedy 2014; Smith et al. 2008). However, our finding, using TEX_{86}^H, that water temperature has increased coincident with anthropogenic climate change is not controversial (e.g. Zinke et al. 2015), and beyond this our main use of this SST proxy is to attempt to separate the extent to which increased phytoplankton biomass since the mid 1990's could be attributed either to increased sea temperature or increased rainfall in the Kimberley.

Thirdly, that as our results are drawn from few cores at usually only two sites (impact and reference), per study area that this lack of replication constrains both the confidence of the interpretation and the spatial scale at which the results can be extrapolated. We accept this as a constraint which besets almost all palaeoecological studies (because of the high cost and time consuming nature of the analytical methods) and is in stark contrast to many ecological studies which demand a high level of replication. However this is why paleoecological studies use multiple proxies to reinforce each other and our methods are no different than most published studies. For example, the well regarded study by Abelmann et al. (2006) relies on a single core to demonstrate that levels of productivity in the entire Atlantic sector of the Antarctic Circumpolar Current were much higher during the previous interglacial period than today. In times of the extent of applicability of our results, for the Cygnet Bay oyster farm site, we only suggest the results are likely to be indicative of the farm site itself not outside, and in terms of the increase in phytoplankton productivity since the mid-1990s, our results are very consistent across all six sites at three locations stretching from south of Broome to the King George River.

Lastly, it was pointed out that our use of the term "brassicasterol" (for the diatom biomarker) implies 24-beta stereochemistry, but our methods are actually a measure of 24-methylcholesta-5, 22-dien-3β-ol (brassicasterol or epi-brassicasterol depending on C-24 stereochemistry). Rather than change this throughout, we have retained the term brassicasterol, but the reader should be aware of the distinction, which does not affect the reliability of our use of the parameter as a proxy for diatom biomass.

2 Introduction

The remote Kimberley coast of north-western Australia is one of the few marine environment domains on earth largely unaffected by human use. However, the region is undergoing increasing economic importance as a destination for tourism and significant coastal developments associated with oil and gas exploration. As a result of the increase in human usage there is an imperative to gain an understanding of the historical and baseline environmental condition ahead of future impacts. In addition, this century, scientists and managers will for the first time, face having to untangle impacts from local and global impacts on the environment. This process is difficult without a good time series of data collected pre-impact. This is not always possible, especially in remote areas, and this project sought to establish through a series of proxies, baseline and historical water quality information in the Kimberley ahead of major local impacts. It is also hoped the information will help enable interpretation of the changes that may have already occurred in recent years as a result of climate change.

Water quality and the pelagic biological oceanographic environment is influenced by natural climate variability, greenhouse induced climate change and other anthropogenic influences e.g. nutrients from grazing, agriculture and other catchment uses including those in coastal towns and cities. Complacency over impacts to water quality has contributed to the decline in environmental health of the Great Barrier Reef (Brodie and Waterhouse 2012) and it will be important to avoid this scenario in the Kimberley.

The key objective of this research is to reconstruct a timeline of indicators of water quality changes as recorded in sediment cores using paleoecological and biogeochemical techniques for a selected set of sites in the Kimberley that have contrasting human uses and/or environmental influences. The results provide an indication of the level of variability and change in water quality over the last 100 years and provide a baseline against which future changes can be measured.

Three study locations in the southern, central and northern Kimberley were selected each offering a different perspective in comparison of levels of human use or natural environmental variability in addition to looking for long-term environmental changes:

- Cygnet Bay where pearl farming has been undertaken since the 1960s offered a comparison of pearl farm and non-pearl farm sites;
- Koolama Bay at the entrance to the King George River offered a chance to examine the influence of significant seasonal riverine input to the coastal environment and was compared with a reference site in a bay nearby without direct river flow into it; and
- Roebuck Bay offered a comparison of sites near/far from Broome city's anthropogenic inputs such as runoff from Dampier Creek as well as the waste water treatment plant, the golf course and an abattoir all built close to the coastline.

Sediment cores (up to 1.5 m) were obtained from each of these locations in the expectation that they would provide a time series for about the last 100 years. By obtaining an age profile in the sediment along with the time course of any change in sediment biogeochemical conditions, phytoplankton biomass and type it possible to evaluate changes in water quality and local biological oceanographic features which can be matched to changes in climate and human use, including impacts such as pollution.

The following set of parameters was measured along the core length (every 1-2 cm) for some or all cores depending on the particular focus for the location:

- ^{210}Pb and ^{137}Cs isotopes – age of core, integrity of age structure in sediment;
- ^{15}N isotope – a proxy for nitrogen source – anthropogenic or natural;
- ^{13}C isotope – proxy for carbon source – land or marine derived carbon;
- Carbon/Nitrogen ratio – can also be used to infer whether primary carbon source is marine or

terrestrial;

- Sedimentation rate and grain size shows the variation of sedimentary environment (e.g. river input, sediment texture, other factors governing deposition and preservation);
- Total Organic Carbon (TOC) and Total Nitrogen (TN) indicate levels of productivity and deposition of organic matter;
- Biosilicate indicates siliceous phytoplankton deposits (e.g. diatoms, silicoflagellates), enhanced productivity;
- Biomarkers – sterols can be used as proxies for dinoflagellates (dinosterol), diatoms (brassicasterol) haptophytes (alkenones); TEX_{86} index for sea temperature; and long chain *n*-alkanes (C_{27}+C_{29}+C_{31}) for terrestrial influence; and
- Black carbon – indicator of biomass burning (e.g. from bushfires) or hydrocarbon burning (fossil fuels).

This report sets out the work undertaken, describes the results of analyses in each location, provides an interpretation of the variation in parameters over the timeline for cores at each location, where possible referencing these changes against know historical events or changes and finally discusses the relevance of the results to understanding historical changes in water quality at each location and in general for the Kimberley.

3 Materials and Methods

3.1 Sediment cores

Sediment cores taken at each site were obtained using a polycarbonate sleeve 6 cm in diameter within a 1.5m long steel casing. Two methods of coring were employed. At Cygnet Bay, cores were collected by SCUBA divers that pushed the core casing vertically into the seabed. At Broome and King George River the same core casing was lowered from a winch on the RV Solander and a Vibecore-D (Speciality Products, USA) weighted vibrating head powered by onboard 24-volt batteries was used to work the corer into the seabed before retrieval (Figure 2.1). In each case, a core catcher prevented loss of sediment from the core as it was withdrawn from the seabed. At each site, three or four replicate sediment cores with a length of approximately 1.0 – 1.4 meters each were collected. The cores were then frozen on board the ship in a vertical position and were later thawed as they stood vertically and were then sectioned into sub-samples at 1 cm intervals (Figure 2.2), weighed and freeze dried before being reweighed and then stored in a freezer at -20°C before being analysed.

Figure 2.1. Coring method using a Vibecore-D (Speciality Products, USA) weighted vibrating head lowered from the CTD winch on the RV Solander.

Figure 2.2. Close-up of sediment core prior to sectioning.

3.2 Chronology

^{210}Pb and ^{137}Cs radiometric-dating techniques (Appleby 2001) were used to measure the core ages. Supported ^{210}Pb ($^{210}Pb_{supported}$) is derived from the ^{226}Ra activity obtained by gamma spectrometry. Excess ^{210}Pb ($^{210}Pb_{ex}$) activity in each section is then obtained by subtraction of $^{210}Pb_{sup}$ activity from the total ^{210}Pb activity (Appleby, 2001).

For the Cygnet Bay cores, radiochemical measurements were performed using well-type Ge detectors (GWL-120210-S). The ^{210}Pb and ^{137}Cs activities were measured after correction with standard samples provided by the Chinese Institute of Atomic Energy Research and the University of Liverpool. Based on the relative variations of excess ^{210}Pb ($^{210}Pb_{ex}$) concentrations, sedimentation rates were calculated using the Constant Initial Concentration (CIC) model (Appleby 2001).

For the King George River and Broome cores, sediment samples were analysed for ^{210}Pb through the measurement of its decay product ^{210}Pb, in equilibrium, by alpha spectrometry after addition of ^{209}Po as an internal tracer and digestion in acid media using an analytical microwave (Sanchez-Cabeza et al. 1998) The concentrations of excess ^{210}Pb used to obtain the age models were determined as the difference between total ^{210}Pb and ^{226}Ra ($^{210}Pb_{supported}$).

Sediment accumulation rates (and thus ages) were obtained using the CRS (constant rate of supply) and/or the CF:CS models (Appleby and Oldfield 1978, Robbins 1978, Masqué et al. 2002). The CRS model assumes a constant $^{210}Pb_{ex}$ flux to the sediment surface, and the age of a certain level in a given depositional sequence would depend on the remaining ^{210}Pb activity beneath this level relative to the integrated ^{210}Pb activity of the sequence. This model can be used in most sedimentary systems where the sediment supply may vary in response to climatic or anthropogenic changes. Sedimentation rate (g $cm^{-2}y^{-1}$) is calculated taking into account the dry bulk density (g cm^{-3}) in order to eliminate possible errors that may arise from the sediment compaction.

3.3 Sediment grain size measurement

Grain sizes of each core, at 1cm interval, were measured using a Malvern Mastersizer 2000F Laser Particle Sizer, to get the trend. They were classified into three groups (less than 4 µm, 4-63 µm and larger than 63 µm) according to Folk's triangle classification and nomenclature (Folk et al. 1970). Prior to the grain-size measurements, small shells visible to the naked eye in the sediments were removed, and then the samples treated using 10% H_2O_2 and 10% HCl to remove organic matter and carbonate, respectively; the samples were then dispersed in a 0.05% $(NaPO_3)_6$ solution to separate particles for measurement.

3.4 Biogeochemical parameters

Freeze-dried sediment samples were homogenized by grinding, and then weighed aliquots were acidified by adding 2 ml of 1 M HCl to every 100 mg of sample. The acidified samples were dried at >60 ºC under flushing filtered air, then mixed with 1 ml Milli-Q water and freeze-dried again. Samples were weighed again to account for the change of weight occurring during the acid treatment. Aliquots of about 20 mg were weighed into 5×8 mm tin capsules for the measurements of total organic carbon (TOC), total nitrogen (TN), carbon and nitrogen isotopes ($\delta^{13}C$ and $\delta^{15}N$) using a continuous-flow isotope-ratio mass spectrometer (Delta V Advantage, Thermo Scientific, Germany) coupled to an elemental analyzer (Flash EA 1112 Thermo Scientific, Italy). These measurements were carried out at the Littoral Environment et Sociétés (LIENSs)-UMR7266, France. The measurement results are expressed relative to Vienna PeeDee Belemnite and atmospheric N_2 for $\delta^{13}C$ and $\delta^{15}N$, respectively. Replicate sample measurements of an acetanilide standard (Thermo Scientific), indicated that the analytical errors were <0.1‰ for both $\delta^{13}C$ and $\delta^{15}N$. The C/N ratios were determined as mol/mol ratios, which were transformed from the %TOC and %TN weight data obtained as part of the stable isotope analyses. Replicate measurements of a certified reference material (Low Organic Content Soil, Elemental MicroAnalysis, UK) indicated analytical errors of 0.025% and 0.002% for %TOC and %TN, respectively.

The wet alkaline leaching method was used to measure biosilica (BSi) in the sediments (DeMaster et al. 1991, Kamatani and Oku 2000). Approximately 0.2 g of freeze-dried and well-ground sediments was used for sample pre-treatment. First, 10 ml of 10% H2O2 and 10% HCl were added to the samples to remove organic matter and carbonate, respectively, and then the extra hydrochloric acid and peroxide were washed out using Milli-Q water. The wet samples were placed in an oven to dry overnight at 60 ºC and then extracted with 2 M Na2CO3 at 85 ºC for an 8-h digestion. It was necessary to gently swirl the samples for homogenization during the digestion processes. At 1-h intervals, 0.1 ml of alkaline solution was extracted for measurement by the molybdate blue spectrophotometric method using OUXI TU-1810. Replicate measurements indicated that analytical errors were below 0.005%.

Measurement of black carbon or elemental carbon followed that given in Fang et al. (2015). Briefly, freeze dried sediment samples were homogenized followed by removal of carbonates, metals and metal oxides (5 ml 0.5 M HCl, 24 h); removal of silicates (5 ml mixture of 6 M HCl and 48% HF, v/v=1:2, 24 h); removal of secondary minerals (5 ml 4 M HCl, 24 h). The residues were then loaded onto quartz fiber filters and quantification of black carbon was made a on a DRI model 2001A Thermal/Optical Carbon Analyzer.

3.5 Biomarkers

Sample processing and instrumental analyses of biomarker proxies were performed at Ocean University of China, following analytical methods in previous studies (Zhao *et al.* 2006; Li *et al.* 2013). Briefly, about 5 g of dry sediment sample was extracted four times with dichloromethane/MeOH (3:1, v/v), after adding internal standards (*n*-$C_{24}D_{50}$, C_{19} *n*-alkanol and C_{46} GDGT). The extracts were hydrolyzed with 6% KOH in MeOH. The neutral lipids were extracted with hexane and then separated into two fractions using silica gel chromatography. The nonpolar lipid (containing *n*-alkanes) fraction was eluted with hexane and the polar lipid fraction (containing sterols and GDGTs) was eluted with dichloromethane/methanol (95:5, v/v). Subsequently, the polar fraction was divided into two parts, one was derivatized using N, O-bis (trimethylsily)-trifluoroacetamide (BSTFA) at 70°C for 1 h and the other was filtered by PTFE membrane (0.45 μm) before instrumental measurements.

The long chain *n*-alkanes, brassicasterol and dinosterol were quantified by GC (Agilent 6890N) with an FID detector and a HP-1 column (50 m × 0.32 μm × 0.17 μm). The oven temperature was programmed from 80°C for 1 min and then increased to 200°C at 25°C/min, followed by 4°C/min to 250°C, then 1.6°C/min to 300°C (holding for 12 min), 5°C/min to 320°C (holding for 5 min). GDGT analysis was performed by HPLC-MS (Agilent 1200/Waters Micromass-Quattro UltimaTM Pt) with an APCI probe and a Prevail Cyano Column (150 × 2.1 mm, 3 µm). Separation was achieved with a flow rate of 0.3 mL min^{-1} at 30.0°C using a gradient program: 88% A (hexane) and 12% B (hexane/isopropanol, v/v = 9:1) at first, a linear gradient to 14% B in 3 min and to 24% B in 6 min; 76% A and 24% B for 5 min; a linear gradient to 100% B in 2 min; 100% B for 8 min; returning to 88% A and 12% B for 13 min.

The TEX_{86}^H index, a modified version of TEX_{86}, was calculated based on the relative abundance of GDGTs defined by Kim et al. 2010 (Eq. 1) and converted into SST according to the global equation (Eq. 2) based on 255 core-top dataset sediments with modern annual surface temperature (Kim *et al.* 2010).

$$TEX_{86}^H = \log\left(\frac{[GDGT\ 2]+[GDGT\ 3]+[Cren']}{[GDGT\ 1]+[GDGT\ 2]+[GDGT\ 3]+[Cren']}\right) \quad \text{Eq. (1)}$$

$$SST = 68.4 \times TEX_{86}^H + 38.6,\ R^2 = 0.87,\ n = 255 \quad \text{Eq. (2)}$$

where H stood for high temperature regions, the numbers 1-3 indicated the number of cyclopentane rings in GDGTs and Cren' was the regioisomer of crenarchaeol.

The input of terrestrial isoprenoid GDGTs can impact the accuracy of TEX_{86}^H in coastal waters. This error can be assessed by the BIT index (Branched and Isoprenoid Tetraether index), as TEX_{86}^H index is not suitable for SST reconstruction when BIT value is above 0.3 (Weijers *et al.* 2006). Thus, we investigated the BIT index to evaluate the potential influence of soil-derived GDGTs on TEX_{86}^H index. The BIT index was calculated based on the relative abundance of branched GDGTs and crenarchaeol defined by (Hopmans *et al.* 2004) (Eq. 3).

$$BIT = \frac{[GDGT\text{-}Ia]+[GDGT\text{-}IIa]+[GDGT\text{-}IIIa]}{[GDGT\text{-}Ia]+[GDGT\text{-}IIa]+[GDGT\text{-}IIIa]+[Cren]} \quad \text{Eq. (3)}$$

where the Roman numerals (Ia, IIa, and IIIa) referred to branched GDGTs and Cren was crenarchaeol.

In order to verify the accuracy of TEX_{86}^H reconstructed temperature, we used the extended reconstruction of SST (ERSST; resolution: 2°×2°; location: 16°S, 124°E; (apdrc.soest.hawaii.edu/las/v6/constrain?var=286) (Smith *et al.* 2008) during the period of 1940-2011 as a comparison. To understand the impact of terrestrial input, we collected the data of rainfall data from the Australian Bureau of Meteorology (www.bom.gov.au/); Broome rainfall station) during the period of 1941-2011 and river discharge from Department of Water, the State of Western Australia (www.water.wa.gov.au/home); Fitzroy River-Dimond Gorge station) during the period of 1963-2011.

The magnitudes of the shift changes of four biomarkers and observational data over time were assessed using the sequential t-test analysis of regime shifts (STARS) (Rodionov 2004, Rodionov & Overland 2005). The STARS algorithm was converted to VBA for Excel (the analysis software is available for download at www.BeringClimate.noaa.gov). The cut-off length (l) was set to 10 years (rarely 5 years for short time series) and the probability level to $p = 0.05$, representing a significant regime shift. After the shift point was established, the value of the regime shift index (RSI) indicated the shift magnitude. The correlation between phytoplankton biomasses and environmental factors was analyzed using principal component analysis (PCA), and the eigenvalues were used to determine the fraction of total data variance explained by each principal component. PCA was performed using SPSS 16 for windows (IBM Statistical Package for the Social Sciences Inc.).

3.6 Sources of environmental and historical data

Rainfall data was obtained from the Australian Bureau of Meteorology website (www.bom.gov.au). Stream flow data was obtained from the Western Australian Department of Water website (www.water.wa.gov.au). Historical bushfire data was obtained from the Western Australian Department of Parks and Wildlife.

3.7 Time series analyses

The magnitude of the shift changes in geochemical and biomarker parameters over time were assessed using sequential t-test for a regime shift (STARS, Rodionov 2004, Rodionov & Overland 2005). The STARS algorithm was converted to *VBA for Excel* and the analysis software is available for download at www.BeringClimate.noaa.gov. The cut-off length (*l*) was set to 10 years and the probability level to p=0.05, representing a significant regime shift. After the shift point is established, the regime shift index (RSI) was used to reflect the magnitude of the shift changes in the confidence of the regime shift. For the spatial comparison between cores, the ratios of geochemical parameters (e.g., $TOC_{site\ 1}$/ $TOC_{site\ 2}$) were calculated after the interpolation analyses of chronological data using *Origin 8.0* software (Mathematics: *interp1xy*) to reduce asynchronous errors caused by different sedimentation rates between reference and effect sites.

4 Cygnet Bay, King Sound, central Kimberley

4.1 Site description and sample sites

Cygnet Bay is a semi-enclosed coastal bay, located in King Sound, in the Kimberley, which is the northernmost region of Western Australia, with an approximate area of 150 km^2 and an average water depth of 10 m (Figure 3.1a-c). King Sound is the receiving water body of the Fitzroy River catchment (Figure 3.2) and has an average depth of 18 m (Figure 3.1b). It is characterized by a typical semi-arid tropical climatic regime, with an annual temperature range of 20–33 ^{o}C and rainfall range of 600–1000 mm, about 70% of which falls between January and March, and moreover the evaporation is about 3000 mm yr^{-1}, greatly exceeding the rainfall. King Sound has well developed mangrove systems (Figure 3.3) and has second largest tidal range in the world, and hydrodynamic processes are mainly controlled by tide driven currents (Wolanski & Spagnol 2003, Semeniuk & Brocx 2011). The maximum tidal range can reach 11 m (mean spring range=7.75 m, mean neap range=5.72 m), with strong current movement from two-way tidal velocities, with an average >0.2 ms^{-1} and a peak flow of 0.75 ms^{-1} (Wolanski & Spagnol 2003).

Pearl oyster farming is set up within the top 2–3 m of water (total depth ca. 10 m) using floating long lines that are approximately 200-m-long and spaced approximately 50 m apart and occupy approximately 40% of the bay area; oysters are suspended in vertically held cages with 8–15 oysters per cage (Figure 3.4). The industry standard for the stocking density of pearl oysters is no more than 16,250 shells per square nautical mile, and no artificial feed or chemicals are required in the culture of pearl oysters (Jelbart et al. 2011). The seabed in the study area is soft sediment without any macroalgae or seagrass present, although reef and intertidal habitats elsewhere in Cygnet Bay do support these plant types.

Sediment cores were collected at the two sites in November of 2011. Site 1 (16°28′28″S, 123°02′06″E) is in the aquaculture area just west of Shenton Bluff and Gilbert Rock with a water depth of 11.5 m, and site 2 is 8.6 km southwest of the aquaculture area (16°32′25″S, 122°59′45″E) with a water depth of 9.8 m (Figure 3.1c). Site 2 is similar to site 1 in that both are approximately 1.5 km south of small peninsulas that run from west to east (Figure 3.1c). At each site, three replicate sediment cores with a length of approximately one meter each were collected by scuba divers using a push core with 6 cm internal diameter. The cores were sectioned into sub-samples at 1 cm intervals and stored in a freezer at -20^{o}C before analysis. To confirm the replicate cores at each site were similar to each other in sedimentary structure, the variation in median grain size (d50), at each 1 cm interval, between two cores from each site were compared using regression analysis, and the result showed they were significantly correlated at a 95% confidence level (See Figures 3.10, 3.11). Further, the replicate cores from each site were used for different analyses. One was used for chronology and the other was used for geochemical analyses as described below. The third core was retained frozen as a spare for future analysis and in case of loss of samples during shipping or handling during analysis by third parties. It is acknowledged that in the absence of samples at multiple locations within the culture area (site 1) and the non-culture (reference) area (site 2), our replicate cores are actually pseudo-replicates.

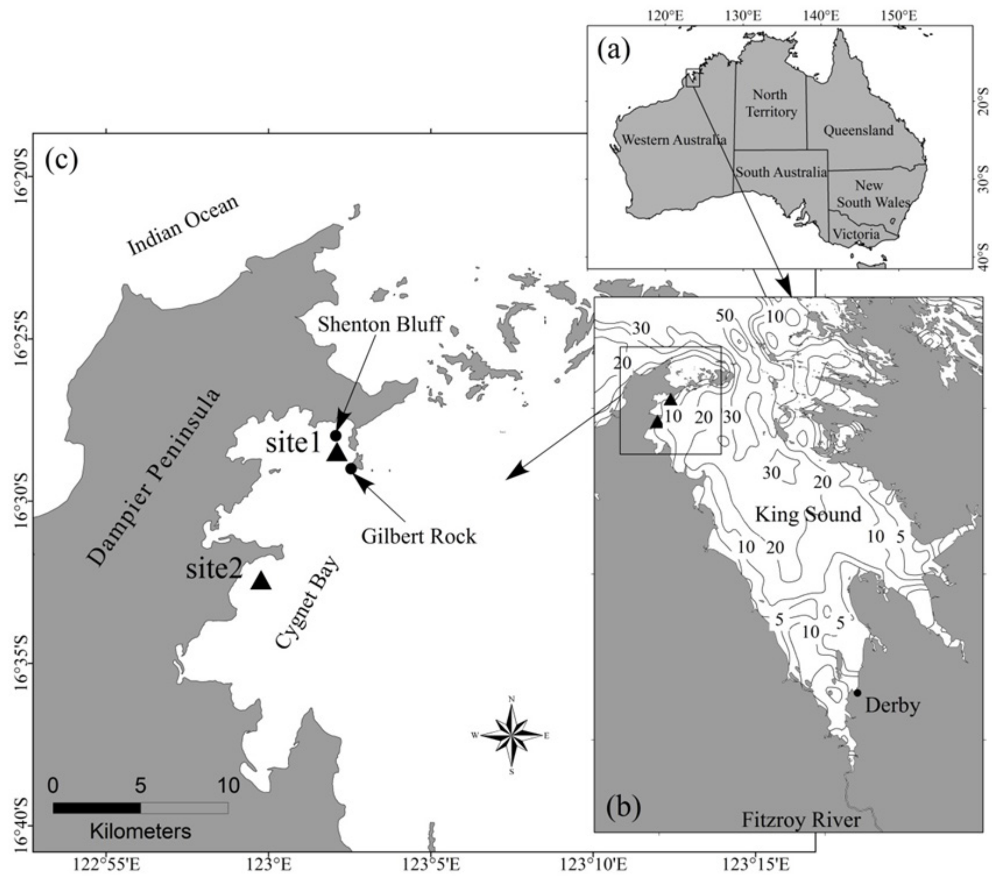

Figure 3.1. Map showing the location of study area with water depth (figures a, and b with depths in meters) and two sampling sites in Cygnet Bay (c), Kimberley Region, northern Western Australia.

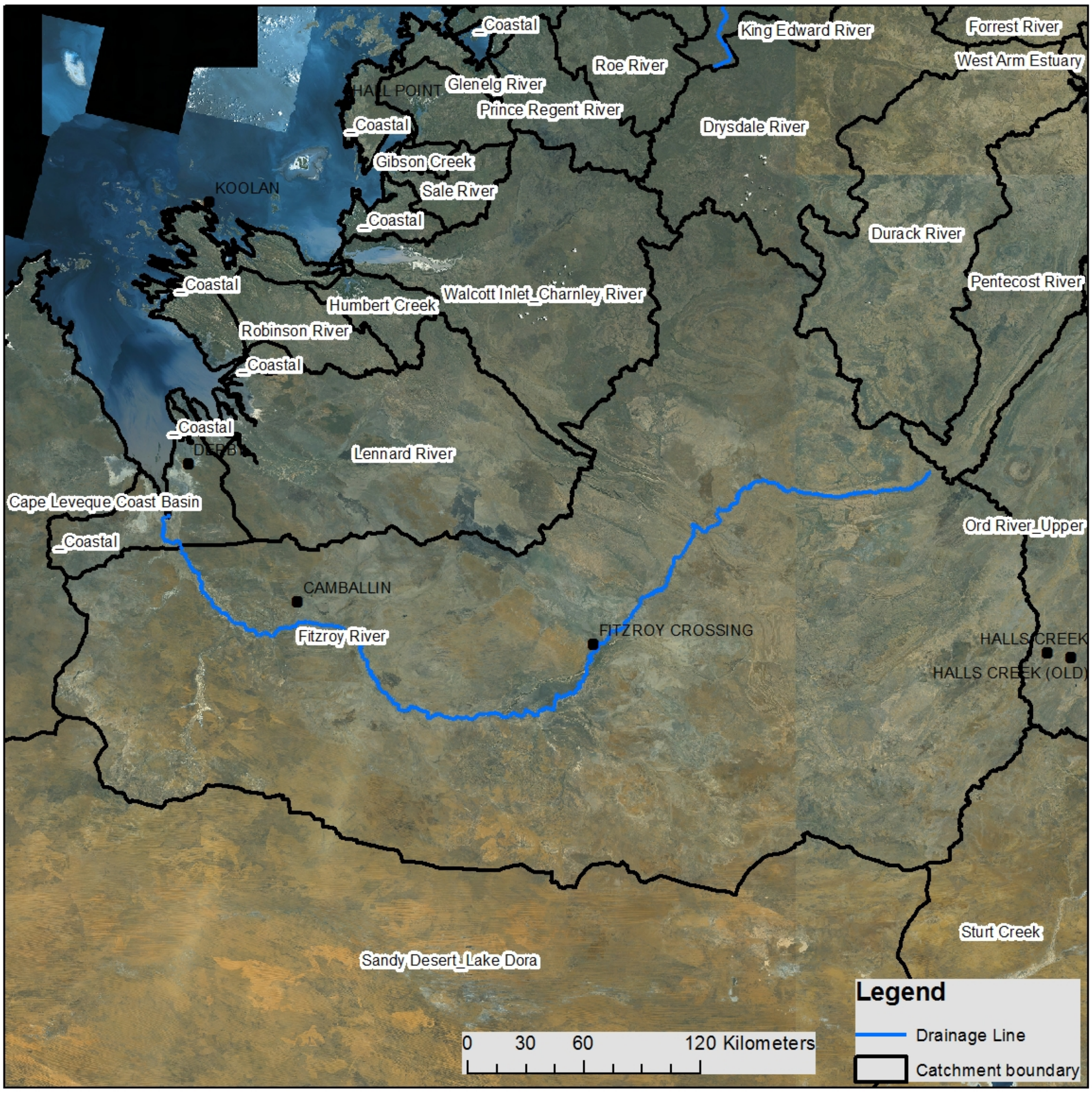

Figure 3.2. Fitzroy River catchment flowing into King Sound.

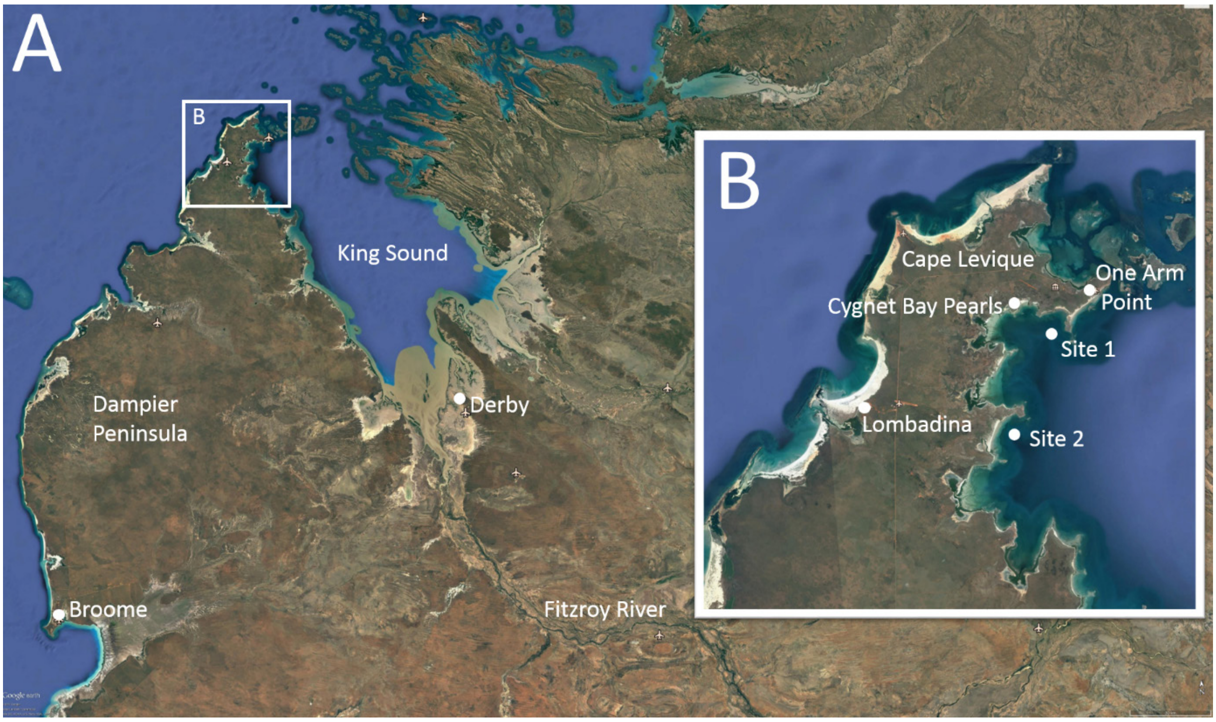

Figure 3.3. Google Earth imagery showing, A. the location of study area in relation to King Sound and the Fitzroy River and influence of tidal creek systems and B, close up of Cape Leveque and sampling sites.

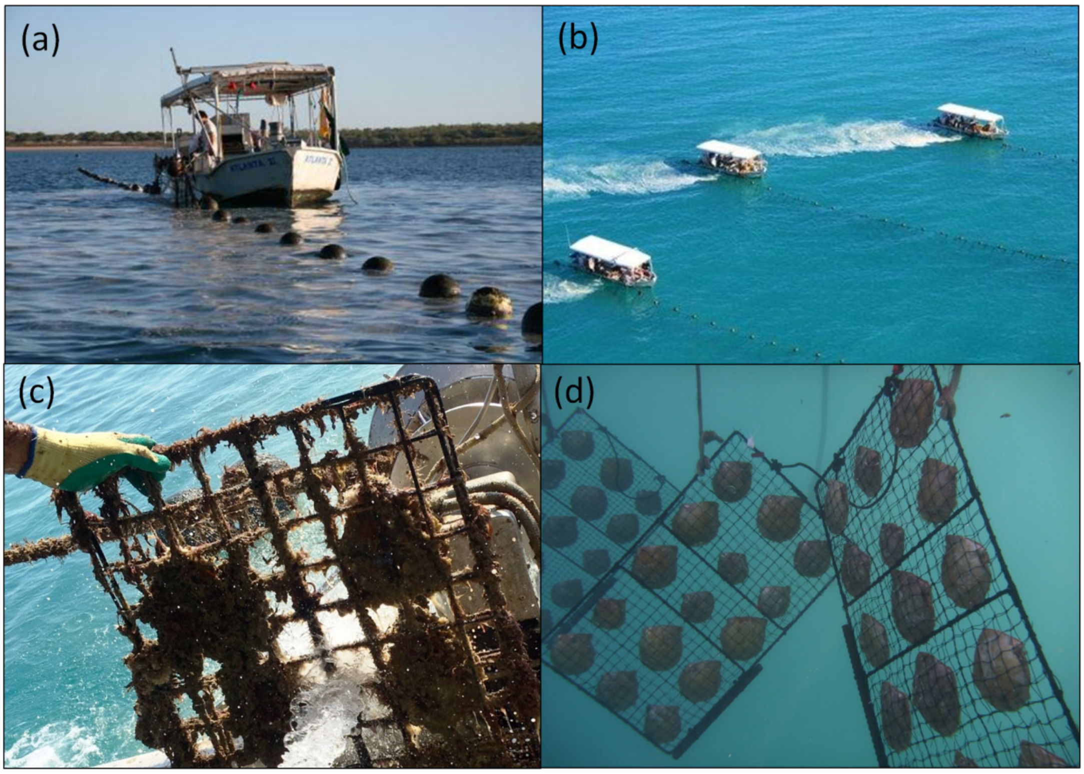

Figure 3.4. Modern long-line culture of pearl oysters in Cygnet Bay (a & b: cleaning/maintenance vessels tending long lines; c: biofouling of 8 shell culture cage before cleaning; d: 15 shell culture cages hanging on long line after cleaning).

4.2 Impact of aquaculture on coastal water quality and sediment characteristics

4.2.1 Introduction

Large scale and intensive bivalve farming can significantly impact aquatic environments by changing a series of physical and chemical conditions such as, reducing tidal current, accelerating organic accumulation, and altering sediment properties (Plew et al. 2005, Callier et al. 2008, Dumbauld et al. 2009). The impact levels depend on a set of integrative factors (Read & Fernandes 2003, Dumbauld et al. 2009), including the species involved (e.g., oyster, mussel and clam), culture methods (e.g., cages and rafts), density, sites, scales, and aquaculture history. For example, compared with mussel aquaculture, which has a significant contribution to sediment accumulation and nutrient input (Prins & Smaal 1994, Strang 2003), pearl oyster aquaculture displays much lower impacts on sediment properties and nutrient concentrations due to its low-density culture and no artificial feed or chemicals (Cheney et al. 1995; Yokoyama 2002; Wells & Jernakoff 2006; Gaertner-Mazouni et al. 2012).

However, small environmental changes accumulating over a long period of time can still cause a regime shift in an ecosystem (Lees et al. 2006; Andersen et al. 2009), and the underlying processes and changing rates can only be realized by careful analysis of long-term continuous observation data. For example, Sarà et al. (2011) found that nutrient and chlorophyll *a* concentrations in the Gulf Castellammare, Italy have been steadily increasing since the establishment of aquaculture facilities in 1999, although they had not reached a eutrophic status. In addition, hydrodynamic conditions at aquaculture sites are important for determining the rate of change. The rate of impact is a slower process at sites with high current (average velocity>0.1 ms^{-1}; and maximum velocity>0.3 ms^{-1}) (da Costa & Nalesso 2006), whereas it is a faster process at sites with low current (average velocity <0.05 ms^{-1}; and maximum velocity <0.1 ms^{-1}) (Hartstein & Rowden 2004; Callier et al. 2008). In contrast to the time span of marine aquaculture activity supporting human life, our ability to understand environmental effects of aquaculture is limited to knowledge on decadal scales. Continuous long-term monitoring data are expensive and rare and, usually, they record environmental information post-impact of human activities. The development of paleo-ecological methods has made it possible to acquire a chronological footprint of past environmental change, and the time span can extend from decades through centuries to millennia (Meyers, 1997; Meyers & Teranes 2001; Pancost & Boot 2004). A number of geochemical proxies (e.g. stable carbon and nitrogen isotopes, biogenic silica, lipid and biomarkers) deposited in the sediments have been used to reconstruct environmental events, such as eutrophication, industrialization, and climate change (Andersen et al. 2004; Turner et al. 2006; Dale 2009; Liu et al. 2013) and these studies not only provide effective environmental information, but also help to minimize long-term monitoring effort and costs.

The organic matter preserved in sediments can provide powerful evidence for interpreting coastal eutrophic processes, and the application of stable isotopes of carbon and nitrogen ($\delta^{13}C$ and $\delta^{15}N$) makes it possible to elucidate the source and fate of organic matter (Meyers 1994). In transitional waters (e.g., coasts and estuaries), organic matter sources are generally a mixture of allochthonous (e.g., river inputs) and autochthonous sources (e.g. marine primary production). They carry their overlapping source-suggestive signatures and display these in the values of $\delta^{13}C$ and $\delta^{15}N$, for example a typical range of $\delta^{13}C$ values for terrestrial C_3 plants is from -26‰ to -28‰ and for marine phytoplankton it is from -19‰ to -21‰ (Fry & Sherr 1984; Meyers 1997), and a mixture of marine and terrestrial organic matter could result in a $\delta^{13}C$ value of approximately -23‰ (Pancost & Boot 2004). The value of $\delta^{15}N$ originating from marine nitrate generally ranges from 3‰ to 6‰; however, sewage and manure can significantly elevate this value from 10‰ to 25‰ (McClelland & Valiela 1998, Savage 2005). C:N ratios can be another potential indicator for elucidating organic matter source, for example a ratio of 5 to 7 is measured for marine-derived organic matter (Redfield et al. 1963), and >12 for terrestrial-derived organic matter (Meyers 1997). However, mineralization, oxidation and significant fractions of inorganic nitrogen can impact C:N ratios and limit their usefulness as source indicators (Andrews et al. 1998, Kuwae et al. 2006). Thus, the application of multiple proxies ($\delta^{13}C$, $\delta^{15}N$ and C:N ratios) is important for verifying the organic matter source. Biogenic silica (BSi) stored in sediment is an important proxy representing siliceous marine organisms (e.g., diatoms, radiolaria, siliceous sponges, and silicoflagellates), particularly for diatoms, which are a major phytoplankton group with a significant contribution to marine primary production in this region and also a sensitive indicator responsive to varied environmental conditions (DeMaster et al. 1991, DeMaster 2002, Smol & Stoermer 2010). Silicon is an essential element for the growth of diatoms. In water bodies dominated by diatoms the BSi concentration in sediment can be an important proxy to indicate modern- or paleo-productivity (Bernárdez et al. 2005; Krause et al. 2011). If we can form an environmental picture combining BSi information with organic matter composition it is possible, to a certain degree, to assess the impact of past environmental changes (e.g. climate and hydrodynamic changes, nutrient cycling) on siliceous phytoplankton.

In this study, we applied paleo-ecological methods for tracking the long-term environmental impact of pearl oyster farming in Cygnet Bay, Kimberley, Western Australia. The farming of the silver- or gold-lip pearl oyster *Pinctada maxima* in the Kimberley region has a history of approximately 50 years and is the foundation of the Australian pearl industry and a major contribution to the world's total South Sea pearl production with an average annual value of around $220 million (Tisdell & Poirine2008, McCallum & Prince 2009). Theoretically, the variety of culture apparatus used in pearl oyster farming, such as rafts and panel nets, and harvesting processes, could increase the deposition of organic matter, nutrient flux and fouling species in the ecosystem (Forrest et al. 2009, Kishore et al. 2014). Actually, a few investigations (Wells & Jernakoff 2006; McCallum & Prince 2009, Jelbart et al. 2011) found only small environmental impacts with low ecological risk, with the reasons attributed to passive farming, low stocking density (<16,250 shells per square nautical mile) and high current flows. However, the environmental assessment still has some uncertainty because compared to pearl farming with a 50-year history, limited short-time frame studies (as described in the publications above) make it difficult to recognize the underlying process of environmental change over the course of the pearl farming activities, especially if the environmental change rate is very slow. In this work a 90-year environmental record was reconstructed using marine sediment cores to assess the environmental change rate after the initiation of pearl farming in Cygnet Bay.

Cygnet Bay is located in King Sound (Figure 3.1); The Fitzroy River, the largest river draining into King Sound, has a catchment largely in a wilderness setting (Semeniuk & Brocx 2011) which is sparsely populated (3,261 persons living around Derby, Australian Bureau of Statistics 2011 data) with low density agriculture. There is a diamond mine currently operating (Ellendale Mine, approximately 120 km east of Derby) and there was a short-lived gold rush in the 1880s, while lead and silver mining was discontinued in the 1980s. These industries are not thought to have had a major impact on the water quality in King Sound (CENRM 2010) and Cygnet Bay is more than 150 km seaward of the entrance of the Fitzroy River into King Sound. Pearl oyster farming is the only significant anthropogenic activity in Cygnet Bay. It was established in the 1960s by the Brown Family and is Australia's oldest and longest continually operated pearl farm. This provided an opportunity to assess decadal aquaculture effects without much disturbance from other human activity. Sediment cores were collected at two sites, located inside and outside the pearl farming area respectively, enabling us to compare their contrasting environmental characteristics over time. Multiple geochemical proxies in the cores, including organic matters, carbon and nitrogen isotopes, biogenic silica, and grain sizes, were measured for elucidating the underlying processes of environmental change in response to pearl oyster farming. The magnitude of the shift change between the farming site and the control site over time was assessed using a sequential t-test for a regime shift (Rodionov 2004), and the impacts of pearl farming and climate change are discussed in relation to the variations of geochemical parameters over time.

4.2.2 Results

Core chronology

The profiles of $^{210}Pb_{ex}$ concentrations in the two cores are shown in Figure 3.5a and c. They exhibited a pattern with exponential regression and showed some disturbance in surficial sediments. The disturbance is common in coastal and estuarine sediments, due to physical mixing, bioturbation and erosion (Ruiz-Fernández & Hillaire-Marcel 2009, Johannessen & Macdonald 2012). Tidal action and burrowers were regarded as the main impact factors on sedimentation in King Sound (Semeniuk & Brocx 2011). Sand bubbler crabs and sand tube worms are common organisms causing burrow-mixed sediment at the upper section of cores. Although cyclonic storms are a feature of Australia's tropical regions, their influence on the indented sheltered gulf embayments in the Kimberley, like those in our study, is generally limited to abnormally high tides and storm surges as they are protected from storm magnified swell and wind waves (see Semeniuk 2011 for detailed explanation of sedimentary dynamics in this region). The CIC model will be prone to large errors if there is significant mixing of surficial sediment, compared with the CRS model (Appleby 2001). The average sedimentation rates were calculated over a time span of ca.1890−2011 at site 1 (0.82 cm yr^{-1}) and ca.1920−2011 at site 2 (1.11 cm yr^{-1}).

The ^{210}Pb geochronology must be validated using at least one independent age control (Smith 2001). ^{137}Cs activity is widely used as an independent tracer of coastal sediments, although only 40% of atmospheric fallout ^{137}Cs (up to 3−5 Bg kg^{-1}) can be detected in marine sediments of Australian northern tropical region (Pfitzner et al. 2004; Logan et al. 2011; Hollins et al. 2011). Generally, appreciable ^{137}Cs was first introduced into the environment in 1954 and peaked in 1964 (Amos et al. 2009), but it is often difficult to find a distinct "1954 depth" in a mixed core (Johannessen & Macdonald 2012). In this study, ^{137}Cs activity peaked at the core depth of 35 cm at site 1 and 49 cm at site 2 (although a later peak also occurred) (Figure 3.5b, d), corresponding to ^{210}Pb geochronology of 1968 and 1967, respectively. This suggested that the calculated ^{210}Pb geochronology was reasonable at the decadal scale.

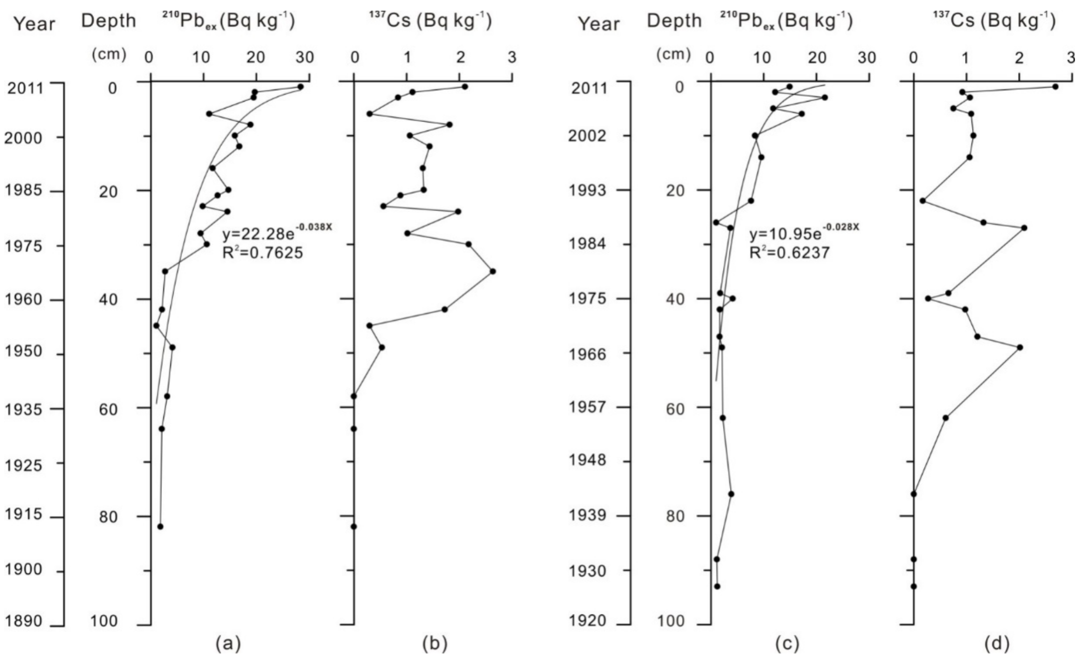

Figure 3.5 Profiles of $^{210}Pb_{ex}$ and ^{137}Cs at site 1 (a, b) and site 2 (c, b).

The profiles of grain sizes at two sites

The median grain size (d_{50}) in the sediment cores varied greatly over a range of 17.8−107.5 µm at site 1 (Figure 3.6a) and 74.9−118.2 µm at site 2 (Figure 3.6c), respectively, indicating that the sediment type was silty sand, and this is consistent with previous studies in King Sound and Fitzroy River delta (Semeniuk 1981, Semeniuk & Brocx 2011). In a spatial comparison, d_{50} between the two sites gradually varied in an opposite trend over time (Figure 3.6a, c). At site 1, finer particles (silt and clay) increased gradually and became evident in the upper section of the core (>50%; Figure 3.6b); whereas at site 2, sediments became coarser with decreasing silt and clay, particularly in the upper section of the core (<40%; Figure 3.6d).

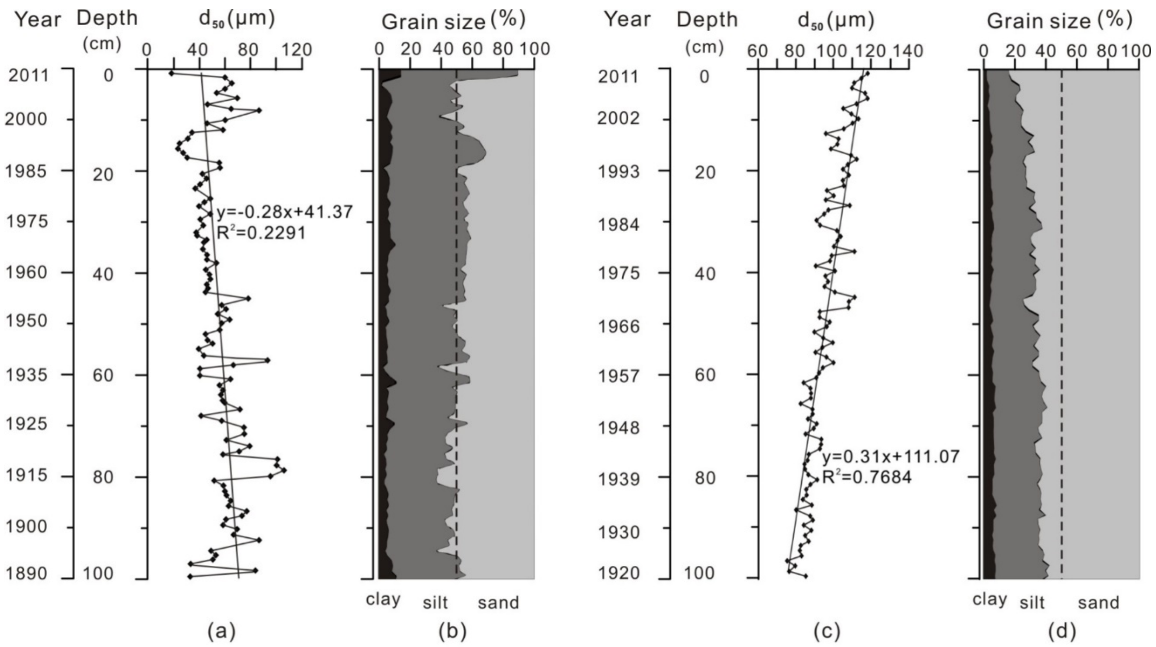

Figure 3.6. Profiles of grain sizes at site 1 (a, b) and site 2 (c, d), showing median values (d_{50}) with linear trend, and the proportions of clay, silt and sand.

Two significant shifts in C/N ratios and $\delta^{13}C$ values also observed after 1950s (at the depth of approximately 50 cm; Figure 3.7c, d). C/N ratios (5 to7 for marine-derived organic matter by Redfield et al. 1963; and >12 for terrestrial-derived organic matter by Meyers 1997) shifted from a phase with terrigenous dominance (12.0 to 19.8; Figure 3.7c) to a phase with marine and terrestrial mixture (7.5 to 12.0; Figure 3.7c). $\delta^{13}C$ values (-19‰ to -21‰ for typical marine-derived organic carbon, and -27.0‰ for typical river-derived terrigenous fraction by Fry & Sherr, 1984) increased from -24‰ to -22‰ to -22‰ to -20‰ at the depth of approximately 50 cm (Figure 3.7d). The trends of C/N ratios and $\delta^{13}C$ indicated a significant increase in the proportion of marine organic carbon.

$\delta^{15}N$ is used as a subsidiary factor to detect anthropogenically enriched organic nitrogen (McClelland &Valiela 1998; Savage 2005), for example farm runoff, animal and human wastes; and the values of $\delta^{15}N$ originating from typical marine nitrate generally fall into a range of 3‰ to 5‰ (Owens 1988). The values of $\delta^{15}N$ in the core ranged from 3.62‰ to 5.73‰ with a slight increasing trend (Figure 3.7e), indicating a dominance of marine nitrate with low anthropogenic impact. BSi concentration in the core range from 0.44% to 1.04% (Figure 3.7f) and displayed a significant increasing trend after 1950s (at the depth of approximately 0 to 50 cm), particularly during 1970s to 2011 (at the top 35 cm). The variations in BSi appear to match the increasing trend in TOC and TN.

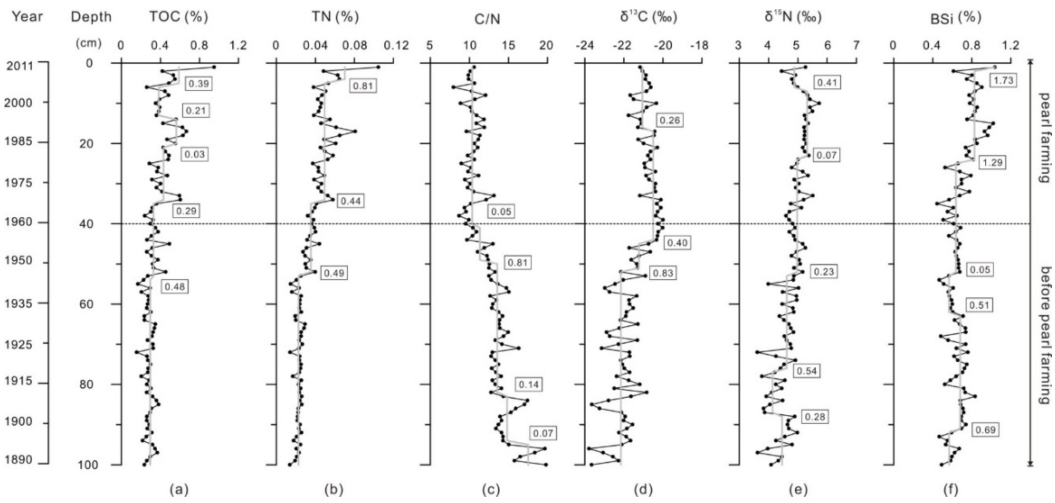

Figure 3.7. Profiles of geochemical parameters at site 1 (a: TOC; b: TN; c: C/N; d: δ13C; e: δ15N; f: BSi); the grey lines showing shift changes assessed by sequential t-test analysis of regime shift, and solid square showing regime shift index.

The profiles of geochemical parameters at site 2

The chronological variations of TOC, TN, C/N, $\delta^{13}C$, $\delta^{15}N$, and BSi at site 2 are shown in Figure 3.8. TOC and TN contents (Figures 3.8a, b) varied in a narrow range (TOC: 0.16% to 0.36%; TN: 0.02% to 0.04%), respectively, and the absolute values were much lower than at site 1 (Figures 3.7a, b). Based on the assessment of STARS, both TOC and TN showed increased shift changes after 1970s (at the depth of 40 cm), and a significant increase occurred after 2000s (at the depth of 10 cm; Figures 3.8a, b). The patterns of C/N ratios (9.0 to 19.0) and $\delta^{13}C$ values (-22.7‰ to -18.7‰) were similar to site 1, shifting to a phase with increased marine organic matter since 1950s (at the depth of approximately 60 cm; Figures 3.8c, d).

In the depth range of 0 to 60 cm (1950s to 2011) most $\delta^{15}N$ values were within 4‰ to 5‰ indicating a stable status with a dominance of marine nitrogen and very low anthropogenic derived nitrogen; however, there were some high values at the bottom of the core (1920s−1940s; Figure 3.8e) indicating a possible anthropogenic disturbance. BSi concentrations at site 2 were much lower than at site 1, and most values were between 0.2% and 0.4%, with decreasing shift changes at the depth of 0 to 60 cm (Figure 3.8f).

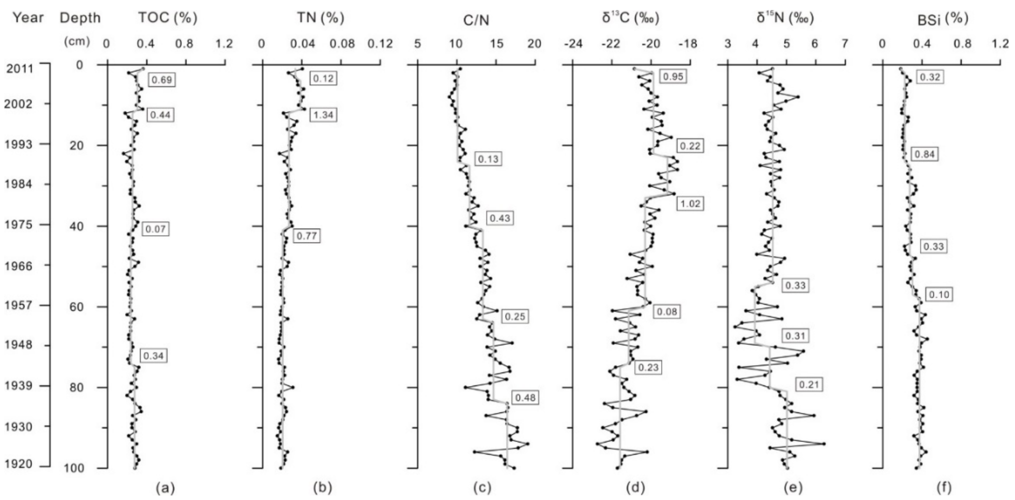

Figure 3.8. Profiles of geochemical parameters at site 2 (a: TOC; b: TN; c: C/N; d: $\delta^{13}C$; e: $\delta^{15}N$; f: BSi); the grey lines showing shift changes assessed by sequential t-test analysis of regime shift, and solid square showing regime shift index.

Magnitude of environmental change between the two sites

The ratios of four chronological parameters (BSi, silt, TOC and TN) between the two sites were processed by STARS (Figures 3.9a-d), with the aim of making a spatial comparison to assess the magnitude of environmental change with and without pearl farming. Before pearl farming started in Cygnet Bay (~1960), the variations in BSi and silt ratios were low without significant shift change (Figures 3.9a, b); and TOC and TN ratios showed similarly stable patterns except for small shift changes in the late of 1940s (RSI: 0.19, 0.39; Figures 3.9c, d). The results indicated that the two sites experienced similar environmental conditions with low variability before pearl farming.

After pearl farming (since 1960), the ratios of the four parameters exhibited higher values and frequent shift changes, particularly after 1980s (Figures 3.9a-d). Significant increases in BSi ratios (RSI: 1.23, 2.04, and 0.32), occurred three times, corresponding to the periods of 1960s, 1980s and 2000s (Figure 3.9a), respectively. The ratios of silt, TOC and TN presented similar patterns (Figures 3.9b-d); they all showed a first significant increase in 1980s, and then shifted back to a relatively lower level in the late 1990s and early 2000s, followed by a sudden increase again in surface sediment after 2005. The results suggested that the magnitude of environmental change at site 1 with pearl farming was much higher than at site 2 without pearl farming.

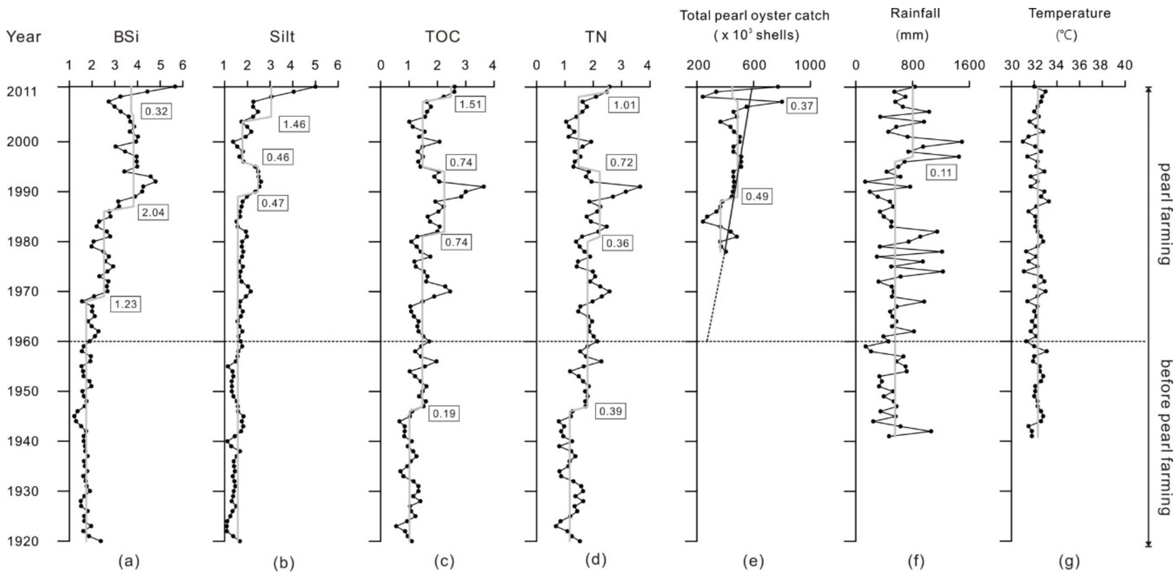

Figure 3.9. Profiles of spatial comparison between the two sites, based on the geochemical ratios (a: BSi; b: Silt; c: TOC; d: TN; e: total pearl oyster catch in Broome area during 1978−2011 (data from Hart et al. 2013); f: annual rainfall; g: mean maximum temperature during 1941−2011 (data from Bureau of Meteorology, 2014b); and the grey lines showing shift changes assessed by sequential t-test analysis of regime shift, and solid square showing regime shift index).

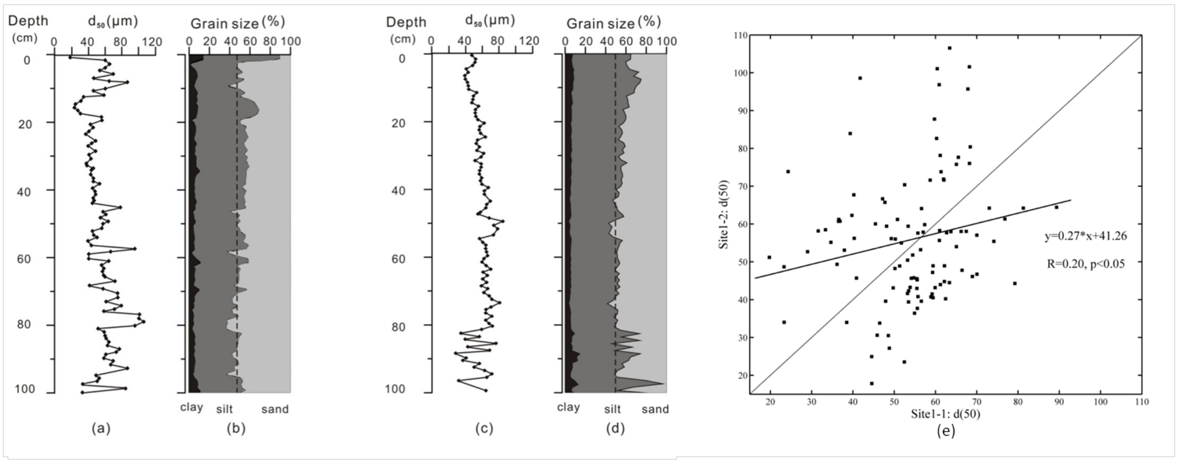

Figure 3.10. Assessing the similarity of two parallel cores at site 1 using median grain size d50 (regression analysis for d50: r=0.20; p< 0.05). (a) d50 for core 1-1, (b) % clay, silt and sand for core 1-1, (c) d50 for core 1-2, (d) % clay, silt and sand for core 1-2, (e) regression for d50 core 1-1 vs core 1-2, R=0.20, p<0.05.

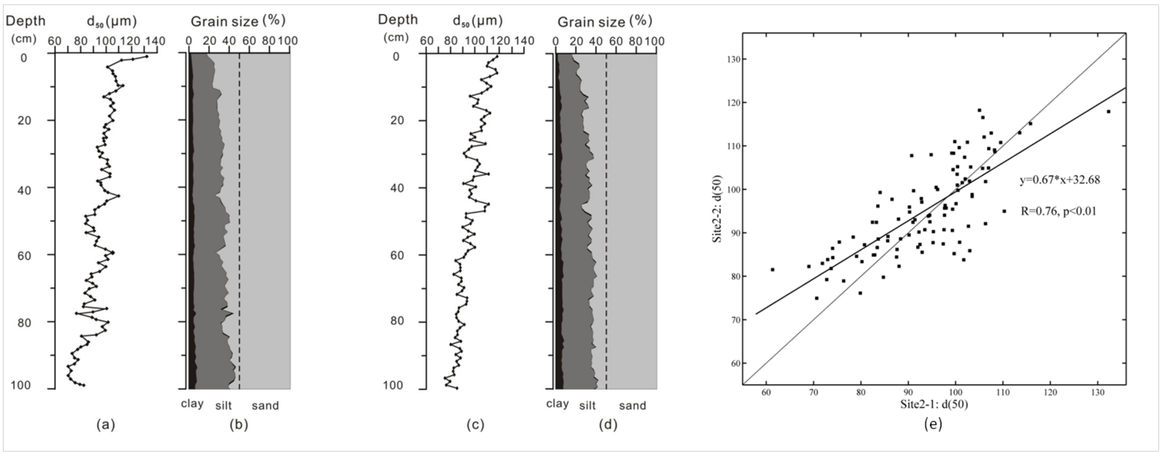

Figure 3.11. Assessing the similarity of two parallel cores at site 2 using median grain size d_{50} (regression analysis for d_{50}: r=0.20; p< 0.05). (a) d_{50} for core 2-1, (b) % clay, silt and sand for core 2-1, (c) d_{50} for core 2-2, (d) % clay, silt and sand for core 2-2, (e) regression for d_{50} core 2-1 vs core 2-2, R=0.76, p<0.01.

4.2.3 Discussion

In this study, contrasting patterns in geochemical parameters between the two sites indicated that a faster environmental change occurred at site 1 after the initiation of pearl oyster farming in 1960s. The corresponding variations in C/N ratios, δ13C and δ15N further suggested that increased TOC and TN in the upper section of the cores were mainly contributed by increased autochthonous sources rather than allochthonous input. In the sections below, for better understanding of the long-term environmental consequences of pearl oyster farming, we discuss the possible mechanisms of geochemical changes in the cores, according to the history of pearl oyster farming and natural disturbance in Cygnet Bay.

Changes of grain sizes in response to pearl farming

One of the environmental consequences of bivalve aquaculture is altering the properties of the sediment, which includes reducing the grain size and increasing the concentration of organic matter (Mesnage et al. 2007; Hargrave et al. 2008; Dumbauld et al. 2009). For example, the incidental source of organic enrichment below bivalve culture apparatus was recognized as important in a review of ecosystem effects of bivalve culture by the USA National Academy of Sciences (Ocean Studies Board 2010). Gaertner-Mazouni et al. (2012) estimated the sediment flux in Ahe Atoll lagoon (French Polynesia) using a sediment trap, and found that the sedimentation rates beneath the pearl oyster culture can be five times higher than in the control zone, and the percentage of small particles (⩽63 μm) was about double, although the impact of pearl farming is generally much lower than fish or other bivalve farming (Gifford et al. 2004, Yokoyama et al. 2006, Andréfouët et al. 2012).

The Brown family, who own and manage Cygnet Bay Pearls, indicated that the family started farming shell near site 1 (bottom farming near Shenton Bluff reef) in 1960 at low density; culture apparatus of modern long lines was started in the 1980s; and stock levels and farm size ramped up appreciably through the 1990s, and these changes are reflected in the total pearl oyster catch in Broome area during 1978−2011 (Figure 3.9e). In this study, fine-grained sediment (clay and silt) at site 1 with pearl farming displayed significant increases after 1960s (Figure 3.6b), with an average increasing rate (≈0.2% yr-1). Silt proportion at site 1 over time was approximately one to five-fold higher than at site 2 without farming (Figure 3.9b), indicating a similar trend to that in Ahe Atoll lagoon; and STARS detected the shift change of silt between the two sites in the late 1980s, which is matched the expansion of modern long-line culture at site 1 since the 1980s (Figure 3.9b, e). The organic wastes produced by pearl farms, e.g. the deposition of faeces and pseudo-faeces from pearl oysters, and the debris fallout from the culture apparatus, including from regular maintenance cleaning of the cages (Figure 3.4), might be important source of organic enrichment in sediment. At site 1, reduced grain size in the core over time well matched the increases of TOC and TN organic matter, displaying significantly positive correlations (Table 3.1).

Table 3.1 Pearson correlation between grain sizes and geochemical parameters at site 1 and site 2 in Cygnet Bay

	Site 1				Site 2			
	d_{50} (μm)	clay (%)	silt (%)	sand (%)	d_{50}(μm)	clay (%)	silt (%)	sand (%)
TOC (%)	-0.541**	0.241**	0.641**	-0.623**	0.087	-0.081	-0.194	0.172
TN (%)	-0.541**	0.185*	0.682**	-0.644**	0.678**	-0.621**	-0.697**	0.698**

Note: ** Correlation is significant at the 0.01 level (2-tailed) * Correlation is significant at the 0.05 level (2-tailed)

In addition, it is necessary to consider the impact of modern long-line culture on the hydrodynamic processes in Cygnet Bay. Previous studies pointed out that the degree of sediment change mostly depends on the density of aquaculture relative to current speed (Plew et al. 2005, Richard et al. 2007). For example, the aquaculture density in New Zealand's coastal waters has reached 800 mussels per meter of long-line (Hartstein & Rowden 2004); the average current speed is 0.4−0.5 ms-1 in the absence of farms, but the speed can be reduced by 36-63% within the farm, indicating a significant drag of mussel lines on currents and waves (Plew et al. 2005). However, this was previously not considered to be important in Cygnet Bay, because current speeds are fast in King Sound (average speed > 0.2 ms-1, a maximum of 0.75 ms-1; Wolanski & Spagnol 2003). The pearl oyster industry in Australia is expanding at a considerable rate (Kuchel et al. 2011), and there is a need to better understand the correlation between rate of environmental change and the intensity of pearl farming for long-term sustainable management.

Changes of organic matter in response to pearl farming

As the variations in grain size, TOC and TN contents at site 1 were higher and had more frequent shift changes than those at site 2 after the 1980s (Figures 3.7-3.9), corresponding to increased stock level during 1980s to 2000s (Figure 3.9e). In contrast, TOC and TN contents at site 2 only showed two slight shift changes (1970s and 2000s, Figure 3.8a-b), which were in response to increased rainfall in this area (Figure 3.9f: 30–40 mm 10 yr-1 since 1970s, and 40−50 mm 10 yr-1 around 2000s; Bureau of Meteorology 2014a, www.bom.gov.au/climate). However, the disturbance of rainfall at site 1 was obscured by the additional impact of pearl farming (Figure 3.7). In general, the elevated carbon and nitrogen contents in sediment are evident after a period of aquaculture (Hatcher et al. 1994; Hargrave et al. 2008), but it was necessary to determine whether allochthonous input may have been an alternative explanation.

Three parameters (C/N ratio, δ13C and δ15N) have been successfully used for identifying organic matter source (e.g. Meyers 1994; Cifuentes et al. 1996, Bratton et al. 2003). Their patterns over time are very similar at the two sites (Figure 3.7, 3.8) indicating a shift of organic matter source from a phase dominated by terrestrial input to a phase with marine and terrestrial mixture since the 1950s. The fate and source of organic matter before the 1950s is beyond the scope of this study, which is to identify the effect of pearl farming. In King Sound, the Fitzroy River is an important vector bringing terrestrial organic sources to the river delta and coastal embayment during the wet season, and, in the high intertidal zone, buried mangrove materials also can contribute to the terrestrial organic matter in mud (Semeniuk 1981). The distance and scale over which terrestrial organic matter is transported to the ocean are strongly related to tidal levels in this region, particularly for fine particles (Semeniuk 1981, Semeniuk & Brocx 2011). At site 2 without farming, the trend of grain size in the sediment was coarser over time, indicating a possible process of coastal erosion due to strong tidal action, which can change the ratio between marine and terrestrial inputs. However, this kind of sedimentary feature requires exploration of the long-term variation of oceanographic setting and climate change.

After the 1950s, most C/N and δ13C values at site 1 are within a range of 6.7 to 10 and -22‰ to -19‰, respectively, indicating that the increased organic carbon arises from marine phytoplankton (Meyers & Teranes 2001; Lamb et al. 2006). Furthermore, the ranges of δ15N in the cores were relatively stable, and most values were around 5‰ (Figure 3.7), indicating that the dominant nitrogen source originated from marine nitrate (Owens 1988) with low impact from anthropogenically enriched organic nitrogen (McClelland & Valiela 1998, Savage 2005). This is in accord with the fact that there are almost no pollution sources around Cygnet Bay due to few towns and little anthropogenic activity, except for pearl farming. Therefore, we can confirm that the increased TOC and TN contents at site 1 were mainly a consequence of pearl farming.

Changes of BSi in response to pearl farming

The phytoplankton of the shelf waters in North-West Australia is basically a diatom flora (Hallegraeff & Jeffrey 1984), and diatoms in the sediment of King Sound are one of the important biogenesis contributors to mud-sized skeletons (Semeniuk 2011). Thus, it allows us to use BSi concentration in the sediment as a proxy to reflect the variations of diatom biomass in response to pearl farming. In this study, BSi concentrations at site 1 were much higher than those at site 2 after the 1970s (2.0 to 5.6 times; Figure 3.9); and STARS detected a very significant increasing shift change in 1980s (Figure 3.7) corresponding to the development of long-line culture in late 1980s and increased stock level (Figure 3.9e). These results matched the variations in TOC, TN, sediment texture and the indications from C/N and δ13C values, suggesting that pearl farming promoted the growth of phytoplankton, at least for diatoms. From this study, we cannot determine if the enhancement of diatoms by pearl farming reflected in our samples is a result of predominantly enhanced benthic (elongate or chain forming) diatom deposition or whether water column (mainly centric) diatoms were also enhanced. This would require an assessment of the distribution of fossil diatom frustules throughout the sediment profile in a future study.

Modification of trophic status, for example increased nutrient concentration and phytoplankton biomass, was observed in a coastal embayment with a decadal history of aquaculture (Pusceddu et al. 2009, Sarà et al. 2011). Low density pearl farming can create a mutual benefit between the growth of phytoplankton and pearl oyster, which was examined in Gokasho Bay, Japan (Abo & Toda 2001). The excretion of pearl oysters and other organic wastes can provide nutrients for phytoplankton growth, and reduced water flow can prolong the residence time and create a favorable environment for phytoplankton growth. Additionally, the increased TN in sediment can enhance the nitrogen flux and recycling in the water column. For example, in the Ahe Atoll lagoon (French Polynesia), benthic nitrogen fluxes in the area of pearl oyster farming could sometimes contribute up to 28% of the nitrogen demand for primary production (Gaertner-Mazouni et al. 2012). Meanwhile, increased phytoplankton biomass is good for the growth of pearl oysters.

During 1940−2011 in King Sound, STARS detected a significant increase in annual rainfall after 1997 (Figure

3.9f), with an increase of approximately 40−50 mm 10 yr-1; mean maximum temperatures were variable between 31−33°C, with an increase approximately 0.05−0.1°C 10 yr-1 but no significant change (Figure 3.9g). These might impact on diatom biomass (Beaugrand & Reid 2003, Barbosa et al. 2010). However, BSi concentrations at site 2, displayed a decreasing trend with several small shift changes (Figure 3.8f), and this was not consistent with the response of TOC and TN contents to increased rainfall. The opposite variations of BSi concentrations between the two sites indicated that the impact of pearl farming on diatom growth was much heavier than rainfall and temperature.

4.2.4 Summary

Small environmental disturbances accumulating in a long period of time may cause a regime shift in marine ecosystems, particularly in sensitive oligotrophic waters. Pearl oyster aquaculture, with a 50-year history in Australia, has been regarded as an anthropogenic activity with low environmental risk. To assess the long-term environmental effects of pearl oyster farming, sediment cores taken in Cygnet Bay, Western Australia, were used to reconstruct environmental processes covering an approximately 90-year period. Biogeochemical parameters in sediment cores from inside and outside a pearl farming area displayed contrasting characteristics over time. Total organic carbon, total nitrogen, biogenic silica (BSi), and fine-grained sediment at the farming site displayed significant increases with the expansion of oyster stocking. In contrast, only small variations in response to climatic signals (rainfall and temperature) over time occurred in the cores outside the farm. The variation in C/N, δ13C and δ15N ranges over time suggested that increased organic matter was mainly contributed by autochthonous sources rather than terrestrial input. The sequential t-test for a regime shift detected approximately two to three-fold increases in organic matter, one to five-fold increases in silt proportion and two to five-fold increases in BSi concentrations after pearl oyster farming, in contrast to the control site. The rapid development of modern long-line culture since the late 1980s was presumed to be the dominant driver of environmental changes in sediments. The results provide foresight to the magnitude of environmental change, which can occur over decades resulting from even minimal anthropogenic activity.

4.2.5 Conclusions

In this study, the spatial comparison of multiple proxies (grain size, TOC, TN and BSi, C/N ratio, δ13C and δ15N) in sediment cores revealed decadal environmental effects of pearl farming, including alteration of sediment texture and increases in organic matter and diatom biomass. Although sediment quality in King Sound did not reach a eutrophic level (Wells & Jernakoff 2006, McCallum & Prince 2009, Jelbart et al. 2011), the increasing rates of organic matter in sediment were much faster than those due to natural processes. One possible option to manage the rate of environmental change could be to dispose of the waste from cleaning the culture apparatus on land. This was recommended to enhance ecosystem sustainability of bivalve culture in a recent review (Ocean Studies Board 2010) and this measure is also recommended as way of reducing the potential of invasive species becoming established in bivalve farming areas. However, given the very slow rate of environmental change detected in our study, we would not recommend this in the Kimberley pearl farming situation unless a risk assessment proved there was an existing and unacceptable risk to invasive species becoming established and that the measure would not have unintended consequences on the water column productivity on which the oyster culture depends.

4.3 Climate change impacts on phytoplankton patterns

4.3.1 Introduction

Phytoplankton is a key component in marine ecosystems, and its variations in abundance and species composition are sensitively coupled with short- or long-term environmental changes, and consequently influence the structure and function of ecosystem, e.g., biogeochemical cycles, food web (Field *et al.* 1998). Over the last several decades, phytoplankton regime shifts, e.g., the changes in biomass and species composition and shifts between diatom and non-diatom, have been widely observed in many coastal ecosystems (Cloern *et al.* 2007, McQuatters-Gollop *et al.* 2007, Ajani *et al.* 2014). Most evidence demonstrated that nutrient enrichment is a principal driving factor for the phytoplankton regime shift in coastal waters, and meanwhile, ocean warming could enhance this process, affecting the distribution and productivity of phytoplankton in the ocean (Harley *et al.* 2006, Boyce *et al.* 2010, Liu *et al.* 2013, Irwin *et al.* 2015). For instance, the warmer sea surface temperature (SST) and lower turbidity in the North Sea have increased phytoplankton biomass, although nutrient concentrations have been decreasing since 1980s (McQuatters-Gollop *et al.* 2007).

Due to the limited observational data, it is challenging to distinguish the impact of climatic variability and human disturbances on the phytoplankton in coastal waters. Paleo-ecological method, using the geochemical and biological information preserved in the sediment to reconstruct the short- or long-term environmental change, has supported significant findings in marine research, although a series of biological, chemical and physical factors (e.g., water depth, temperature, salinity, grain size and degradation) during sedimentation and preservation can impact the results (Fischer & Wefer 2012). A few proxies have been widely applied for the reconstruction of sea temperature, terrestrial input and phytoplankton biomass, due to their biosynthetic specificity and resistance to degradation in the sediment. Schouten *et al.* (2002) proposed TEX_{86} (TetraEther indeX of tetraethers consisting of 86 carbon atoms) as a proxy for SST, based on the relative distribution of marine archaea isoprenoid glycerol dialkyl glycerol tetraethers (GDGTs). The selected GDGTs are membrane lipids synthesized by Thaumarchaeota, which contain different number of cyclopentane and cyclohexane rings (Schouten *et al.* 2002). It is thought that the addition of rings into GDGTs raises the melting point of the cell membrane and alters membrane packing (Gliozzi *et al.* 1983; Uda *et al.* 2001), enabling archaea to adjust membrane stability in response to temperature changes (Chong 2010). The long chain *n*-alkanes (C_{27}+C_{29}+C_{31}), specific to higher land plants (Eglinton & Hamilton 1967), can help to interpret the impact of terrestrial input in marine sediments in terms of changes in rainfall, river discharge or dust input (Villanueva *et al.* 1997; Seki *et al.* 2003; Smittenberg *et al.* 2004). A few sterols are verified biomarkers for diatoms and dinoflagellates, e.g. dinosterol (4α, 23, 24-trimethyl5α-cholest-22(E)-en-3β-ol) is produced almost exclusively by dinoflagellates (Volkman *et al.* 1998; Volkman 2003), and brassicasterol (24-methylchol est-5, 22(E)-dien-3-ol) is a commonly used diatom biomarker even although it has been reported in many algal classes (Volkman *et al.* 1998; Volkman 2003; Rampen *et al.* 2010). The analysis of these compounds in the sediment core can help to reconstruct the long-term changes in environmental change and phytoplankton community and discover their correlation.

In this study, Cygnet Bay (site 2 from above), located in the Kimberley, northwest of Australia (Fig. 3.1), is chosen for studying the phytoplankton regime shift in response to the climate change. The Kimberley is a remote coastal region with very limited anthropogenic activity (Halpern *et al.* 2008) but significant climatic variability. Annual averaged SST indicated that the northwest coast of Australia has warmed by ca. 0.6°C in the past 50 year (Lough, 2008) and annual rainfall increased approximately 50% since 1950 (Shi *et al.* 2008; Cai *et al.* 2011; Lin & Li 2012; Feng *et al.* 2013). More recently, Furnas & Carpenter (2016) found that the primary production in northern Australia increased more than 2-fold greater in post-1990 than in the 1960s, but considering the insufficient data, they attributed the difference to the improvements in production measurements. Liu et al. (2016) analyzed the variations of organic matters in the sediment cores, which were collected from the Cygnet Bay, and they suggested that the variability in climatic signals (rainfall and temperature) might explain the increase in marine organic matter over decadal scales. Therefore, it warrants further examination of whether the increase in phytoplankton production in the northwest of Australia since the 1990s was related the climate change. Diatoms and dinoflagellates are the dominant phytoplankton in Kimberley coastal waters (Thompson & Bonham 2011; Armbrecht et al. 2015), and thus, this allows us to use brassicasterol and dinosterol to represent diatom and dinoflagellate biomasses. Four proxies (TEX_{86} index, long chain *n*-alkanes, brassicasterol and dinosterol) were chosen and analyzed, using the dated sediment cores from the Cygnet Bay, to reconstruct the variations of SST, terrestrial influence, and the diatom and dinoflagellate biomasses, respectively. Validity of biomarker reconstruction was discussed in the context of historical observation data, and the shift magnitudes of SST and phytoplankton over time were assessed using a sequential t-test (Rodionov 2004).

4.3.2 Results

TEX_{86}^H temperature record

The BIT index in our samples was low, with a range of 0.13 and 0.29, and particularly low values occurred since the 1990s (Fig. 3.12c), indicating a low influence from terrestrial GDGTs input and verifying the validity of the application of TEX_{86}^H index for SST reconstruction in Cygnet Bay. TEX_{86}^H temperature ranged from 25.2 to 28.3°C and displayed three different periods according to the STARS analysis (Fig. 3.12a): 1) the period of 1940-1978 was relatively stable with an average of 26.4°C; 2) the period of 1978-1986 showed a significant decrease with an average of 25.8°C (RSI: -0.3); 3) the period of 1986-2011 displayed two significantly increasing shifts (RSI: 0.5, 1.5), and the averages were 26.5°C (1986-1997) and 27.5°C (1997-2011), respectively. In a comparison, ERSST revealed a range of 26.9- 29.0°C (Fig. 3.12b), which is slightly higher than TEX_{86}^H temperature. The significant warming shift of ERSST occurred in 1956 (RSI: 0.5). The average temperatures of ERSST during the three periods (1940-1978; 1978-1986; and 1986-2011) were 27.9°C, 28.2°C and 28.4°C, respectively. Thus, the increasing trend of SST during 1986-2011 is consistent between TEX_{86}^H and ERSST.

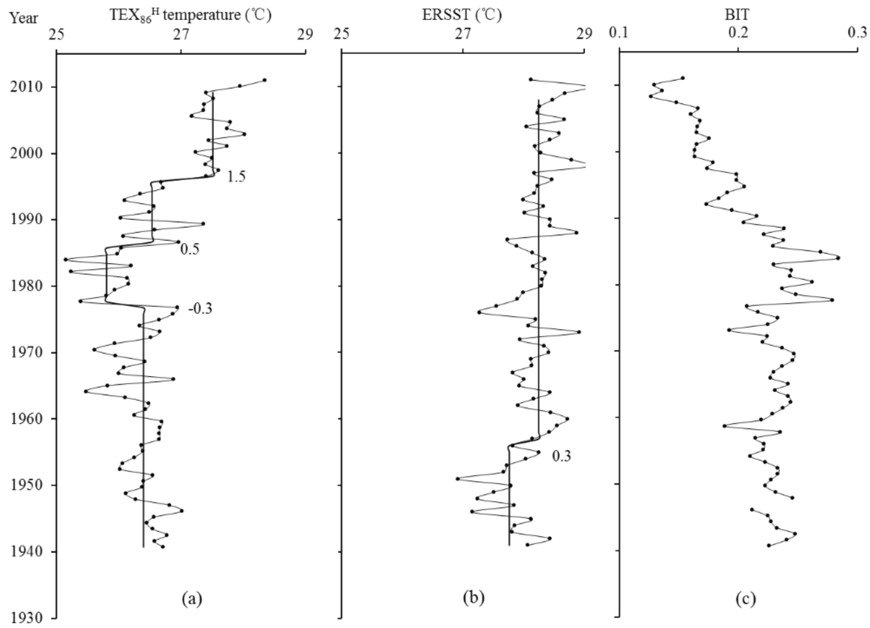

Figure 3.12. Profiles of sea temperature records (a: TEX_{86}^H temperature; b: ERSST from 1940-2011 (data provided by NOAA) (Smith et al. 2008)) and BIT index (c). The lines show shift trends assessed by sequential *t*-test analysis of regime shift and numbers are regime shift index (RSI).

Long chain n-alkanes record

The concentrations of long chain *n*-alkanes in marine sediments can help to interpret the variations of terrestrial input. They ranged from 38.2 to 84.7 ng/g and although variable through the whole time series, showed two periods over time according to the STARS analysis (Fig. 3.13a): 1) the period of 1940-2002 was relatively stable with an average of 51.0 ng/g, although STARS detected a small decreasing shift (RSI <0.1) at 1960; 2) the period of 2002-2011 displayed higher values, with an average of 65.5 ng/g, STARS detected one significant increasing shift (RSI: 0.5) in 2002.

Rainfall and river discharge are important in bringing terrestrial matter into the sea. Fig. 3.13b shows the variation of rainfall in Broome during 1941 to 2011, with a range of 132-1496 mm; and STARS separated them into two periods according to a small increasing shift at 1997 (RSI: 0.1). The average of rainfall during 1997-2011 was 802.2 mm, which is significantly higher than the average of rainfall (553.7 mm) during 1941-1996. In comparison, STARS did not detect the significant shift of annual river discharge of Fitzroy River during 1963 to 2011, but the annual river discharge displayed an increasing trend after 1990s (Fig. 3.13c). The average annual river discharge during 1997-2011 was 3917×10^6 $m^3 yr^{-1}$, which is higher than the average of rainfall (2529×10^6 $m^3 yr^{-1}$) during 1963-1996. Thus, the patterns of long chain *n*-alkanes, rainfall and river discharge are broadly consistent in this region, indicating a significant increase after the late 1990s.

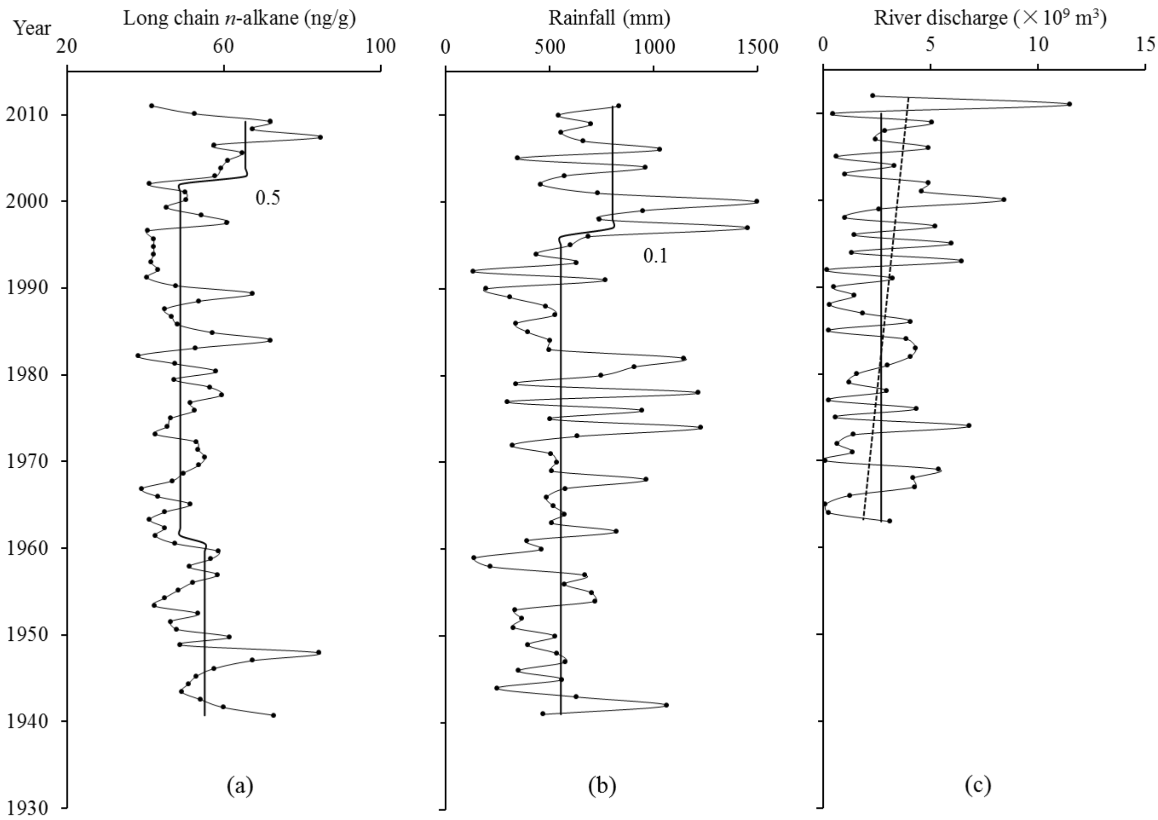

Figure 3.13. Profiles of terrestrial records (a: long chain *n*-alkanes contents; b: annual rainfall from 1941-2011 (data from Australian Bureau of Meteorology); c: Fitzroy River discharge from 1963-2011 (data from Department of Water) and the dashed line shows the linear trend). The solid lines show shift trends assessed by sequential *t*-test analysis of regime shift and numbers are regime shift index (RSI).

Phytoplankton biomarker records

The brassicasterol contents of the sediment representing diatom biomass varied from 14.8 to 244.6 ng/g with two significant periods (Fig. 3.14a): 1) during 1940-1997, brassicasterol contents were lower and stable, with an average of 22.2 ng/g; 2) during 1997-2011, brassicasterol contents increased rapidly, STARS detected three increasing shifts (RSI: 1.0, 1.7 and 1.4), and the average contents during the three shifts were 44.7 ng/g, 103.4 ng/g and 188.8 ng/g, respectively.

The dinosterol contents representing dinoflagellate biomass varied from 38.7 to 207.3 ng/g with two significant periods (Fig. 3.14a): 1) during 1940-1970, dinosterol contents were relative stable, with an average of 52.9 ng/g; 2) during 1970-2011, dinosterol contents increased gradually, including a slow increasing trend during 1970-1997 (RSI: 0.6, 0.5; average contents: 75.6 ng/g and 93.5 ng/g) and a fast increasing trend during 1997-2011 (RSI: 1.6 and 0.7; average contents: 126.6 ng/g and 162.7 ng/g). These results are consistent with the increased temperature and terrestrial input.

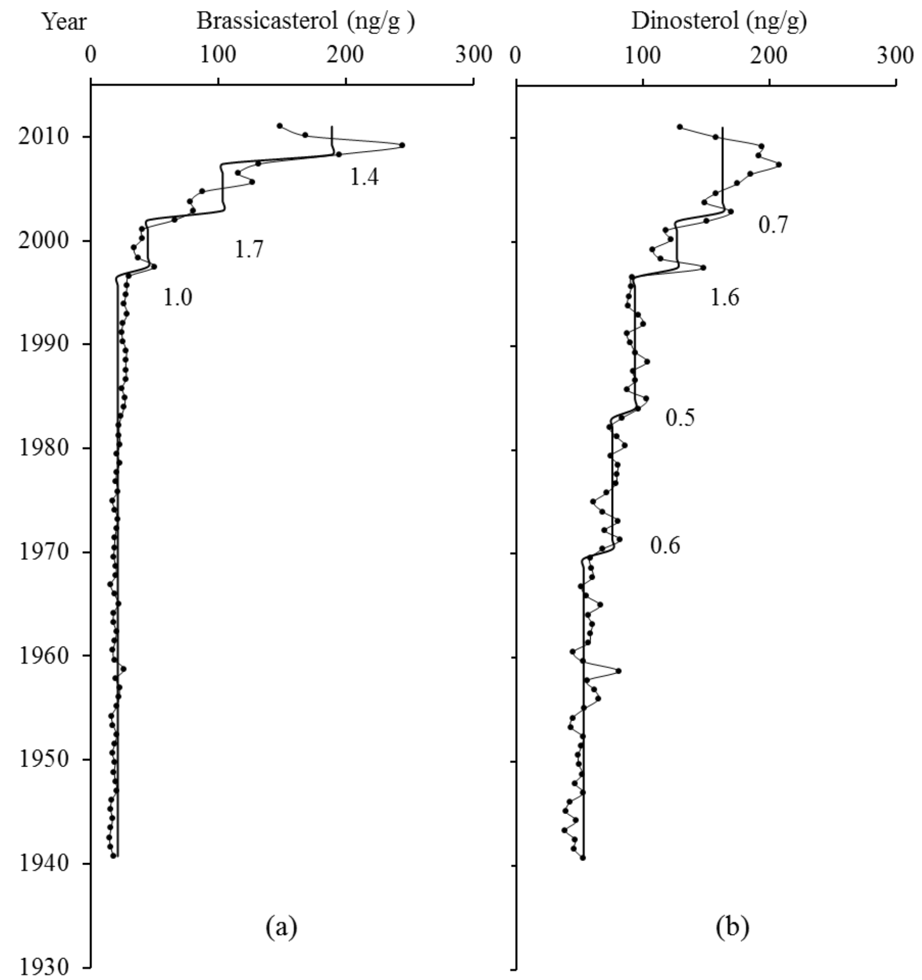

Figure 3.14. Profiles of phytoplankton records (a: brassicasterol contents; b: dinosterol contents). The solid lines show shift trends assessed by sequential *t*-test analysis of regime shift and numbers are regime shift index (RSI).

Principal component analysis (PCA)

PCA was performed on the original data of the four proxies (Fig. 3.15). The first two principal components (PC1 and PC2) were responsible for 82.2% of the total variance. PC1 accounted for 57.7% of the total variance, with high positive loadings on phytoplankton biomarkers (brassicasterol and dinosterol) and TEX_{86}^{H} temperature. In addition, TEX_{86}^{H} temperature showed significant correlations with phytoplankton biomarkers (coefficient of 0.56 for brassicasterol and 0.55 for dinosterol, $p<0.01$), indicating importance of SST on the phytoplankton biomass increase. PC2 accounted for 25.1% of the total variance, with high positive loadings of long chain *n*-alkanes contents. In comparison, long chain *n*-alkanes displayed poor correlations with phytoplankton biomarkers (brassicasterol: $r=0.02$, $p>0.05$; dinosterol: $r=-0.09$, $p>0.05$; Table 3.2).

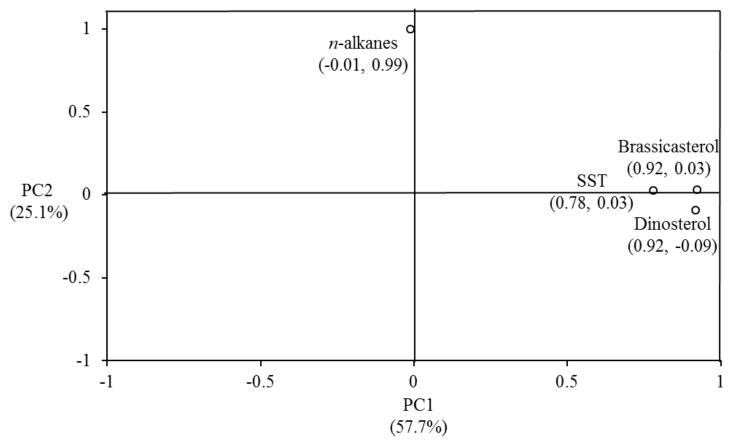

Figure 3.15. Plots of proxy loadings on PC1 and PC2 based on principal component analysis. Numbers in parenthesis correspond to the values of loadings on PC1 and PC2.

Table 3.2. Cross-correlation coefficients for four biomarker proxies.

	Brassicasterol	Dinosterol	*n*-alkanes	SST
Brassicasterol	1			
Dinosterol	0.84*	1		
n-alkanes	0.02	–0.09	1	
SST	0.56*	0.55*	–0.01	1

*: Correlation is significant at $p < 0.01$.

4.3.3 Discussion

Validity of reconstructed proxies

TEX_{86}^H index is suitable for SST reconstruction in tropical or subtropical regions (>15°C) (Kim et al. 2012, Chen et al. 2014, Hertzberg et al. 2016). It has been applied in some Australian regions (e.g. south-eastern Australia, west Sumatra) and displayed a good linear correlation with the instrumental annual SST (Smith et al. 2013, Chen et al. 2014). The warming trend of TEX_{86}^H temperature and ERSST in the Cygnet Bay is similar, but there are some discrepancies in the warming rate (Fig. 3.12). This phenomenon has been reported in previous studies, e.g., northwest Africa (McGregor et al. 2007), northeast Hong Kong (Kong et al. 2015), shelf of Western Australia (Zinke et al. 2015). A few factors could lead to the difference between TEX_{86}^H temperature and ERSST. One is the errors from the measurement of ERSST: 1) sporadic SST measurements over the historical period can result in large uncertainties in ERSST, and thus the accuracy of ERSST is based on a compilation of observational data (Smith *et al.* 2008; Woodruff *et al.* 2011; Kennedy 2014). Observational data in the Kimberley are fewer than the other regions, due to its remote geographic location; 2) the 2°×2° resolution of ERSST could underestimate the temperature variability in shallow waters, because the rapid warming rate was more frequently observed in the nearshore than offshore (Belkin 2009; Lima & Wethey 2012). The other possible errors are from TEX_{86}^H index: 1) The TEX_{86}^H temperature using the global calibration has a large calibration error (2.5°C), which reduce the accuracy of TEX_{86}^H temperature; 2) some studies have shown that the TEX_{86}^H temperature may be skewed to specific season due to seasonality in growth or export of Thaumarchaeota (Leider et al. 2010, Jia et al. 2012, Lü et al. 2014). In general, TEX_{86}^H temperature captured the warming trend in the northwest of Australia, e.g., both observed air and sea temperatures revealed significant warming since the 1950s and accelerated warming rates since the 1980s (Lough 2008, Lough & Hobday 2011); an increase in episodes of anomalously warm ocean conditions along the western Australian coastline since the late 1990s which were strongly influenced by the strengthening of the Indonesian Throughflow in response to increases in Pacific trade winds (Feng et al. 2011, 2015); coral temperature records in the shelf of northwestern Australia also indicated long-term warming with highest temperature anomalies during 1980s-2010 (Zinke et al. 2015). Thus, these similar warming patterns suggested the applicability of TEX_{86}^{H} index in our study area.

Long chain *n*-alkanes have been widely used to evaluate the terrestrial influence to the ocean (Zhao *et al.* 2006; Eglinton & Eglinton 2008). In this study, the increasing trend of long chain *n*-alkanes during 2002-2011 matches up with the increased rainfall and river discharge after about 1997, although there is a small time-lag (Fig. 3.13). Meanwhile, rapid increases in brassicasterol and dinosterol after about 1997 are in response to the increased TEX_{86}^{H} temperature and long chain *n*-alkanes in time scale (Fig. 3.14). Liu et al. (2016) discovered a significant increasing trend of total carbon and nitrogen contents in the sediment cores in the Cygnet Bay after 2000; and the ranges of carbon and nitrogen ratio and $\delta^{13}C$ indicated that the increased organic matter are mainly from marine sources. Furnas & Carpenter (2016) found the primary production increase ca. 2-fold in 1990-2013 than in 1960-1962 in the Kimberley Shelf. Thus, there is credible evidence for phytoplankton biomass increase related to climate change in the Kimberley region.

Phytoplankton biomass in response to warming SST and terrestrial influence

Temperature, salinity, irradiance, and macronutrient concentrations are regarded as the key and fundamental environmental factors to determine the phytoplankton niches. Recently, statistical analysis of time series data in the Baltic Sea, North Atlantic Ocean and Caribbean Sea showed that the importance of temperature, salinity and irradiance for the niches of diatoms and dinoflagellates is even higher than macronutrient concentrations (Gasiūnaitė et al., 2005; Irwin et al., 2012; Mutshinda et al., 2013). In this study, a significant concurrent shift occurred around 1997. Compared with the average values of four proxies before 1997, the average TEX_{86}^{H} temperature during 1997-2011 increased approximately 1°C, rainfall increased 248.2 mm, brassicasterol and dinosterol sediment content increased 8.5 and 1.7 times respectively. The PCA indicated that warming temperature has more significant impact on the increases in diatom and dinoflagellate biomass than terrestrial input. The driving mechanism of warming temperature on phytoplankton biomass is complicated, e.g., most results from open sea showed that ocean warming can enhance the vertical stratification, which could reduce the nutrient supply to the mixed-layer and consequently decline the phytoplankton biomass in surface water (Richardson & Schoeman, 2004, Behrenfeld et al. 2006, Doney, 2006); however, some cases indicated that warming temperature can accelerate nutrient recycling by bacteria, and consequently result in phytoplankton increase (Taucher & Oschlies 2011). In Cygnet Bay, the seawater is well mixed due to the shallow depth (9.8 m) and strong tidal action all the year round. Thus, the increase of phytoplankton biomass was more possibly attributed to positive physiological action and fast nutrient turnover. Some studies in northwestern Australia emphasized a mechanism of ocean-coast interaction that could influence the coastal phytoplankton biomass, e.g., in the North West Cape, the increase of phytoplankton biomass in coastal waters could be caused by increased nutrients transport from the deep sea through enhanced upwelling (Furnas 2007); and in Darwin Harbour, Burford et al. (2008) found that the oceanic inputs of nutrient to the estuary were a primary contributor according to calculated nutrient budget. However, due to a lack of observational data, the mechanism of the ocean-coast interaction in the Kimberley needs further exploration.

The sediment core analysis reveals not only the increased phytoplankton biomass since 1997 but also the different shifting pattern between diatoms and dinoflagellates. In comparison, dinoflagellates showed an earlier but slower increasing trend than diatoms (Fig. 3.14). Thompson & Bonham (2011) analyzed the phytoplankton communities collected during a 2010 research voyage in the Kimberley region, and found that the pigment proportion of diatoms in the shallow water (<50 m) was much higher than dinoflagellates. This supported our result in the upper core. In general, diatoms are favored in the niches with higher macronutrients, higher turbulence but lower salinity and temperature than the dinoflagellates, and thus, diatoms often dominate in the coastal and estuarine waters (Margalef 1978, Egge & Aksnes 1992, Hinder et al. 2012, Ajani et al. 2014, Xie et al. 2015). Silicate is a critical, limiting macronutrient for diatom growth but not for dinoflagellates, and the source of silicate in coastal waters is mainly by riverine input. Thus, increased riverine input and rainfall often enhance the supply of silicate and decrease the salinity which can provide more suitable conditions for diatom growth. In this study, diatom and dinoflagellate biomarkers did not display any correlation with long chain n-alkane (proxy for terrestrial inputs), however the increased river discharge and rainfall after 1997 provide a mechanism by which conditions after that time favored diatoms over dinoflagellates.

4.3.4 Summary

Ocean warming can modify the biomass and geographic distribution of phytoplankton on decadal scales. Significant increases in sea surface temperature (SST) and rainfall in the northwest of Australia over recent decades is attributed to climate change. Here, we used four biomarker proxies (TEX_{86} index, long chain *n*-alkanes, brassicasterol and dinosterol) to reconstruct approximately 60-year variations of SST, terrestrial input, and diatom and dinoflagellate biomass in the coastal waters of the remote Kimberley region. The results showed that the most significant increases in SST and terrestrial input occurred since about 1997, accompanied by an abrupt increase in diatom and dinoflagellate biomasses. Compared with the data corresponding to the previous decades, the average TEX_{86}^H temperature during 1997-2011 increased approximately 1°C, rainfall increased 248.2 mm, brassicasterol and dinosterol contents increased 8.5 and 1.7 times. Principal component analysis indicated that the warming SST played a more important role on the phytoplankton increase than increased rainfall and river discharge.

4.3.5 Conclusions

The paleo-ecological evidence from Cygnet Bay demonstrated that SST and terrestrial input have significantly increased since 1997 in the Kimberley region, and the biomasses of diatoms and dinoflagellates corresponded to these changes with an increasing trend. In comparison, warming SST played a more important role for the phytoplankton increase than increased rainfall and river discharge. The graphical abstract in Figure 3.16 summarises the results.

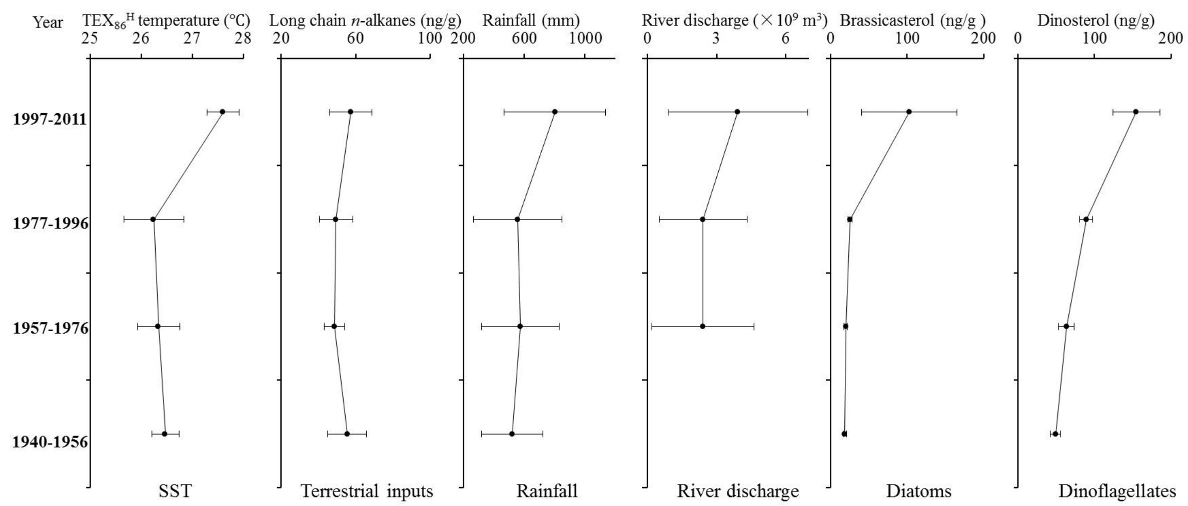

Figure 3.16. Graphical abstract summarising the results of the Cygnet Bay reference site cores.

4.4 Addenda for Cygnet Bay Pearl Farm site

The following analyses were carried out late in the project and are included here for completeness.

They add three pieces of information to the analysis given in sections 3.2 and 3.3. Firstly, the patterns in biomarkers for diatoms and dinoflagellates (Figure 3.17) supports the analysis showing increases in phytoplankton biomass associated with both pearl farming and climate change. Secondly that the contribution of terrestrial material as indicated by long chain alkanes (Figure 3.18) and the pattern of temperature increase (Figure 3.19) are similar between both the farm site (CB1) and the reference site (CB2). Thirdly the comparison of phytoplankton pigments shown in Figure 3.20 separates the influence of the pearl farm since about 1980 and climate change since about 1999. For both parameters, the increases between the late 1980s and the late 1990s at the farm site (only) are interpreted to be due to the effects of pearl farming while the steeper increase in both biomarker pigments at both sites from the late 1990s are interpreted as being associated with the increase in anomalous warming events in the region.

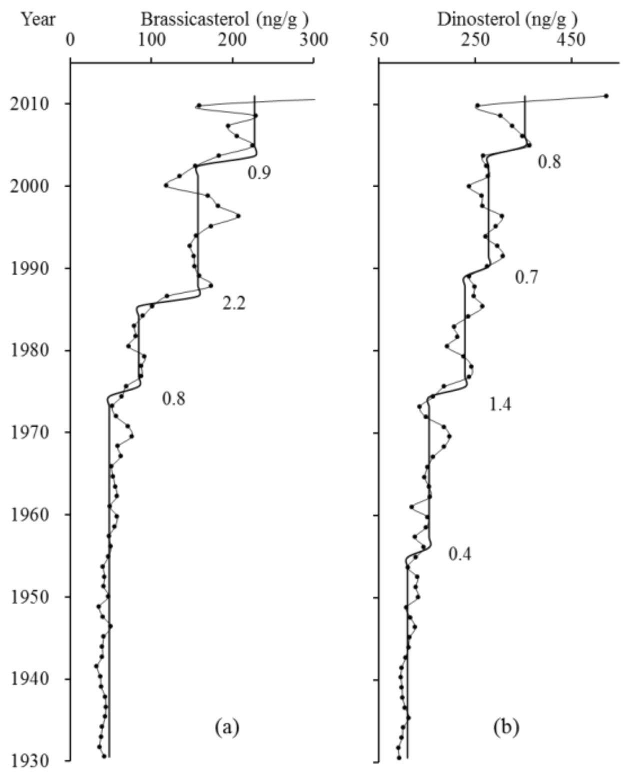

Figure 3.17. Profiles of brassicasterol (a) and dinosterol (b) contents at CB1 (Cygnet Bay pearl farm site). The solid lines show shift trends assessed by sequential t-test analysis of regime shift and numbers are regime shift index (RSI).

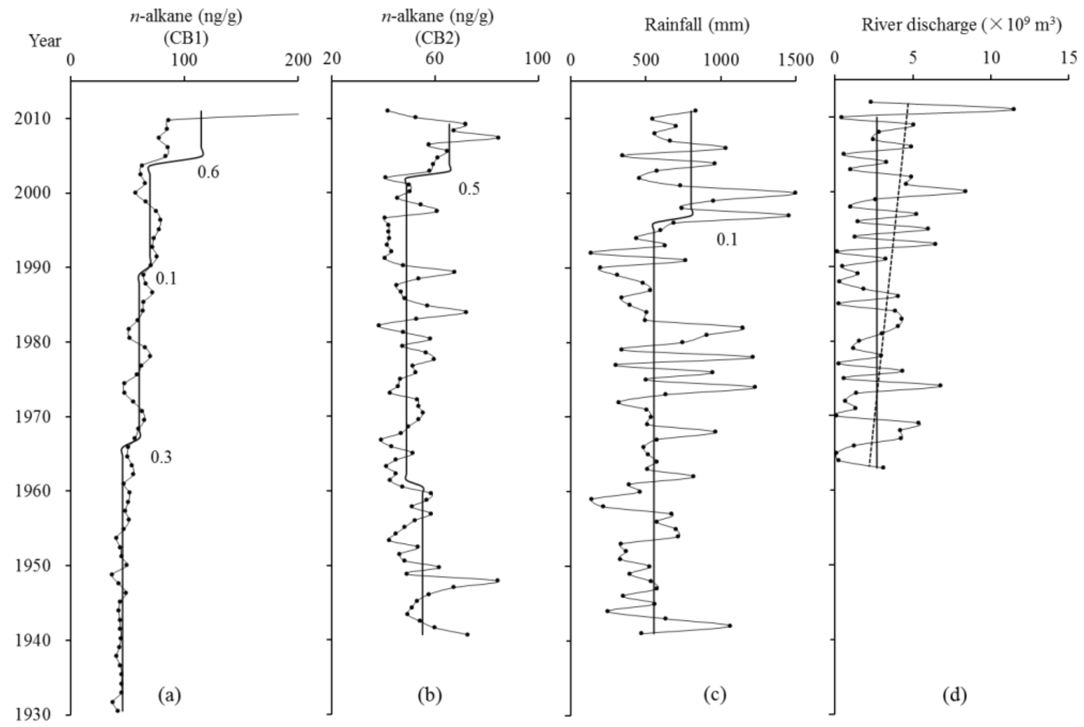

Figure 3.18. Profiles of terrestrial records: long chain n-alkanes contents at CB1 (a) and at CB2 (b); annual rainfall at Broome (c, data from Bureau of Meteorology); Fitzroy River discharge (d, data from Department of Water). The solid lines show shift trends assessed by sequential t-test analysis of regime shift and numbers are regime shift index (RSI).

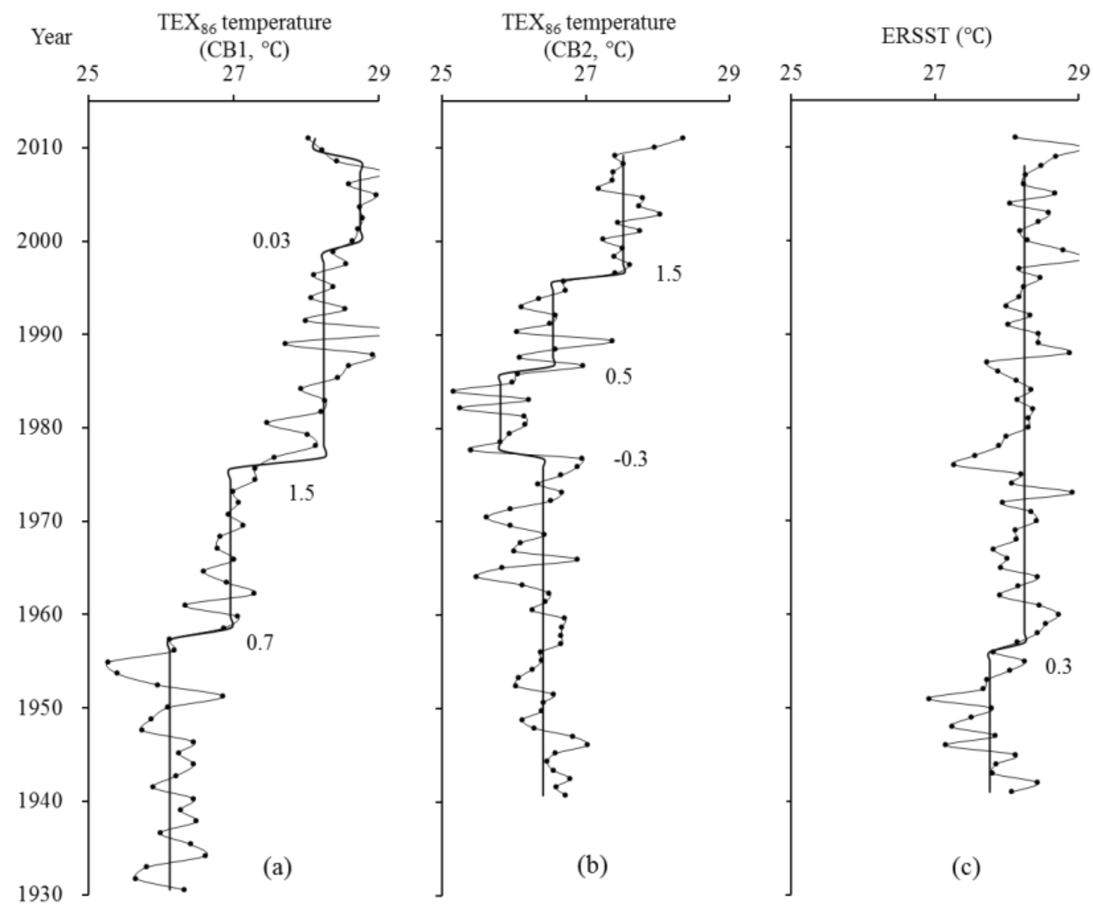

Figure 3.19. Profiles of sea temperature records (a: TEX86H temperature at CB1; b: TEX86H temperature at CB2; c: ERSST from 1940-2011). The solid lines show shift trends assessed by sequential t-test analysis of regime shift and numbers are regime shift index (RSI).

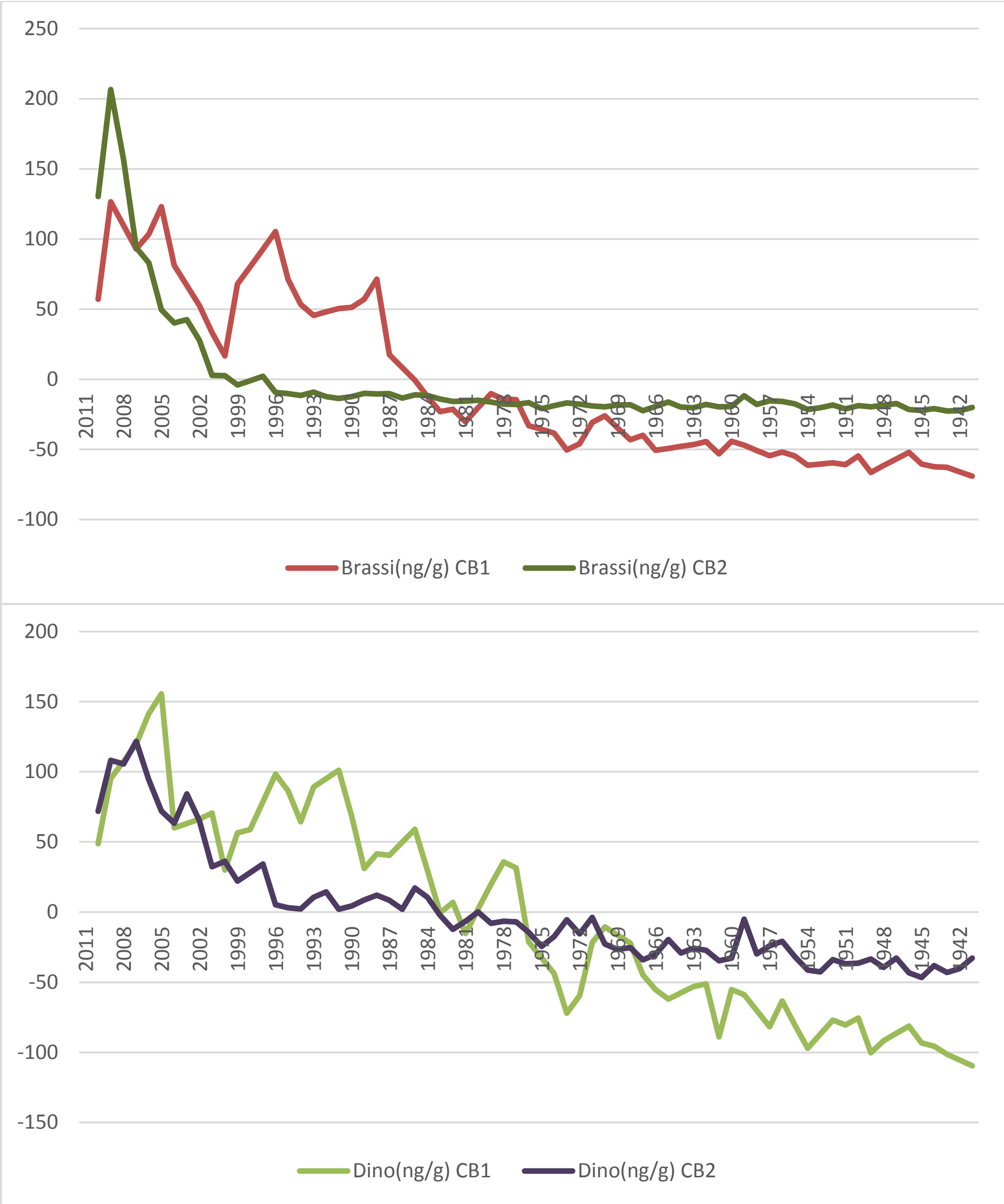

Figure 3.20. Plot of brassicasterol (upper panel) and dinosterol (lower panel) at both the farm site (CB1) and the reference site (CB2). Units are in ng/g and each line is the measured value in the year given minus the long-term average of the aged section of the whole core. The figure nicely separates the influence of the pearl farm since about 1980 and climate change since about 1999. For both parameters, the increases between the late 1980s and the late 1990s at the farm site are interpreted to be due to the effects of pearl farming while the steeper increase at both sites from the late 1990s are associated with the increase in anomalous warming events in the region. The high values in both parameters at the farm site in the late 1980s and 1990s also indicate the very recent (post-2000) high values at the reference site cannot be solely attributed to degradation of the biomarkers in older sediments.

5 King George River, northern-eastern Kimberley

5.1 Introduction, site description and sample sites

The north-eastern part of the Kimberley region of north-western Australia is one of the world's remaining wilderness areas. Sparsely populated by indigenous communities and small tourist operations, access to the region is largely limited to boat and small aircraft. There had been no previous marine scientific studies of the area and the need to form an understanding of the biodiversity, habitat distribution and ecosystem function of this area lead to a study by Keesing (2014) which focused on biodiversity assessment and biophysical characterization.

Despite the growing popularity of the King George River Falls as a tourist attraction, this section of coastline remains largely unsurveyed except for a cursory visit by the Western Australian Museum to the upper reaches of the King George River in 1991 (Morgan 1992). The King George River region includes a full range of typical habitats; river, sandy beaches, rocky shores, mangroves and an island 8km offshore (Lesueur Islet 1.5 km long x 0.6 km wide) which is surrounded by coral reef. The importance of the area as a tourist destination, its proximity to aquaculture and hydrocarbon lease areas, the variety of marine and coastal habitats and the previously unsurveyed nature of the area make it interesting both scientifically as well as from a conservation management point of view.

In addition, the King George River area was chosen as part of this study as it is significantly influenced by the seasonal wet season (December to March) dry season rainfall cycle. The large freshwater output into Koolama Bay from the King George River offered the opportunity to examine the sediment profile influence by the river and for comparison with an un-named adjacent embayment without direct riverine input.

The following description of marine and estuarine habitats in the area is summarized from Keesing (2014). Benthic habitats off the offshore area of King George River and Lesueur Island were of two basic types; soft bottom muddy habitat or filter feeder communities on hard or broken substrates. Soft bottom habitats were the most abundant feature in the region. Inshore these were primarily mud habitats. Within Koolama Bay the subtidal benthos was muddy and becoming sandier inshore where sandy beach habitats and rocky shore habitats occur. Both within the bay proper and in the small bay just to the west of Koolama Bay, small creeks run in an along shore direction behind the beach. During the dry season at least, these are largely lagoon features. The mouth of the King George River transitions from the sandy beaches of Koolama Bay to riverine mangrove habitats. These too are surprisingly sandy rather than the heavy muddy mangrove habitats found elsewhere in the Kimberley. Just inside the mouth of the river a large mangrove creek leads off to the east. Small beds of the seagrass *Halophila decipiens* occur in this area. As the river bends some 4.5 km up stream there are extensive stands of mangroves. Here the river is at its widest, about 800m. The mangroves along the river are principally *Avicenia* and *Rhizophora*. The river is walled with towering red-orange sandstone cliffs on each side and along the length of the river there is rocky habitat of either sheer cliff or rocks that have accumulated at the base of the cliff. The King George River branches to the east, at about 4.5 km from the mouth, for a further 2km where there are further mangrove stands and a waterfall. The main section of the river turns west and then south, again mangrove stands have developed at each bend in the river. The last significant mangrove stand occurs at about 10 km from the mouth. Just past this point the river is at its narrowest below falls section (about 120 m wide) and from there it is about 2.7 km to the majestic twin falls. The water depth at the base of the falls is about 80m

Core sampling was undertaken in June 2013. Sediment cores (ca. 1.2 m long) were taken from 3 sites in the King George River region (Figures 4.1 and 4.2). Two in Koolama Bay (sites KGR1 in 5m depth and KGR2 in 11 m depth) within direct influence of the outflow of the King George River and another from a reference site with similar aspect (site KGR 3 in 11 m) in an unnamed bay, two bays to the west of Koolama Bay where there is minimal riverine input and outside King George River catchment (Figure 4.3). In general, we would expect the historical sediment record in Koolama Bay to reflect catchment wide inputs to the marine environment and for the reference site (KGR 3) to reflect a less variable biogeochemistry dominated by marine influences. Given the potential for riverine input to scour the seabed and disrupt sediment profiles we did not proceed with any analysis on cores from site KGR1.

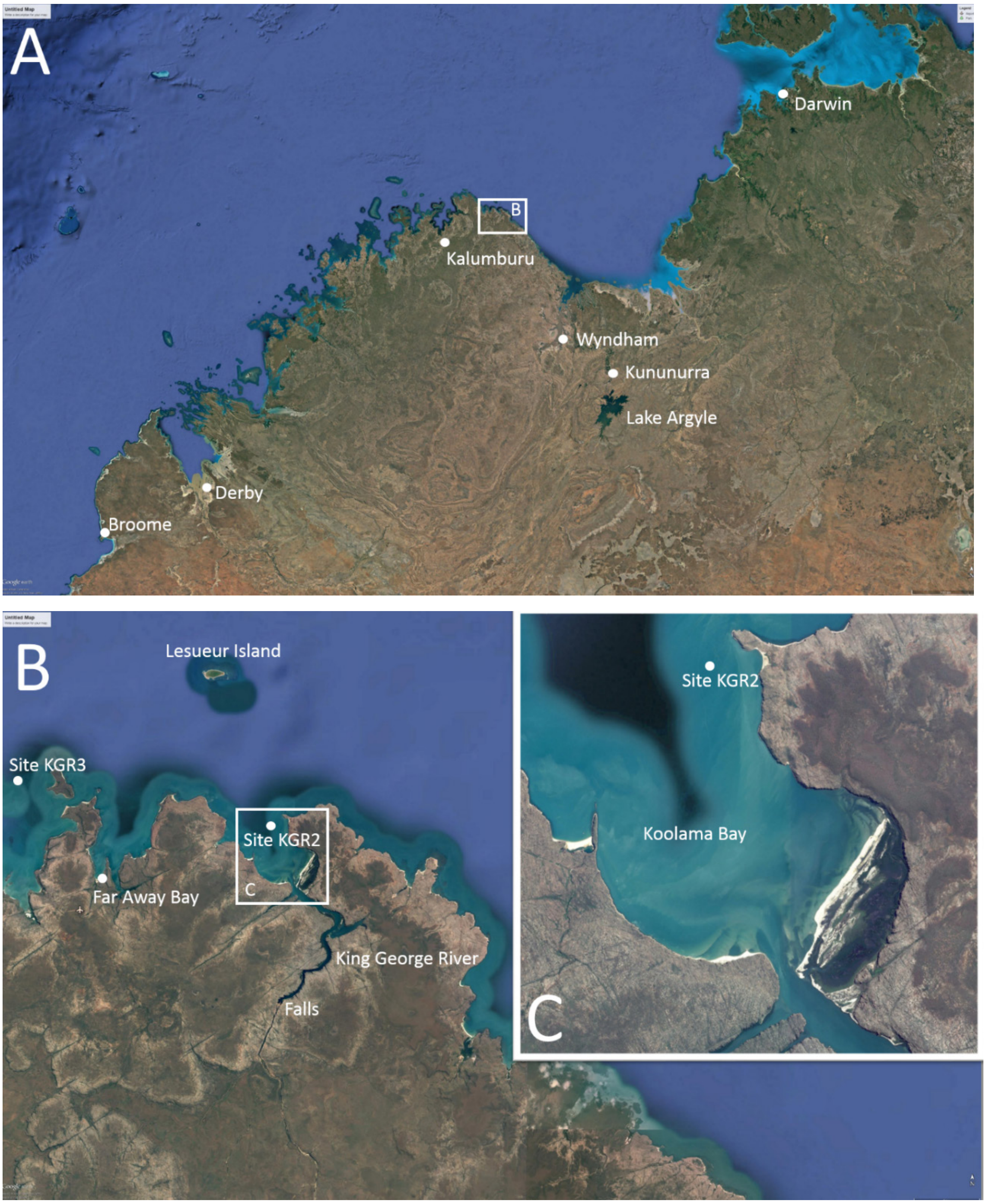

Figure 4.1. Google Earth imagery showing location of King George River sampling sites and mangrove habitats where King George River opens in to Koolama Bay.

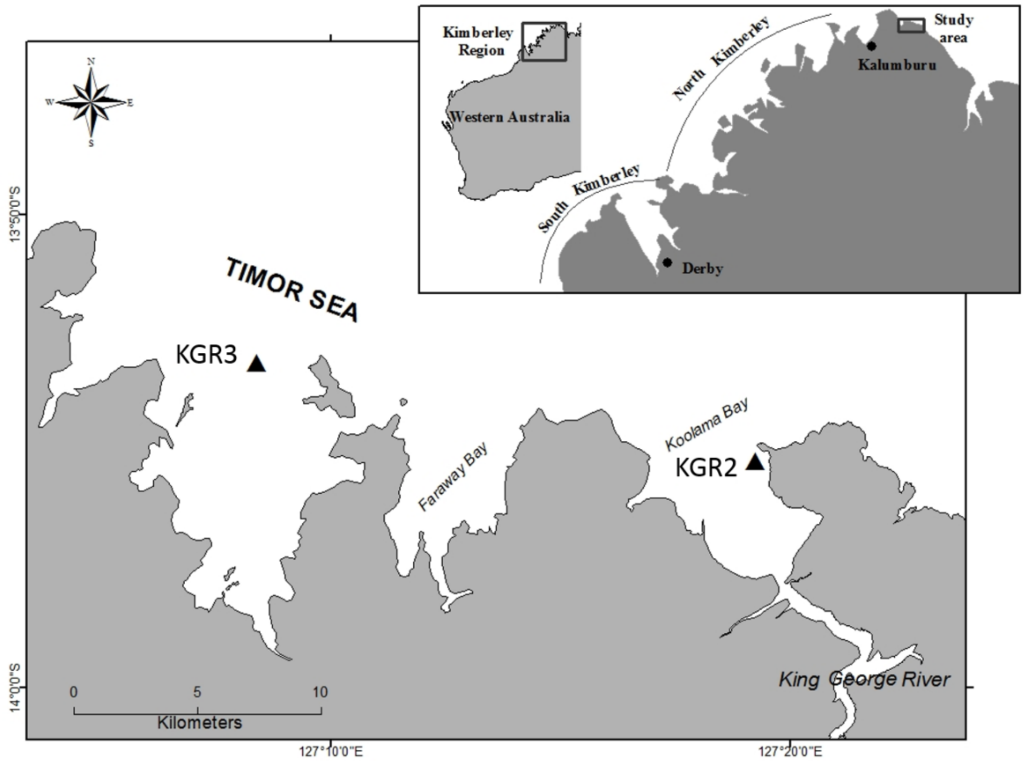

Figure 4.2. Map showing sampling sites (▲) in Koolama Bay in King George River (site KGR2) and an unnamed Bay to the west (site KGR3).

Figure 4.3. King George River catchment.

5.2 Impact of river flows and climate change on coastal water quality and sediment

5.2.1 Core chronology

The profiles of $^{210}Pb_{ex}$ concentrations and sedimentation rates in KGR2 are shown in Figure 4.4a and b. An age-model has been obtained using the CRS model with a time span of 1880–2013 over the top 20 cm. According to this model, the sedimentation rate during the first half of the 20th century was about 0.03-0.04 g cm^{-2} yr^{-1}, increasing by about a factor of 2 during the following decades. The ^{210}Pb profile in the upper part of the sediment core seems to indicate a certain degree of mixing.

The profiles of $^{210}Pb_{ex}$ concentrations in KGR3 are shown in Figure 4.4c. The profiles of $^{210}Pb_{ex}$ concentration provides evidence of mixing of the upper 14 cm of the sediment core, which precludes the determination of an age-model using the CRS model. The CF:CS model can be applied below the mixed layer to obtain an upper limit of the sedimentation rate for the 14-30 cm section: 0.14 ± 0.02 g cm^{-2} yr^{-1}. Given the relatively large part of the core that is mixed, this sedimentation rate could be overestimated by about 25%. This sedimentation rate can be extrapolated to the upper 14 cm of the core if desired, although without certainty. In doing so, the upper 14 cm would correspond to the sediments accumulated since the early late 1970s.

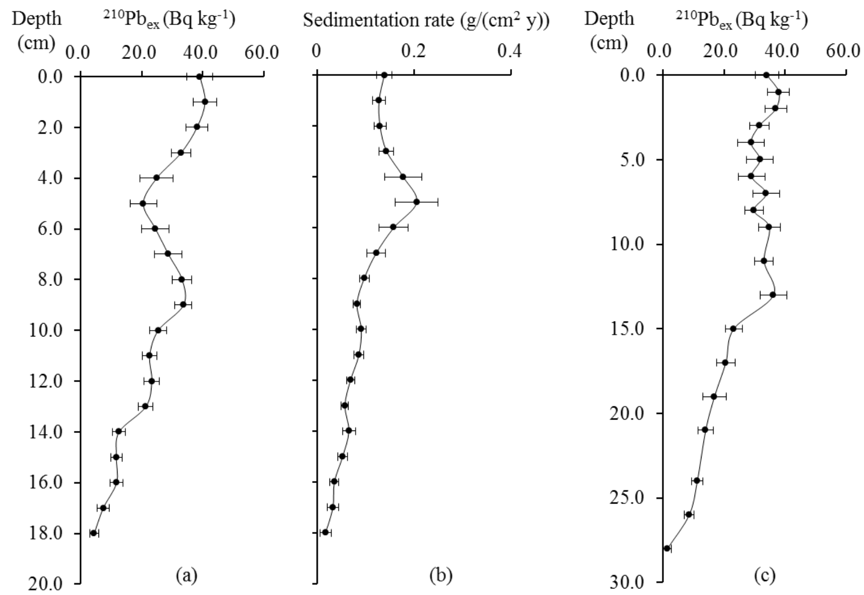

Figure 4.4. Profiles of $^{210}Pb_{ex}$ and sedimentation rates at KGR2 (a, b), and $^{210}Pb_{ex}$ at KGR3 (c) (error bars denote standard deviation).

5.2.2 Sediment grain size

The median grain size (d_{50}) in the sediment cores vary at a range of 6.6–19.9 µm at KGR2 (Figure 4.5a) and 7.8 to 21.9 μm at KGR3 (Figure 4.5c), respectively, indicating that the sediment type was sandy silt. In a spatial comparison, d_{50} between the two sites displayed different trends over time (Figure 4.5a, c). At KGR2, sediments became coarser with decreasing clay, particularly in the upper section of the core (Figure 4.5b), whereas at KGR3, the variation in d_{50} showed slight changes with the sediments consist of homogeneous sand (mean of 12%), silt (mean of 63%) and clay (mean of 25%) (Figure 4.5d).

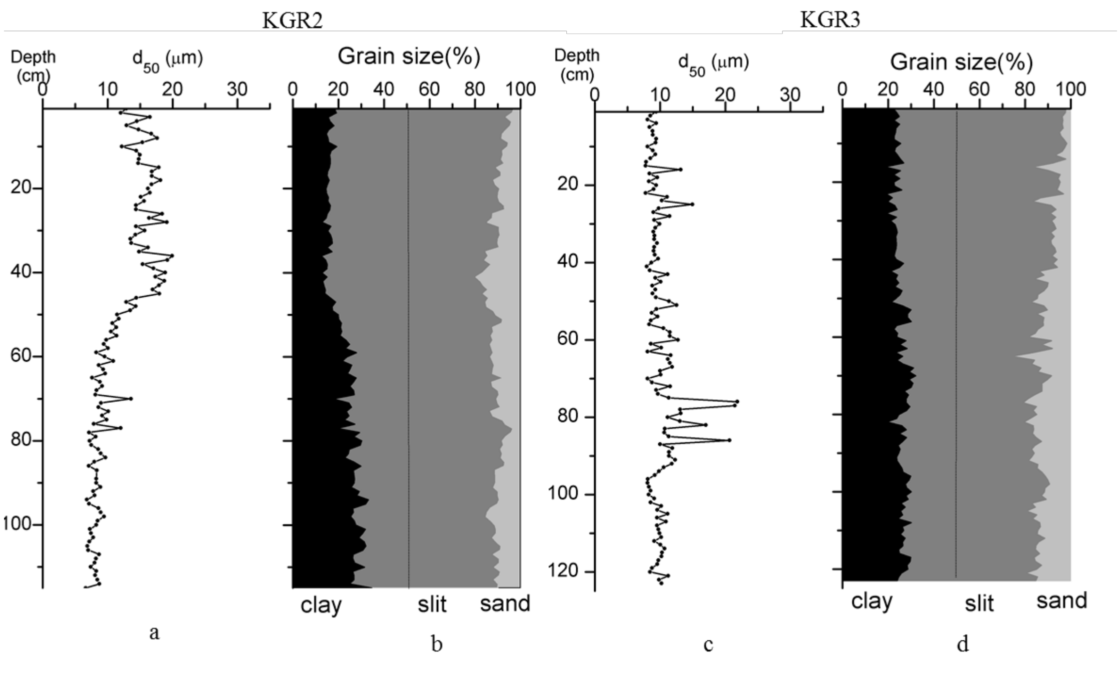

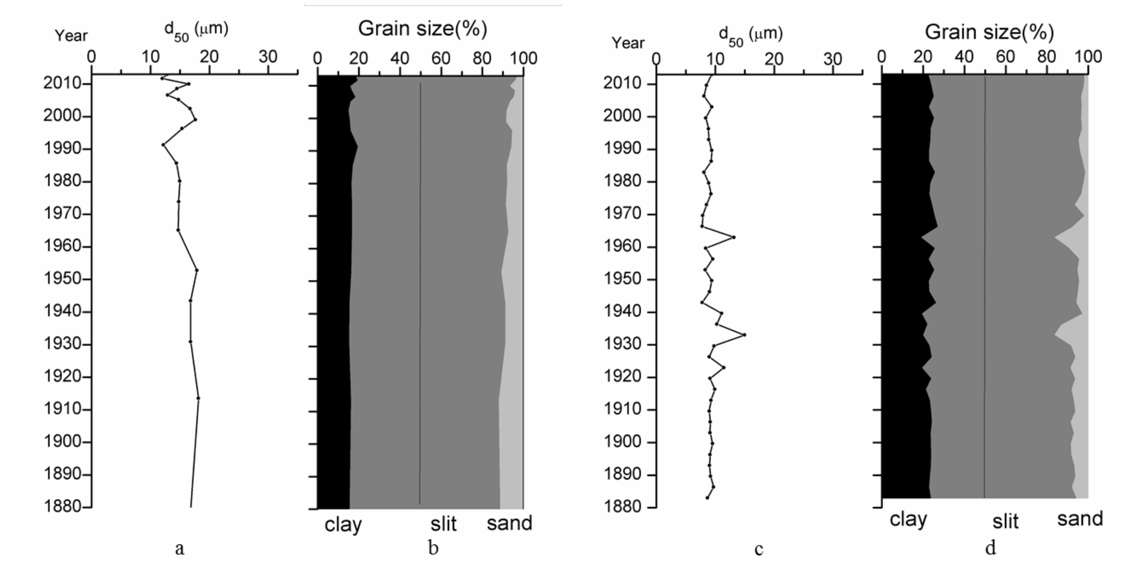

Figure 4.5. Profiles of grain sizes at KGR2 (a, b) and KGR3 (c, d), showing median values (d_{50}) and the proportions of clay, silt and sand. Upper panel shows the whole core and the lower panel just the aged section.

5.2.3 Geochemical parameters

The chronological variations of TOC, TN, C/N, $\delta^{13}C$, $\delta^{15}N$, and long chain *n*-alkanes (C_{27}+C_{29}+C_{31}) at KGR2 are shown in Figure 4.6. TOC and TN contents (Figures 4.6a, b) vary from 0.49% to 0.91% and from 0.03% to 0.10%, respectively. Both TOC and TN display an increasing trend over time. $\delta^{13}C$ values and C/N ratios range from -29.2 to -21.2‰ and 9.6 to 24.1 at KGR2, respectively (Figures 4.6c, d). The variation trend of C/N ratio is synchronous to the $\delta^{13}C$ profile, with positive $\delta^{13}C$ values corresponds well to the low C/N ratio. The $\delta^{13}C$ and C/N ratio trends indicate a significant increase in proportion of marine organic carbon, which shift from a phase with terrestrial dominance to a phase with a marine and terrestrial mixture in the upper 40 cm. The $\delta^{15}N$ values range from 3.6 to 5.7‰, with a slight decreasing (Figure 4.6e). It is clear that the $\delta^{15}N$ values displayed relatively small variations and fell into a range of typical marine nitrate (3 to 5‰), indicating low anthropogenic impact. The long chain *n*-alkanes (C_{27}+C_{29}+C_{31}) range from 76.2 to 178.5 ng/g TOC and are relatively stable with small oscillations, indicating stable terrestrial material input (Figure 4.6f).

The chronological variations of TOC, TN, C/N, $\delta^{13}C$, $\delta^{15}N$, and long chain *n*-alkanes (C_{27}+C_{29}+C_{31}) at KGR3 are shown in Figure 4.7. TOC range from 0.45 to 1.10%, with an average of 0.68% (Figure 4.7a), and TN vary between 0.04 and 0.12%, with an average of 0.06% (Figure 4.7b). $\delta^{13}C$ values and C/N ratios range from -28.2 to -21.9‰ and 9.1 to 25.8 at KGR3, respectively (Figure 4.7c, d). Most $\delta^{15}N$ values were within 3‰ to 5‰. The long chain *n*-alkanes (C_{27}+C_{29}+C_{31}) range from 66.3 to 311.7 ng/g TOC (Figure 4.7f). Both temporal trends and absolute values of these geochemical parameters are similar to KGR2, indicating that the two sites experience similar environmental conditions.

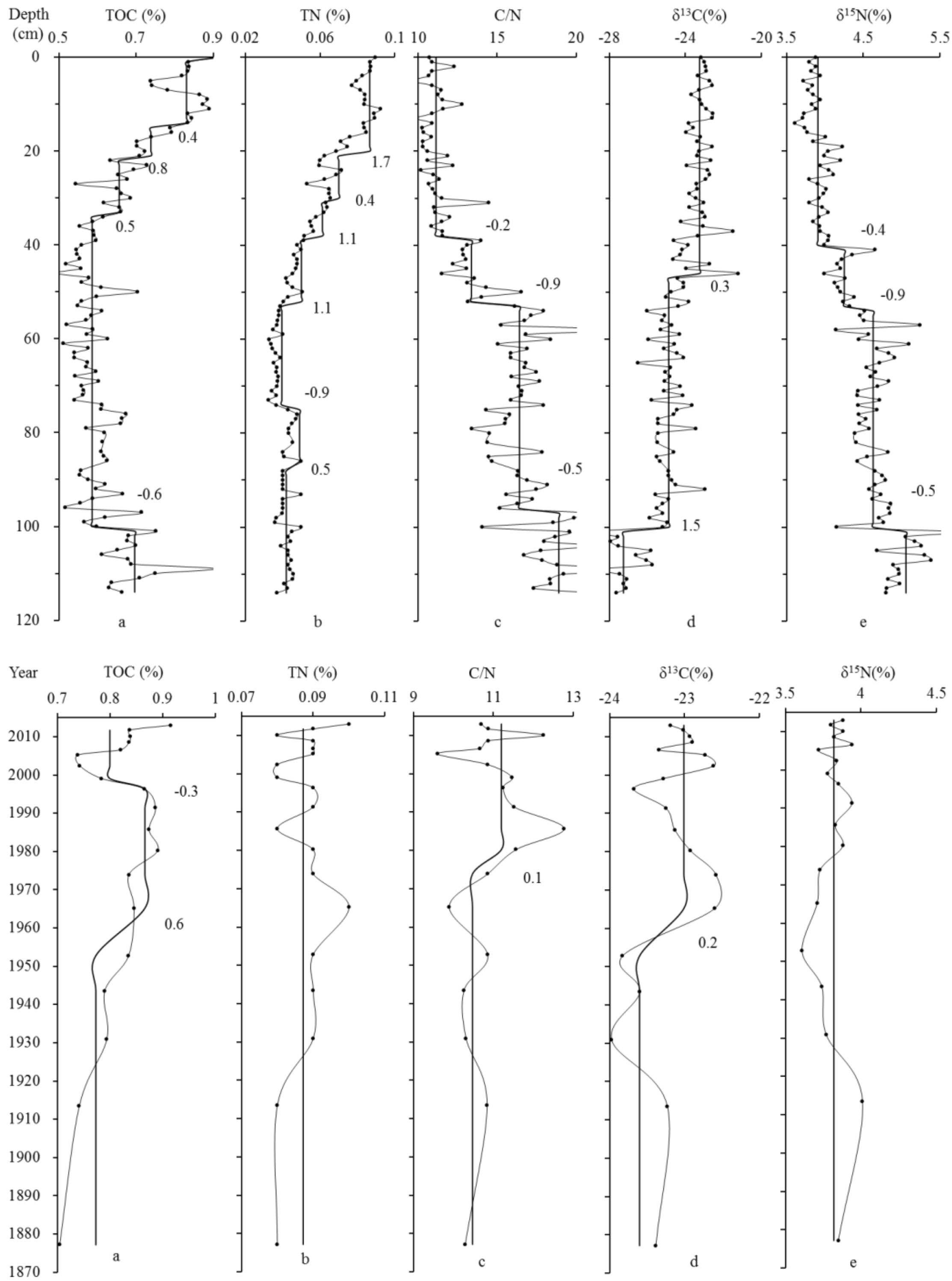

Figure 4.6. Profiles of geochemical parameters at KGR2 (a: TOC; b: TN; c: C/N; d: δ13C; e: δ15N). Upper panel is the data from the full cores and the lower panel is for the aged section only. The solid lines show shift trends assessed by sequential t-test analysis of regime shift and numbers are regime shift index (RSI). The cut-off length (l) was set to 10 for upper panel and 5 for lower panel.

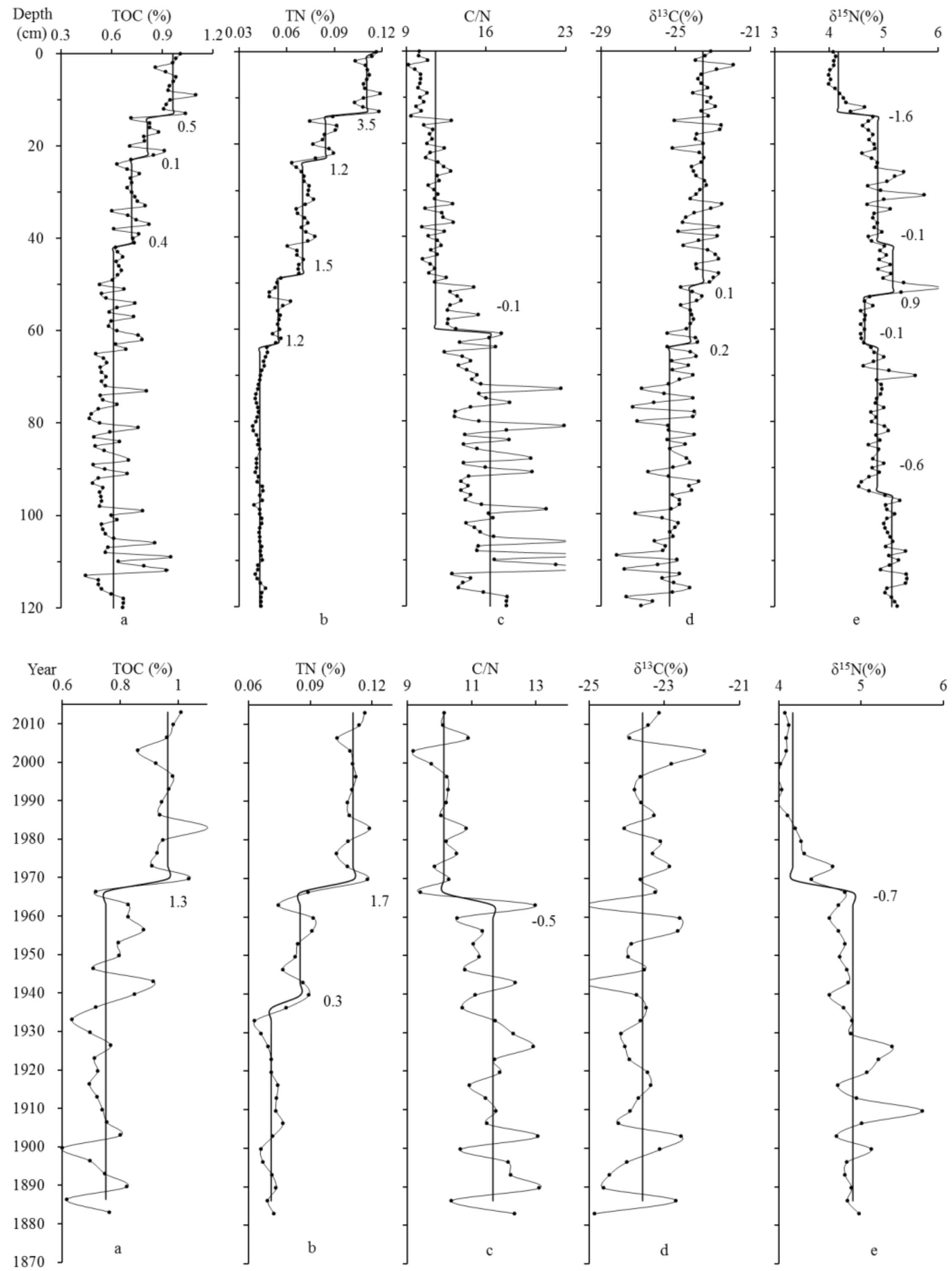

Figure 4.7. Profiles of geochemical parameters at KGR3 (a: TOC; b: TN; c: C/N; d: $\delta^{13}C$; e: $\delta^{15}N$; f: *n*-alkane). Upper panel is the data from the full cores and the lower panel is for the aged section only. The solid lines show shift trends assessed by sequential *t*-test analysis of regime shift and numbers are regime shift index (RSI). The cut-off length (l) was set to 10 for upper panel and 5 for lower panel.

5.2.4 Temperature proxies

TEX_{86}^{H} temperature estimates vary from 26.1 to 29.4°C at KGR2 and from 26.2 to 28.8°C at KGR3 (Figure 4.8a, b). Both the absolute values and temporal variations are in agreement in the two cores. TEX_{86}^{H} temperature display higher values in 125-60 cm, followed by low values in 60-30 cm, and increased to ca. 28°C in 30-0 cm. For the aged section of the cores the temperature indicated in both cores has fluctuated around 28°C since the 1940 and prior to that time it was higher in KGR2 and lower in KGR3.

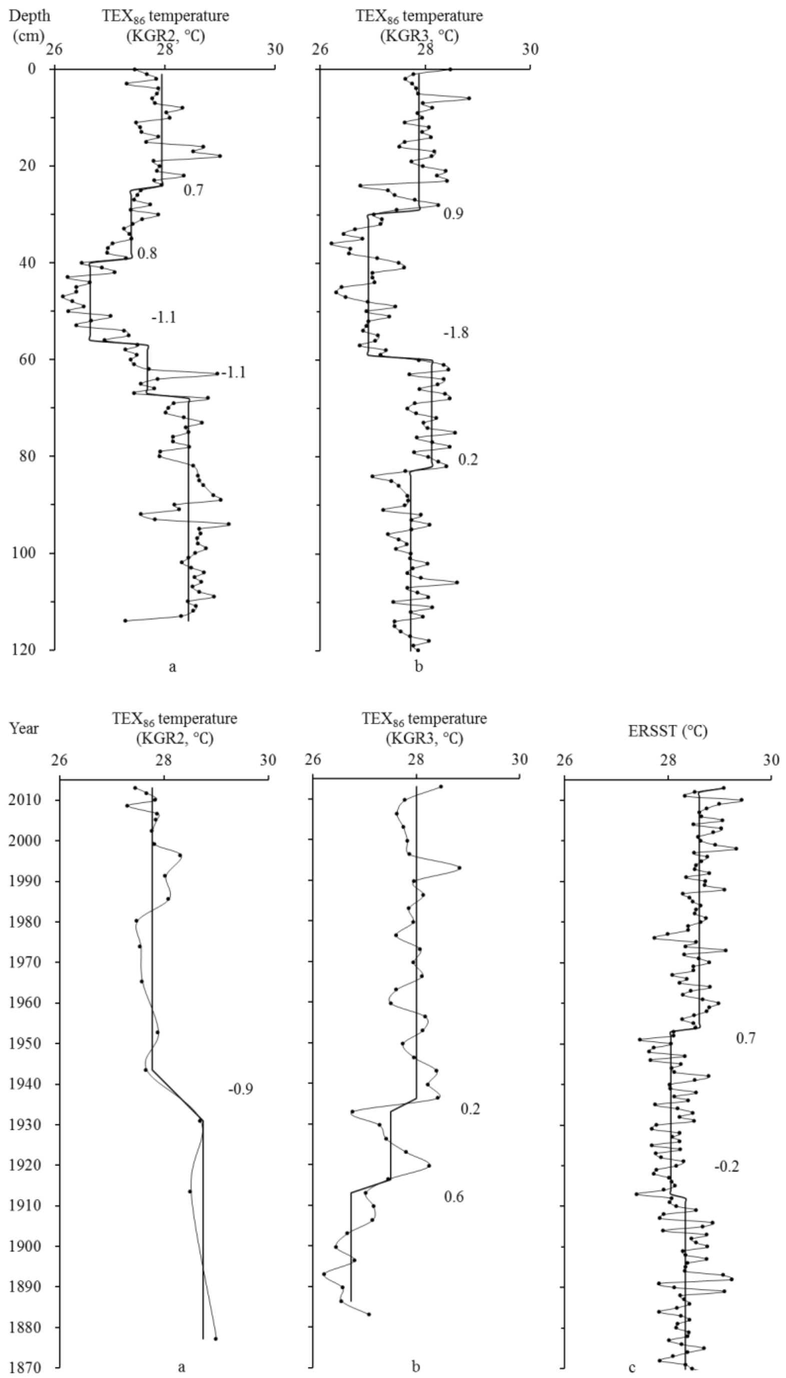

Figure 4.8. Profiles of TEX_{86}^{H} reconstructed temperature at KGR2 (a) and KGR3 (b) and ERSST (c) obtained from the Asia-Pacific Data-Research Center (http://apdrc.soest.hawaii.edu/, location: 14°S, 126°E). Upper panel is the data from the full cores and the lower panel is for the aged section only. The solid lines show shift trends assessed by sequential *t*-test analysis of regime shift and numbers are regime shift index (RSI). The cut-off length (l) was set to 10 for upper panel and 5 for lower panel.

5.2.5 Terrestrial influence proxies

The annual rainfall in Kalumburu varies from 629.9 to 1836.3 mm, with relatively large fluctuations around 1200 mm (Figure 4.9c of lower panel). The long-term average from 1940 is 1212 cm. Long chain alkanes, an indicator of terrestrial plant inputs was measured along the length of the core and showed a significant increase in the top 25-30 cm (last 100 years or so) at both sites (Figure 4.9 upper panel), relative to the deeper parts of the cores. Over the depth of the more recent (aged) profile in the core, there was no pattern or trend except for one very large temporary increase in the 1960s at KGR 3 (Figure 4.9b of lower panel).

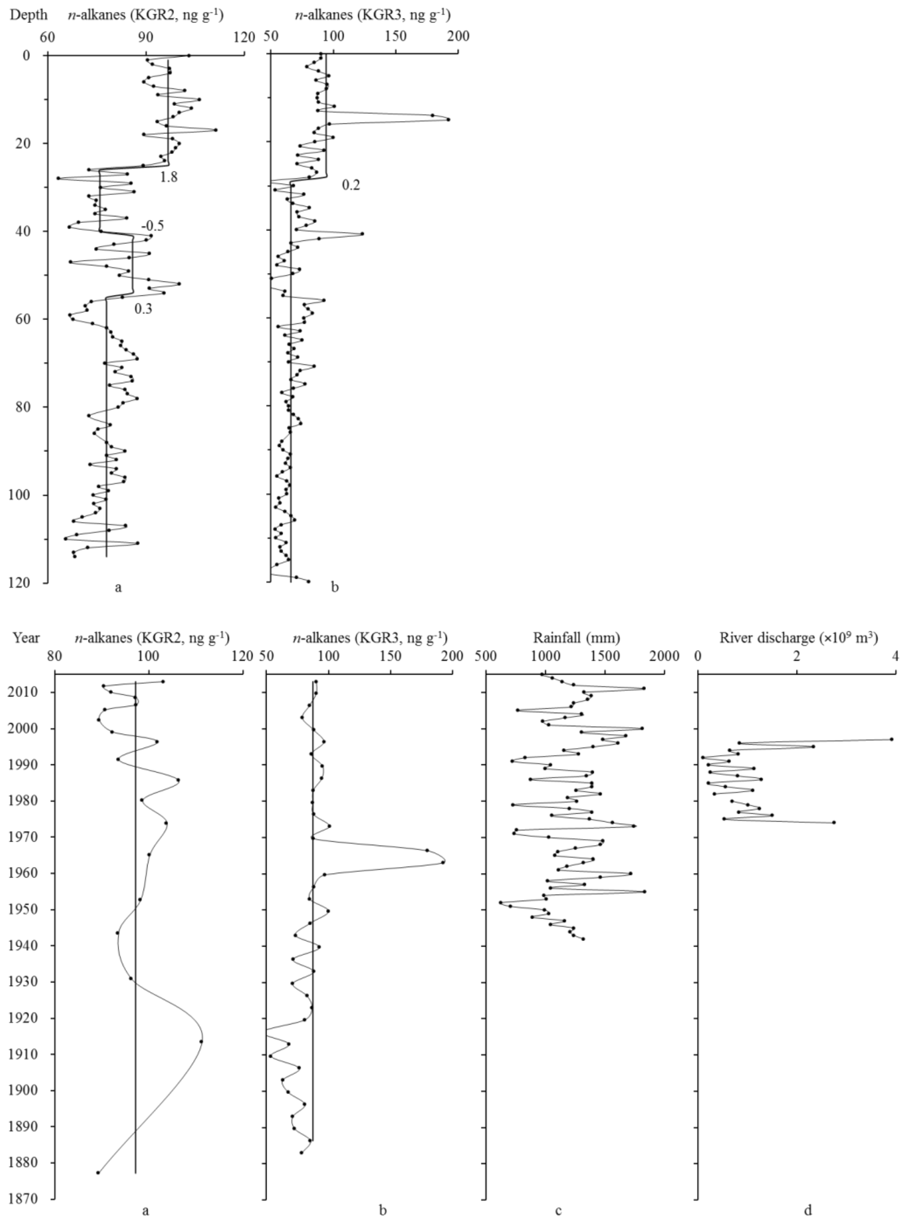

Figure 4.9. Profiles of terrestrial records: long chain *n*-alkanes contents at KGR2 (a) and at KGR3 (b); annual rainfall at Kalumburu (c, data from Bureau of Meteorology); Drysdale River discharge (d, data from Department of Water). Upper panel is the data from the full cores and the lower panel is for the aged section only. The solid lines show shift trends assessed by sequential *t*-test analysis of regime shift and numbers are regime shift index (RSI). The cut-off length (l) was set to 10 for upper panel and 5 for lower panel.

5.2.6 Phytoplankton proxies

Biomarkers are reported as both raw values and normalized to sedimentary TOC content to eliminate the effects of degradation. TOC normalized (nanograms of biomarker per gram of TOC in sediments) brassicasterol and dinosterol content at KGR2 range from 32.1 to 239.3 ng/g TOC and 67.8 to 341.1 ng/g TOC, respectively, and display similar increasing trend over time (Figure 4.10a, b). Both brassicasterol and dinosterol contents show low values in 60-120 cm, start to increase from 50 to 20 cm, and stay high values in the top 20 cm. While BSi contents display different patterns with biomarkers, with some high values around 80 cm and then an increase trend in the upper 30 cm (Figure 4.10c).

TOC normalized brassicasterol and dinosterol content at KGR3 range from 26.8 to 384.3 ng/g TOC and from 41.0 to 297.4 ng/g TOC, respectively (Figure 4.11, b). BSi contents range from 0.78 to 1.48%. Both biomarkers and BSi contents show consistent increasing trend over time (Figure 4.11c). When compared with KGR2, there is a clear similar pattern of biomarkers contents, however, a different pattern of BSi in the two cores. The different behaviours of BSi suggest that other processes besides phytoplankton productivity could affect the BSi content in our study area.

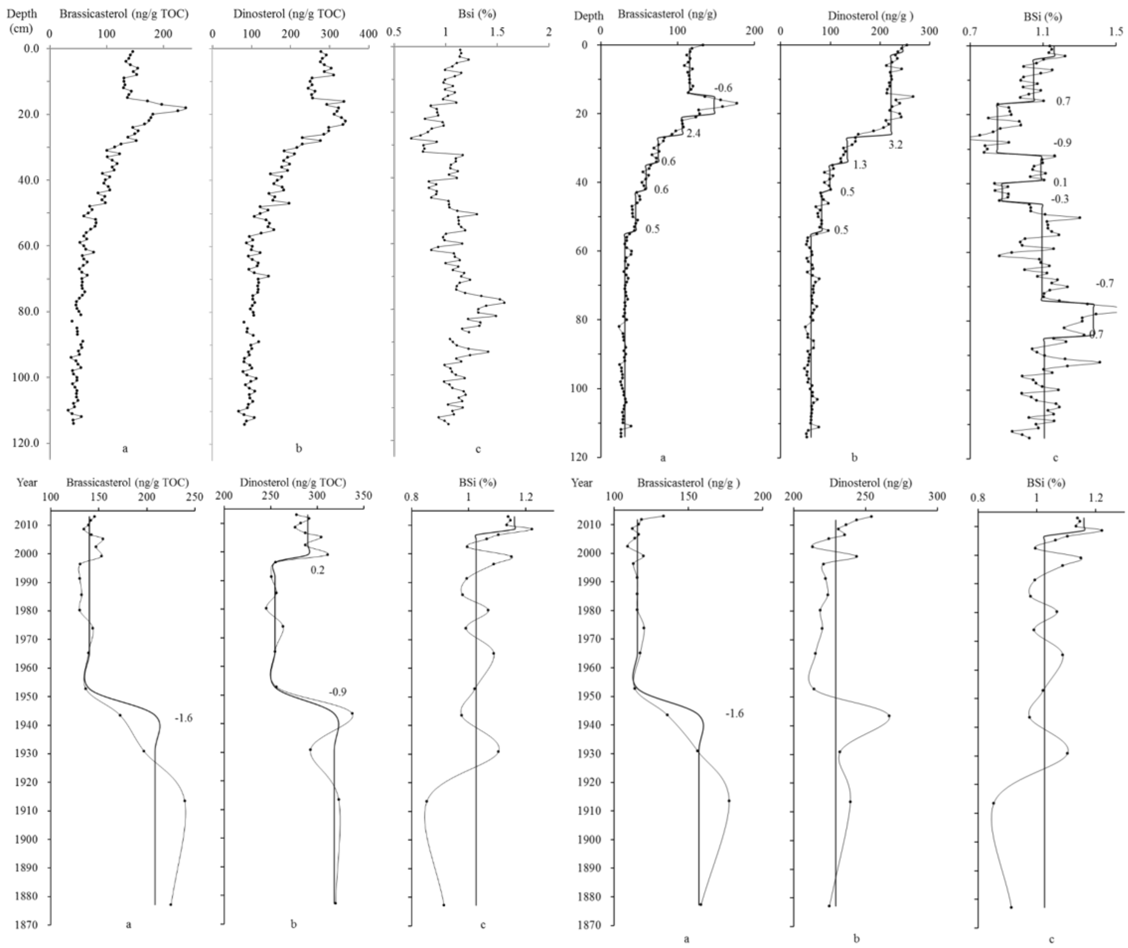

Figure 4.10. Profiles of brassicasterol (a) and dinosterol (b) content; (c) BSi content at KGR2. Left panels show the raw values in ng/g dry sediment. Right panels show the Total Organic Carbon corrected data (ng/g TOC) Upper panels are the data from the full cores and the lower panels are for the aged section of the cores only. The solid lines show shift trends assessed by sequential *t*-test analysis of regime shift and numbers are regime shift index (RSI). The cut-off length (l) was set to 10 for upper panel and 5 for lower panel.

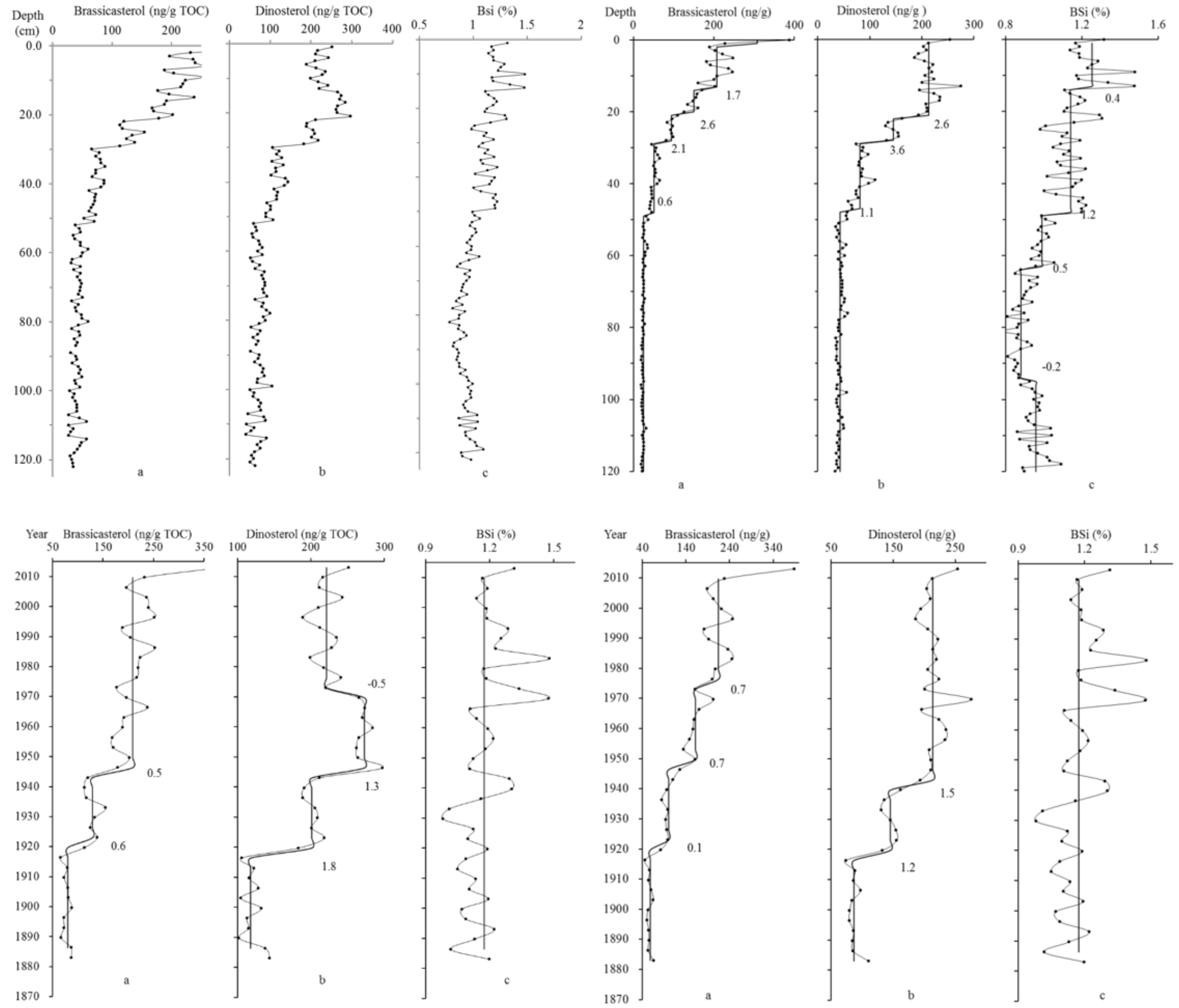

Figure 4.11**.** Profiles of brassicasterol (a) and dinosterol (b) content; (c) BSi content at KGR3. Left panels show the raw values in ng/g dry sediment. Right panels show the Total Organic Carbon corrected data (ng/g TOC) Upper panels are the data from the full cores and the lower panels are for the aged section of the cores only. The solid lines show shift trends assessed by sequential *t*-test analysis of regime shift and numbers are regime shift index (RSI). The cut-off length (l) was set to 10 for upper panel and 5 for lower panel.

5.2.7 Discussion

Differences in the age profile between the cores make comparisons difficult but there are a number of consistencies between the cores at the two sites KGR2 (Koolama Bay) and KGR3 (western bay). Total organic carbon (TOC), total nitrogen (TN), $\delta^{13}C$, brassicasterol and dinosterol all increased over the length of the cores. Long chain alkanes and $\delta^{15}N$ showed little change through the length of the cores at both sites. Biosilicate increased over time at KGR3 but at KGR2 the increase was mainly in the top 30cm. Conclusions that can be drawn from the alkanes, $\delta^{13}C$, and C/N trends are that marine carbon sources of carbon production have increased over time while the importance of terrestrial inputs has remained stable. The TOC (0.9-1.0 %), $\delta^{13}C$ (-23) and C/N values (10-11) near the surface of our cores indicate a mix of marine and terrestrial carbon sources and are similar to those found by Abballe (2012) in nearshore samples of surface sediment the Arafura Sea. The other relevant study in this region is that of Volkman et al. (2007). While their Ord River study was mostly of estuary, their most "marine" sites showed $\delta^{13}C$ values of -14 to -20 indicating marine sources of carbon while values further up the river showed a transition of mixed marine and terrestrial inputs to a $\delta^{13}C$ minimum of -28 consistent with terrestrial sources more than 40 km upstream. The $\delta^{15}N$ data in our study indicates there is no evidence of anthropogenic nitrogen increasing.

Increases in brassicasterol, dinosterol and biosilicate are all consistent with increasing phytoplankton biomass. Sediment diagenesis can affect temporal variations in organic matter and some biomarkers in sediments (Sun and Wakeham, 1994) although sterols such as those used here are regarded as being very stable (Volkman 1986). In addition, in our results, phytoplankton biomarker trends were in agreement with variation trends of C/N and $\delta^{13}C$ in the same cores, which indicate an increasing contribution of marine organic matter at the same time the biomarkers indicate an increasing biomass of marine phytoplankton. These comparisons suggest that preservation changes were not the main cause of the temporal variations of biomarker contents, instead, their increasing trends mainly reflect phytoplankton biomass variation. In-situ primary production measurements by Furnas (1996) showed 2-fold increase post-1990 than in the 1960s (Furnas and Carpenter 2016) although these authors were cautious of their result and concluded that changes in measurement methods over time could have occurred which could be responsible for the trend observed.

Unlike at Broome where rainfall has increased by 40% off its long-term average since 1997, rainfall at Kalumburu has been relatively stable since 1940 with only a 6.8% increase since 1997. At KGR2 only Biosilicate was correlated with averaged rainfall (p=0.049), which is intuitive, given that river runoff is the major source of biosilicate inputs to coastal waters. There were insufficient data points to compare parameters at KGR2 with Drysdale River discharge. For KGR3 there were no significant correlations between Drysdale River discharge and any of the biogeochemical or biomarker parameters. Only Brassicasterol was correlated with averaged rainfall with a one-year lag (p=0.045) or two-year lag (p=0.032). Multiple regression analyses using models of TEX_{86}^{H} combined with rainfall did not provide any greater predictive capability. Few parameters measured were correlated with TEX_{86}^{H} temperature over the full length of the cores. Brassicasterol was weakly correlated with TEX86 at KGR3 (p=0.039) but not at KGR2 (p=0.348)

We expected to find that the KGR2 site in Koolama Bay would show significant differences over KGR3 due the presumed influence of the King George River at KGR2. With the exception of a significant relationship between biosilicate and rainfall at KGR2 and not KGR 3, in fact we found no evidence that the two sites differed greatly, at least not in ways attributable to increased freshwater flows. This may have been due to low sedimentation rates and poor core preservation, however the trends in sediment parameters unrelated to terrestrial input were evident. Both sites showed evidence of increased phytoplankton biomass over time. Although correlations were weak (this may have been due to low sedimentation rates), the increasing trends in biomarker pigments occurred over the same period as increases in temperature indicating that, consistent with what we found at both Cygnet Bay and at Broome, that increased phytoplankton biomass has occurred over the same period as anthropogenic ocean warming.

5.3 Black carbon and its relationship to bush fires in the KGR catchment

5.3.1 Introduction

"Black carbon (BC)" or elemental carbon is produced exclusively from incomplete combustion of biomass and fossil fuels, and is ubiquitous in the environment. BC can be classified into two subtypes, i.e., char and soot. Although char and soot are both produced from combustion activities, different sources contribute different proportions of char and soot to total BC. Biomass burning during a bush fire generates a much higher percentage of char than soot, with a char/soot ratio of >5–10, while motor vehicle exhausts have a ratio of char/soot typically lower than 1 (Han et al., 2015). In remote area catchments like in the Kimberley, we would expect very low levels of soot relative to char.

In general, both aromatic char and soot are resistant to decomposition so they will persist in sediments, making BC a good proxy of environmental variability. BC from bushfires can make its way into marine sediments in two pathways; it can settle from the atmosphere and it can be transported from the site of the fire through river runoff. Thus, the amount of BC in coastal sediments will depend not only on the extent of fires but also of rainfall and other factors affecting runoff.

The preliminary results presented here are from a pilot study to examine the potential for using BC analyses of coastal marine sediment archives to reconstruct the time course of, or at least reflect the temporal variability, in bushfires in the Kimberley. In this case we are using the King George River catchment (Figure 4.3) as an example. We would only expect the results to be applicable to the King George River catchment, not the Kimberley as a whole. The results of the BC analyses are matched to the very recent record (2000 to 2013) of area burnt in the catchment. Additional information about rainfall and river discharge is also considered, although for this study, the nearest rainfall data we were able to obtain was from Kalumburu which is in the King Edward River Catchment and the only river discharge data was from the Drysdale River. These types of data are only sparsely collected in the Kimberley and records are often incomplete or discontinuous.

5.3.2 Results and Discussion

Black carbon (BC) concentrations varied from 0.4 to 1.2 mg/g of sediment (Figure 4.12). This is within the range expected based on other studies on marine sediments in coastal waters (Fang et al. 2015) and the range is significant providing encouragement that we can infer significant changes over time. Less than 10% of the BC is soot, meaning, as expected, that biomass burning is contributing the majority of the BC present. The main source of BC in these sediments can be expected to come from fires burning within the King George River catchment (or nearby if atmospheric deposition is important).

Figure 4.12 shows significantly elevated concentrations of BC in the top 23 cm. This increase, from about 0.60 to 0.85 mg/g BC, is observed at a depth outside the section of the core which can be aged with confidence, but based on sedimentation rates it would have occurred around 1850. Below this, BC concentrations vary little down to about 90 cm depth. We have not aged sediments this deep in the core. The aged section of the core (Figure 4.13) shows peaks of 0.94-1.1 mg/g BC in 1974, 1980, 1996, 1999, 2010 and 2012 and lows of 0.69-0.76 mg/g BC in 1986, 2002 and 2006. These years are best regarded as approximations given uncertainties in sediment ages.

There is good reason to expect that the amount of black carbon (BC) in coastal sediments will be influenced by the extent of fires in the relevant catchment, rainfall and/or river discharge. We looked for correlations between BC and these potential explanatory factors and used multiple regression analyses to determine if any combination of these explanatory factors could explain the amount of BC in the sediment cores. Each of these factors was analyzed over the extent of the record, for example bush fire data was only available from 2000 while rainfall data was available from 1940. Multiple regression analysis only included data for the shorter period in any pairwise comparison. In order to match explanatory factor data to the years for which BC data was available an average which matched the time between BC measurements was used. For example, BC data was available for 2010 and 2012 so the BC data for 2012 was compared with average rainfall and area burnt from 2011 and 2012. Lag periods of 1 and 2 years were also examined.

There were no significant correlations between BC in sediments and an explanatory variable examined. The variable with the highest positive correlation with EC was early season area burnt with a one-year lag (R^2= 0.546, p=0.058). Multiple regression analysis showed that a model incorporating early season area burnt (with a one-year lag, i.e. the year before) and rainfall explained a significant amount of the variability in BC (R^2=0.812, p=0.035). This result is intuitive but needs to be regarded with caution as the sample size is small (bush fire data matched to BC from 2002-2013, Figure 4.14) and the rainfall record is from an adjacent catchment. Nevertheless, the result is encouraging and suggests that a study which sought to optimize the spatial and temporal matching of good time series of explanatory data (area burnt and rainfall) and a sediment core location with a good sedimentation rate and good age preservation would yield results which can be regarded with greater confidence.

In determining a potential site for more work, we consider the King Edward River catchment as offering high potential. This catchment has a good rainfall record at Kalumburu (since 1940), it has a very large catchment area (84,000 km^2) and a much larger area burnt each year (> 600,000 ha compared to <250,000 in King George River). Lastly, the King Edward River flows into a semi enclosed embayment (Napier Broome Bay), which will offer the likelihood of a higher sedimentation rate and less sediment disturbance. Cambridge Gulf is also another location with characteristics that offer the likelihood of a successful application of these techniques.

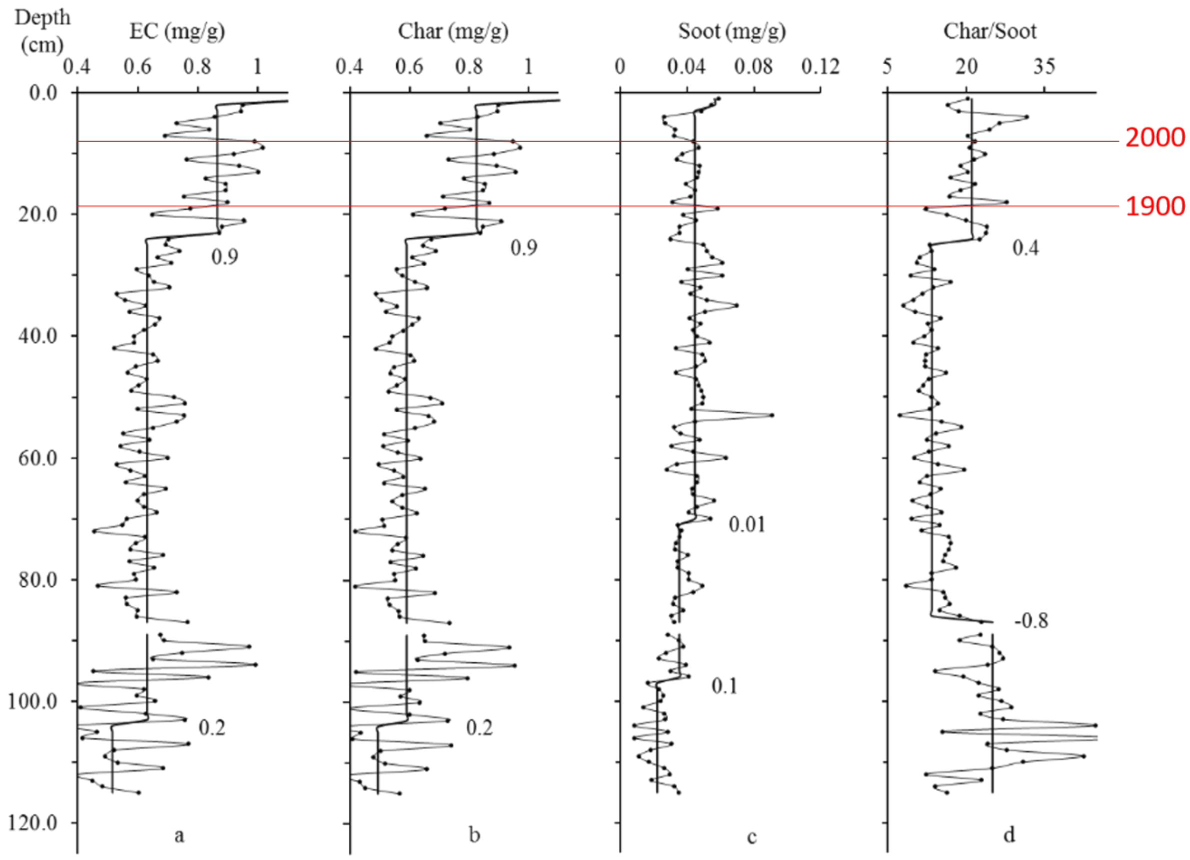

Figure 4.12. Profiles of (a) Black Carbon [EC], (b) Char, (c) Soot in mg/g and (d) ratio of Char to Soot in the Koolama Bay sediment core. Years are indicated for the aged section of the core. The line shows shift changes assessed by sequential t-test analysis of regime shift, and the corresponding regime shift index).

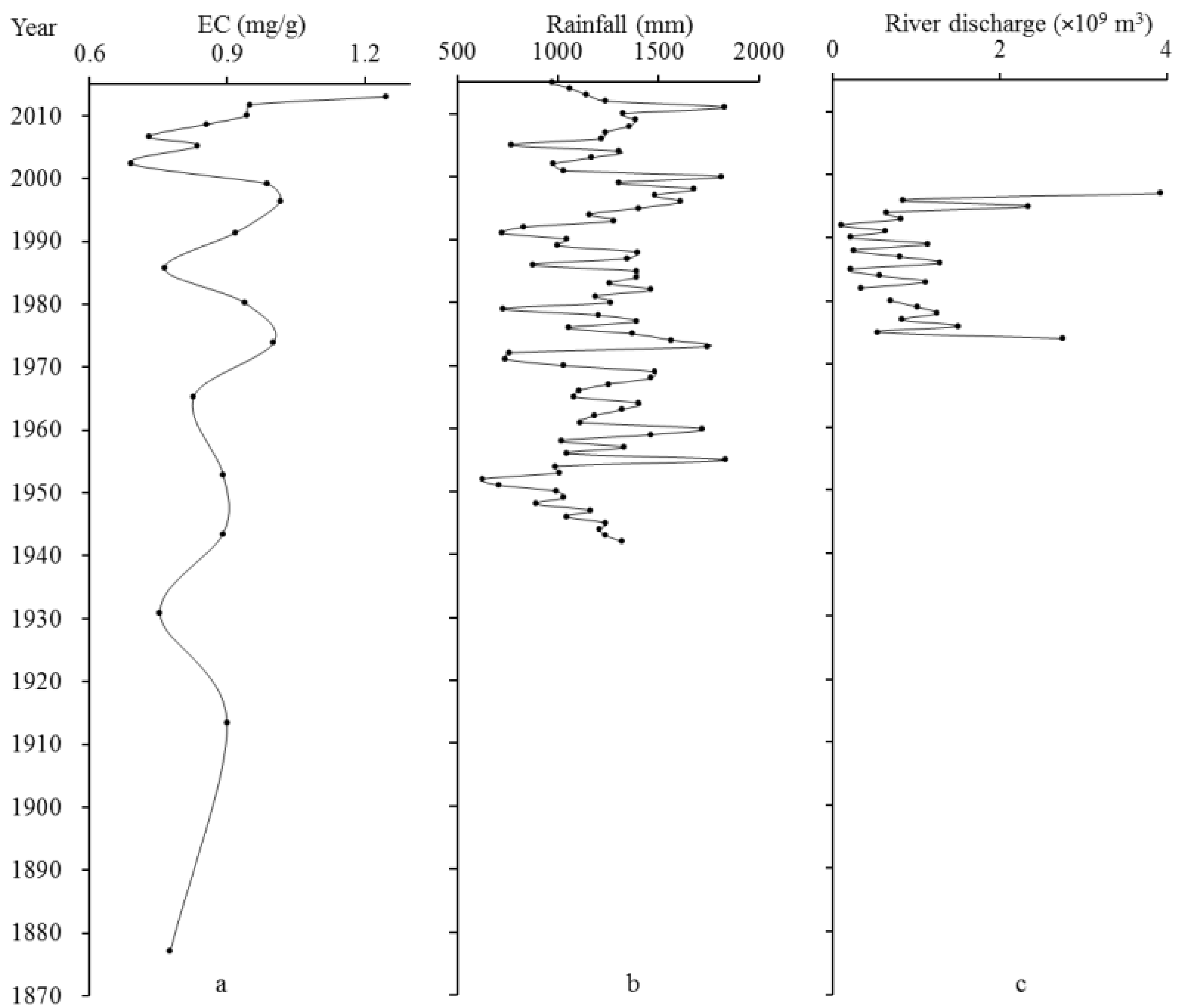

Figure 4.13. (a) Profile of Black Carbon (EC) in mg/g in the aged section of the Koolama Bay sediment core, (b) rainfall records for Kalumburu, (c) Drysdale River discharge records.

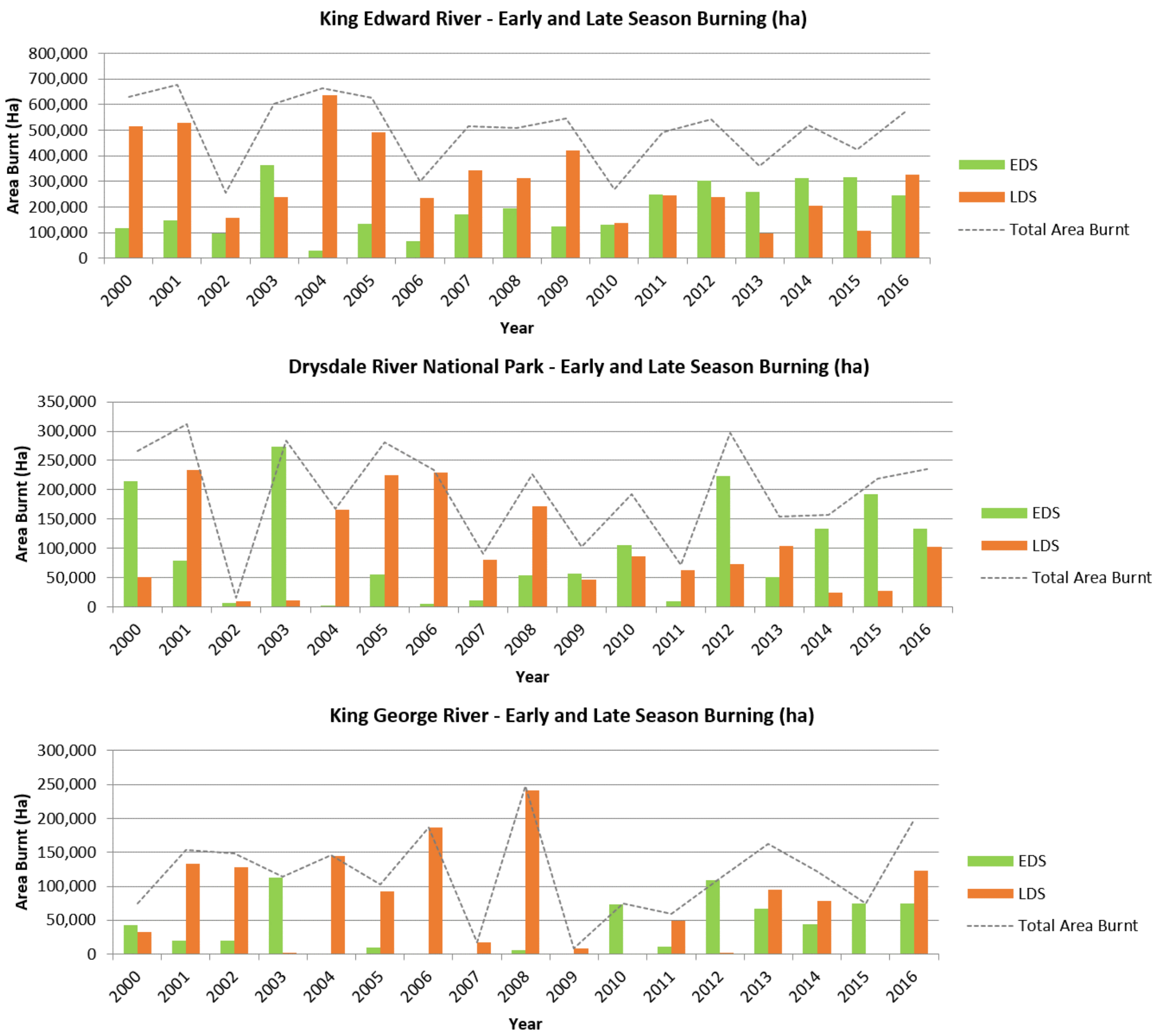

Figure 4.14. Burnt area calculated from fire scars in three Kimberley catchments. Boundaries for the areas calculated for the King George River and the King Edward River catchments are shown in Figure 4.15. EDS is early season fires (January to June) and LDS is late season fires (July to December) Source: North Australian MODIS burnt area imagery mapping by month 2000 – 2016. Data downloaded from http://www.firenorth.org.au/nafi3/ analysis undertaken by Janine Kinloch and Georgina Pitt, Remote Sensing and Spatial Analysis Section, GIS Branch, WA Department of Parks and Wildlife. Note our King George River cores were collected in June 2013.

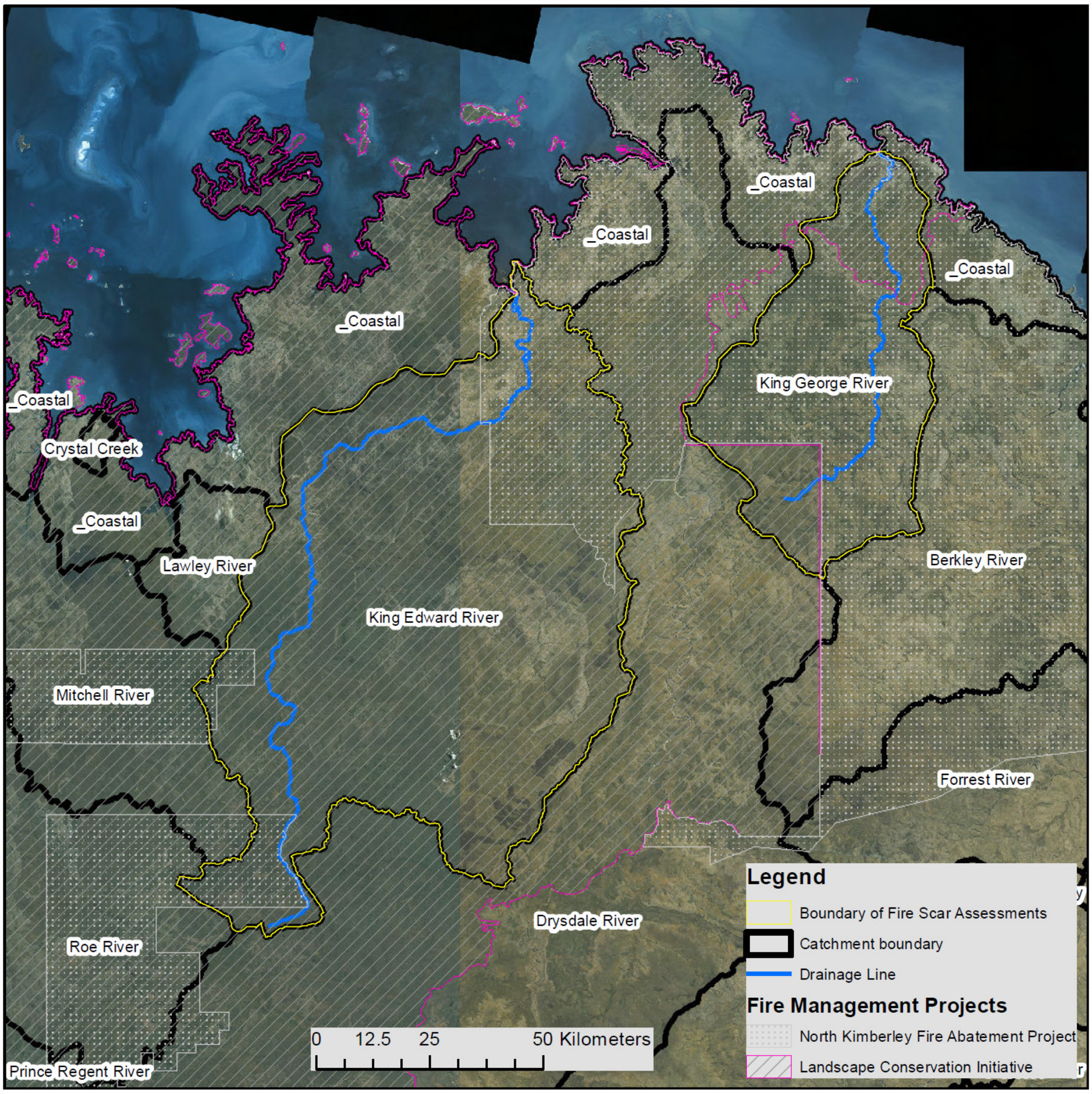

Figure 4.15. Map of northern Kimberley showing the boundaries of the areas within the King George River and the King Edward River catchments from which the burnt areas calculated from fire scars shown in Figure 4.14.

6 Broome, southern Kimberley

6.1 Introduction, site description and sample sites

Broome is located on Roebuck Bay adjacent to Dampier Creek and offered the opportunity to investigate sedimentary records for a Kimberley site potentially influenced by human activity signals typical of a coastal city. In this case we focused on a comparison of two sites, the first potentially influenced by Broome's historical and recent anthropogenic inputs via Dampier Creek, which carries urban runoff into the bay as well as direct intentional or accidental inputs from other sources (such as the wastewater treatment plant, the abattoir and the golf course) (see Figure 5.1), and a second in the south-eastern part of Roebuck Bay which was to serve as a reference site.

Cores were collected from about 15m depth at two sites in Roebuck Bay (Figure 5.2). Four cores were collected at site 1. At site 2, loss of the coring gear meant only two cores were collected. Site 1 is directly within the influence of Dampier Creek and close to a number of industrial sites to the south of the city. Site 2 was selected to be remote to this influence in a similar depth but is not a perfect reference site, as it is influenced by the Cape Leveque coastal basin catchment on Dampier Peninsula (Figure 5.3) to a greater extent than is Site 1 given that Dampier Creek receives little input from the Cape Leveque coastal basin catchment. Nevertheless, there is little if any industrial influences in the part of the catchment which delivers water into the creeks along the eastern coast of Roebuck Bay (Figures 5.1 and 5.3).

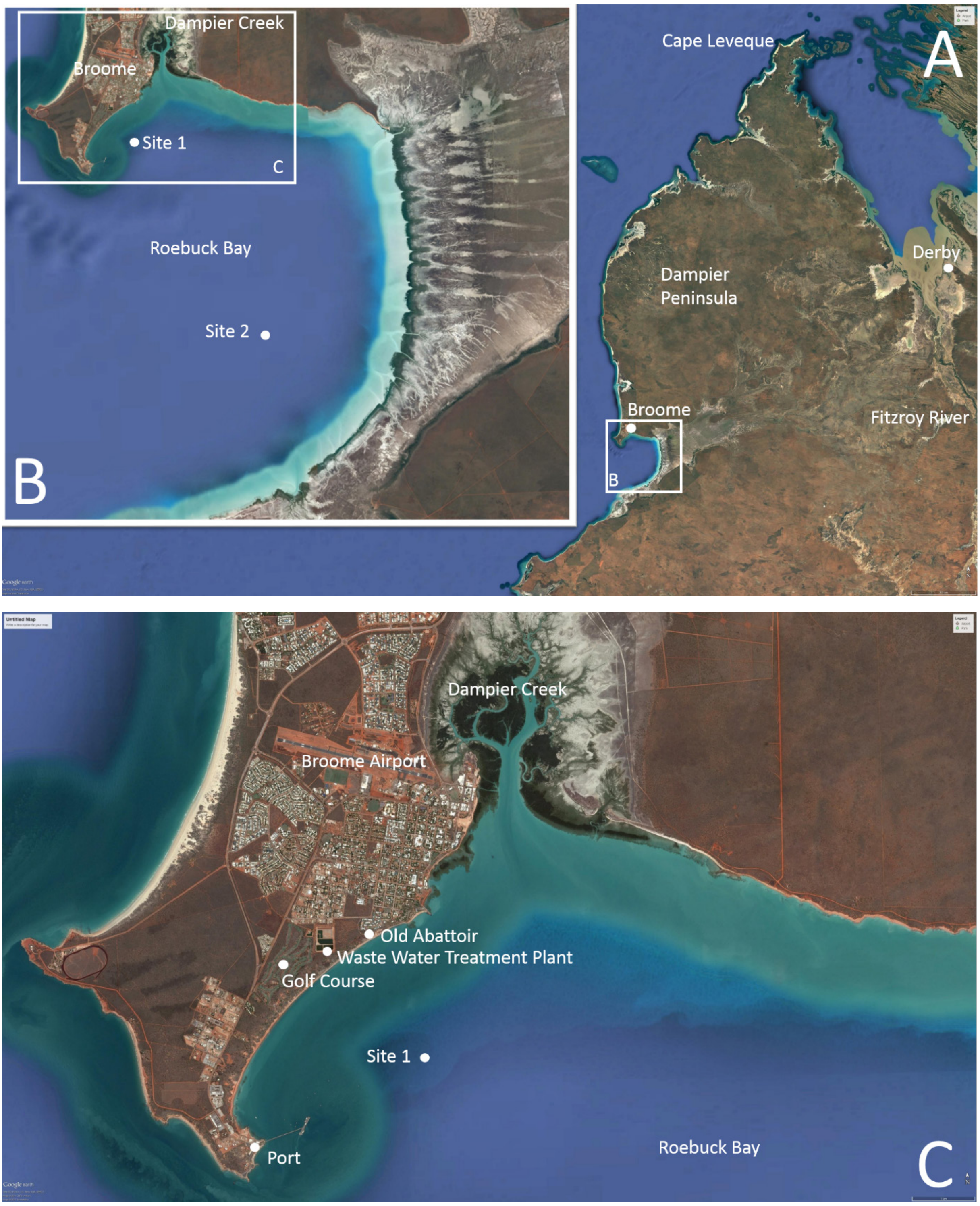

Figure 5.1. Google Earth image of Broome and Roebuck Bay showing sampling sites and locations of industrial sites of interest to water quality studies. Core sampling sites in Roebuck Bay. The northern site (site 1) sits within the influence of Dampier Creek and Broome city while the southern site (site 2) is the reference site. Note the differing influence of the different catchments on the two different sites.

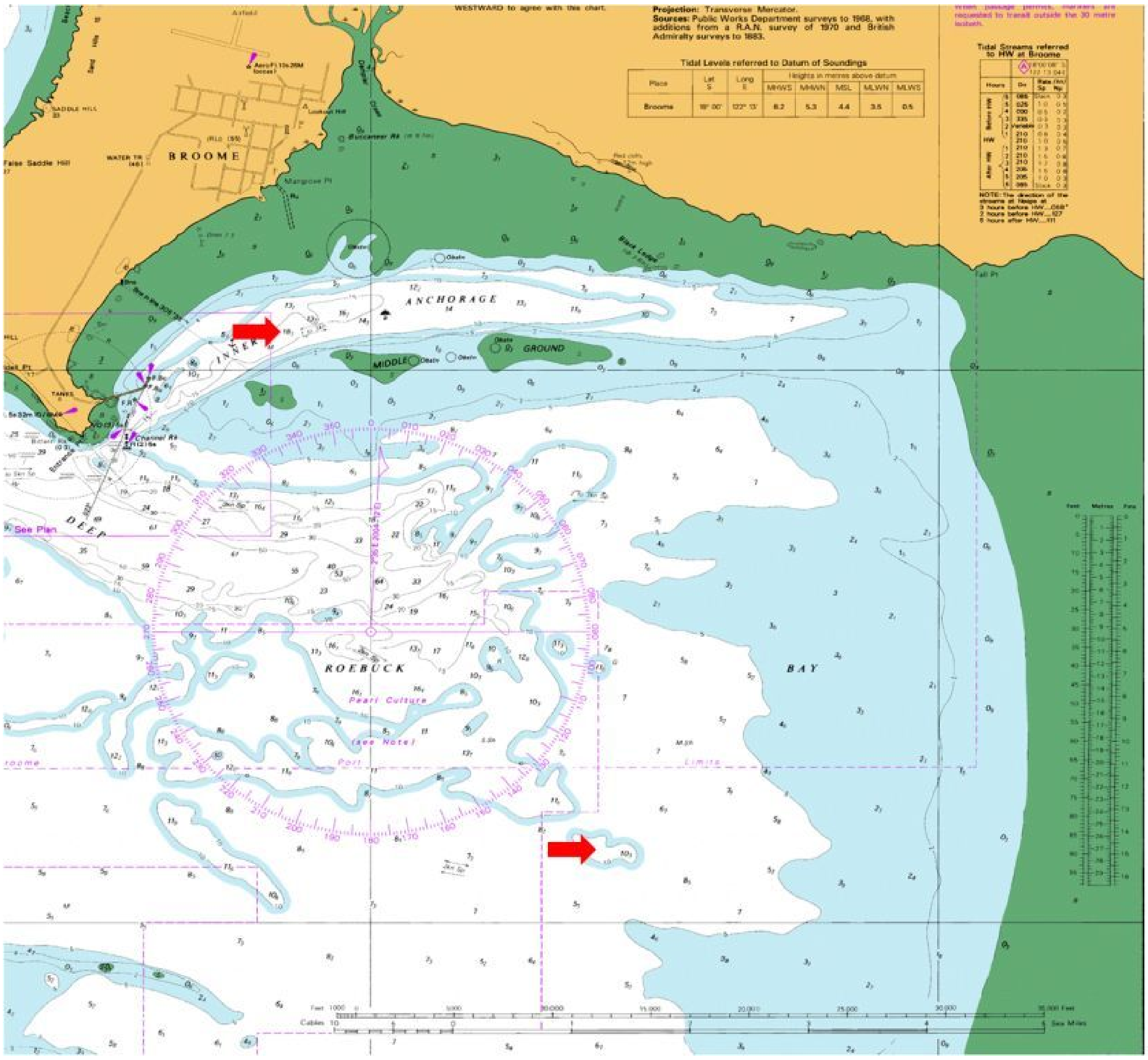

Figure 5.2. Core sampling sites in Roebuck Bay. The northern site (site 1) sits within the influence of Dampier Creek and Broome city while the southern site (site 2) is the reference site.

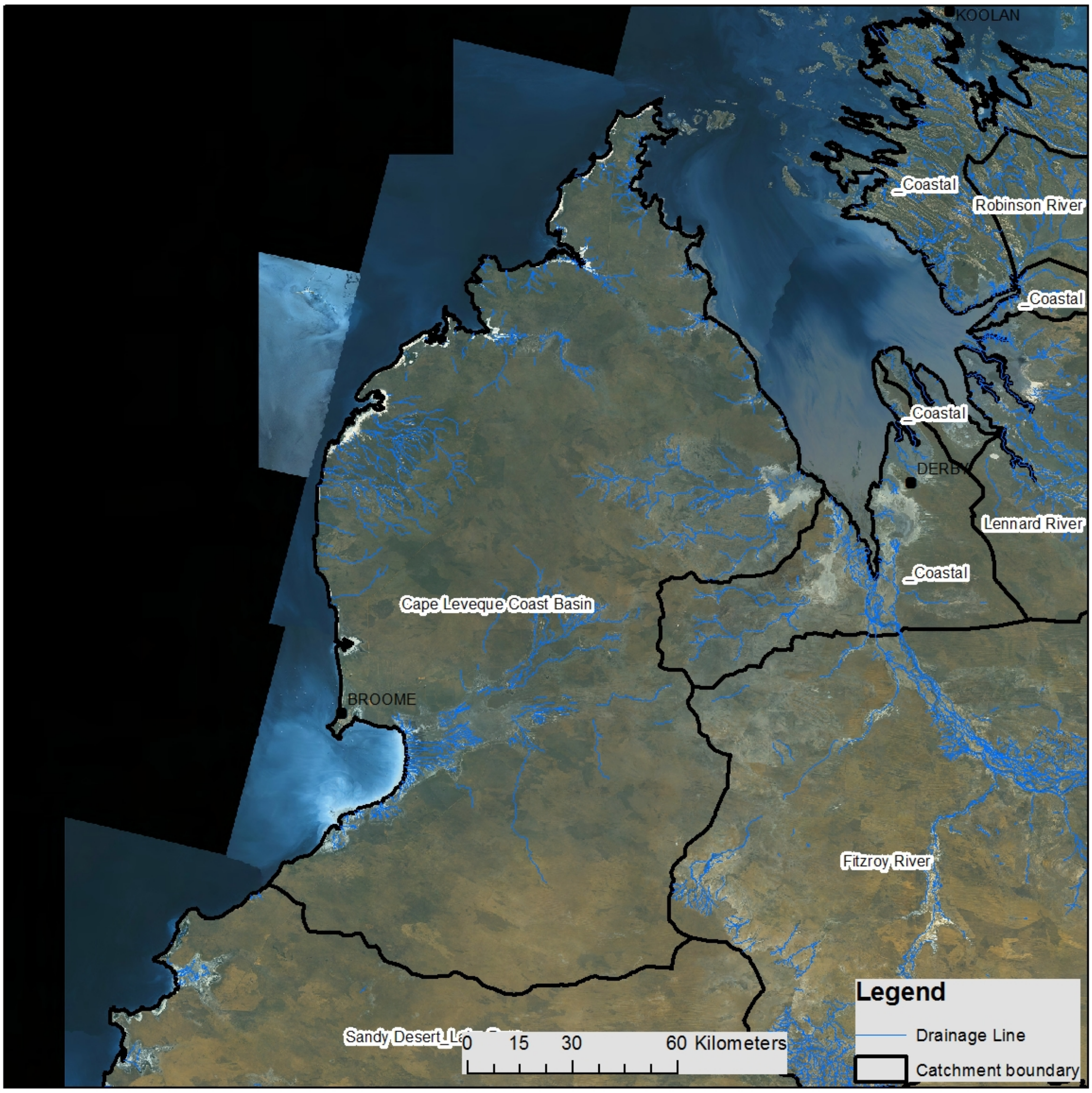

Figure 5.3. The Cape Leveque coastal basin showing catchment influence on the eastern shore of Roebuck Bay to a greater extent than Broome itself.

6.2 Results

6.2.1 Core chronology

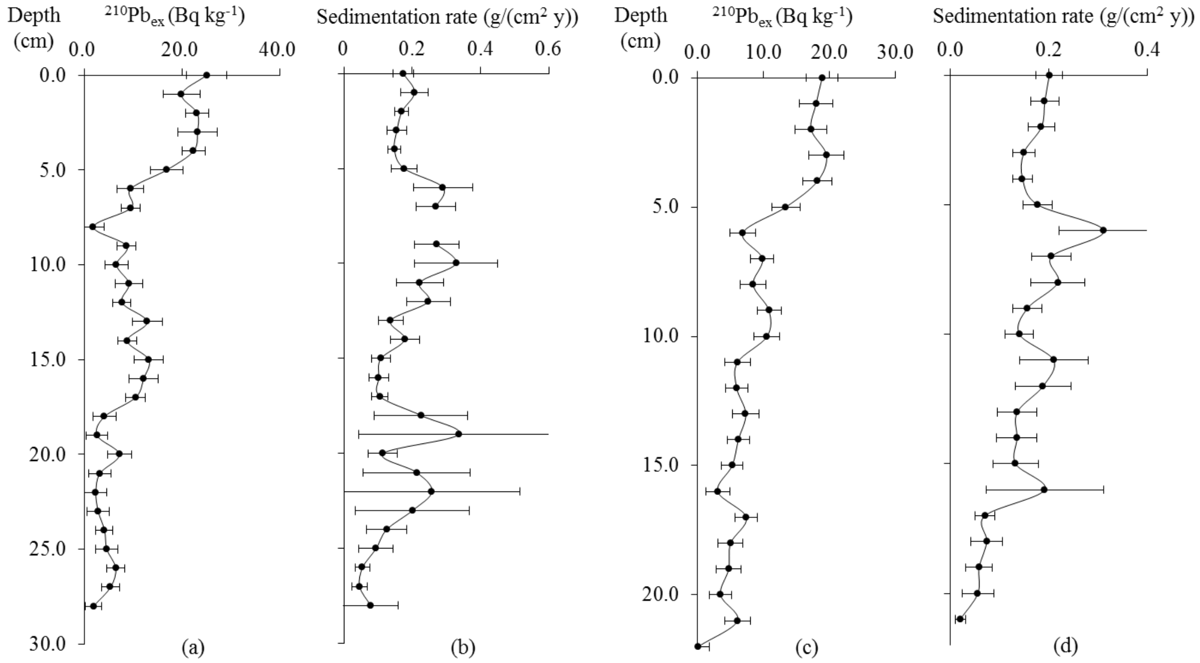

Figure 5.4. Profiles of $^{210}Pb_{ex}$ and sedimentation rates at Broome1 (a, b) and at Broome2 (c, d) (error bars denote standard deviation).

The $^{210}Pb_{ex}$ depth profiles and sedimentation rates in Broome cores are shown in Figure 5.4. A thin mixed layer of the top 4 cm is observed in Broome2. In core Broome1, sedimentation rates range from 0.05 to 0.29 g $cm^{-2}y^{-1}$, with a mean value of 0.18 g $cm^{-2}y^{-1}$. In Broome2, sedimentation rates range from 0.02 to 0.22 g $cm^{-2}y^{-1}$, with a mean value of 0.14 g $cm^{-2}y^{-1}$and an increasing trend over time. The results of the CRS model applied to the Broome cores is shown in Figure 5.5. Broome 1 was aged between 2012 at 1cm and 1904 at 28 cm. Broome to was aged between 2003 at 4 cm and 1903 at 21 cm.

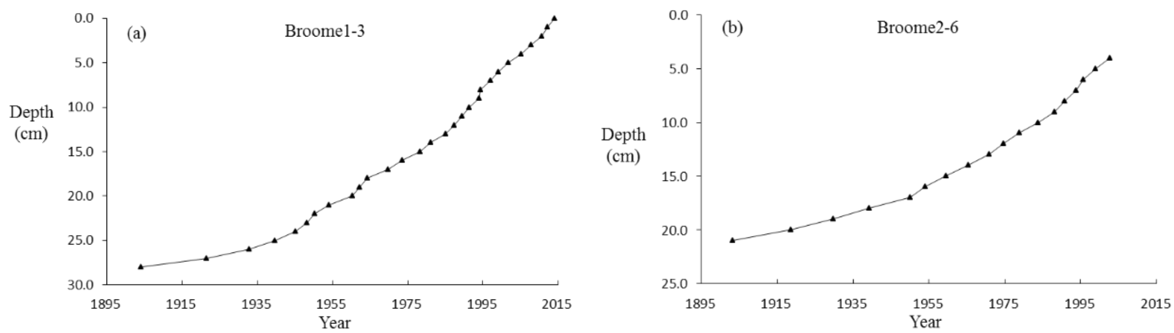

Figure 5.5. Comparison of age profiles from the CRS ^{210}Pb model applied to the two Broome cores.

6.2.2 Sediment grain size

Contents of sand (64 um) in Broome1 varied between 65-70% for most of the upper section of the core to 60cm, although some relative minima about 40% (2-4 and 14-16 cm) and maxima about 80% (7-10 cm) were present. The same pattern was observed for d_{50}, averaging 100 µm along the upper 50 cm but varying between 75 µm and 135 µm in the upper part of the core. Contents of sand (64 µm) in Broome2 increased from 69% to 75% in the upper 50 cm, and then varies between 75-80% below 50 cm. This corresponds to a sustained increase of d_{50} from surface (ca. 120 µm) to around 50 cm (ca. 200 µm), where it remains approximately constant below 50 cm (Figure 5.6).

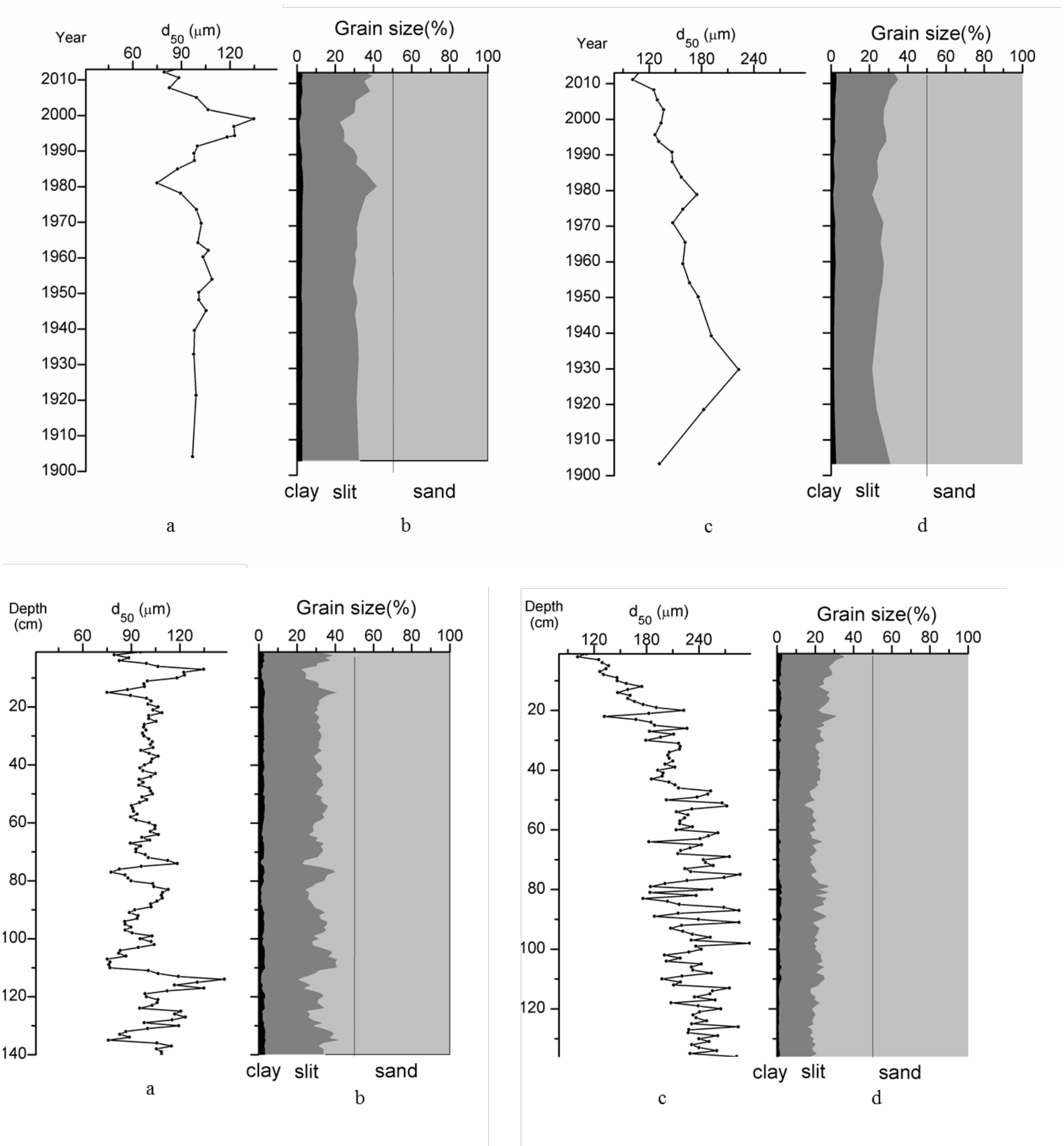

Figure 5.6. Profiles of grain sizes through the entire core profile at Broome1 (a, b) and Broome2 (c, d), showing median values (d_{50}) and the proportions of clay, silt and sand. Upper panels are shown against the aged section of the core and the lower panels are shown for the full depth range of the core.

6.2.3 Geochemical parameters

The chronological variations of TOC, TN, C/N, $\delta^{13}C$, and $\delta^{15}N$ at Broome1 are shown in Figure 5.7. TOC vary from 0.23% to 0.79% (Figures 5.5a). Large oscillations are observed in the upper 30 cm, and are relative stable below that layer. TN contents vary from 0.03% to 0.09% (Figures 5.7b), with a slight increasing trend in the upper layer. C/N ratios range from 4.9 to 17.9 (Figures 5.7c) and high values are observed in 50-80 cm. $\delta^{13}C$ values range from -20.3 to -17.9‰ (Figures 5.7d) and show stable changes, except for some low values in 80-100 cm. The $\delta^{15}N$ values range from 4.4 to 13.3‰ (Figure 5.7e). $\delta^{15}N$ display relatively higher values than that in northern Kimberley, indicating possible anthropogenic impact.

The chronological variations of TOC, TN, C/N, $\delta^{13}C$ and $\delta^{15}N$ at Broome2 are shown in Figure 5.8. TOC vary between 0.28 and 0.90%, with an average of 0.49% (Figure 5.8a); TN vary between 0.04 and 0.12%, with an average of 0.06% (Figure 5.8b). Both TOC and TN show an increasing trend in the upper 10 cm. $\delta^{13}C$ values range from -19.2 to -17.4‰; C/N ratios range from 7.2 to 10.3; and $\delta^{15}N$ range from 7.1 to 10.3 (Figure 5.8c, d, e). These geochemical parameters all exhibit no clear trend and slight variations in this core.

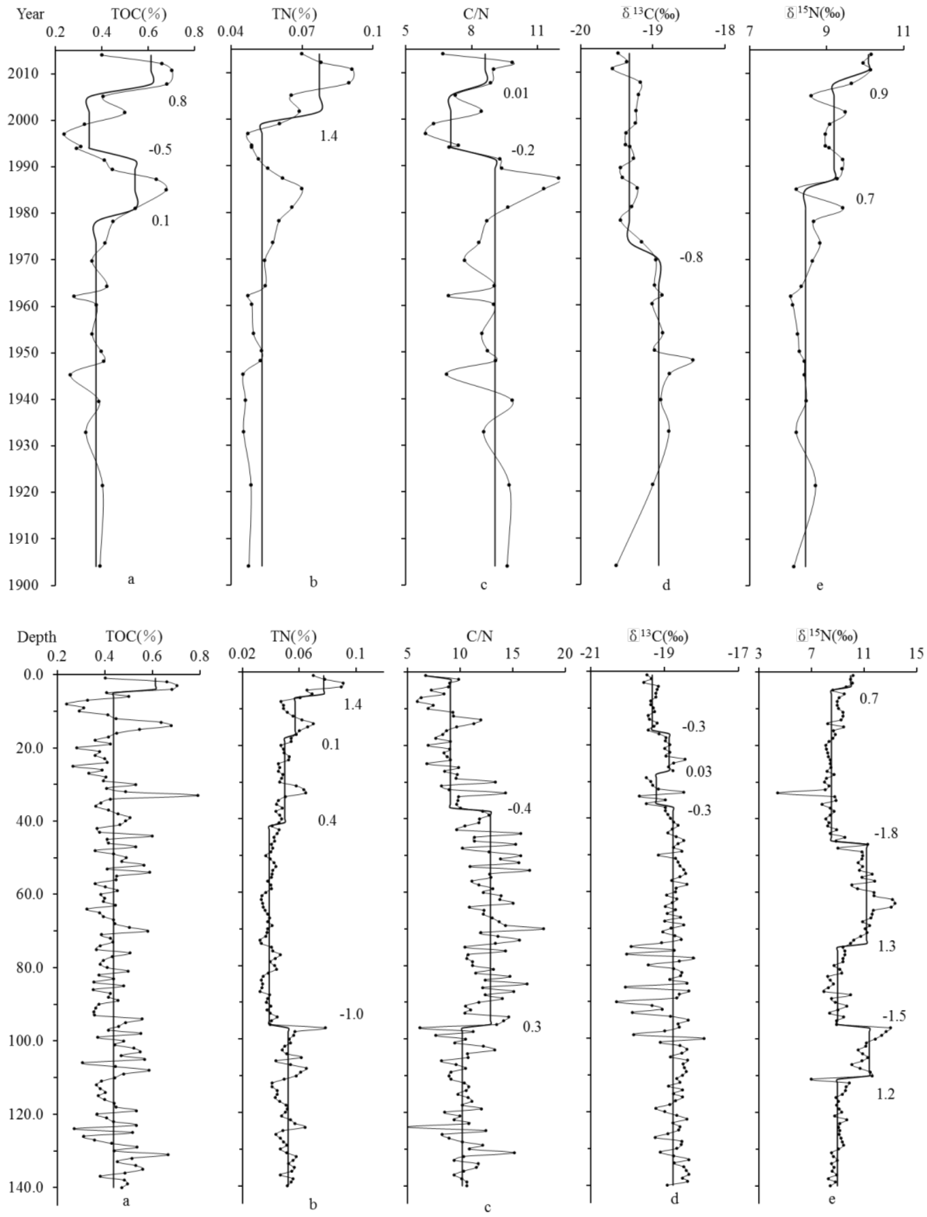

Figure 5.7. Profiles of geochemical parameters at Broome1 (a: TOC; b: TN; c: C/N; d: $\delta^{13}C$; e: $\delta^{15}N$;). Upper panels are shown against the aged section of the core and the lower panels are shown for the full depth range of the core.

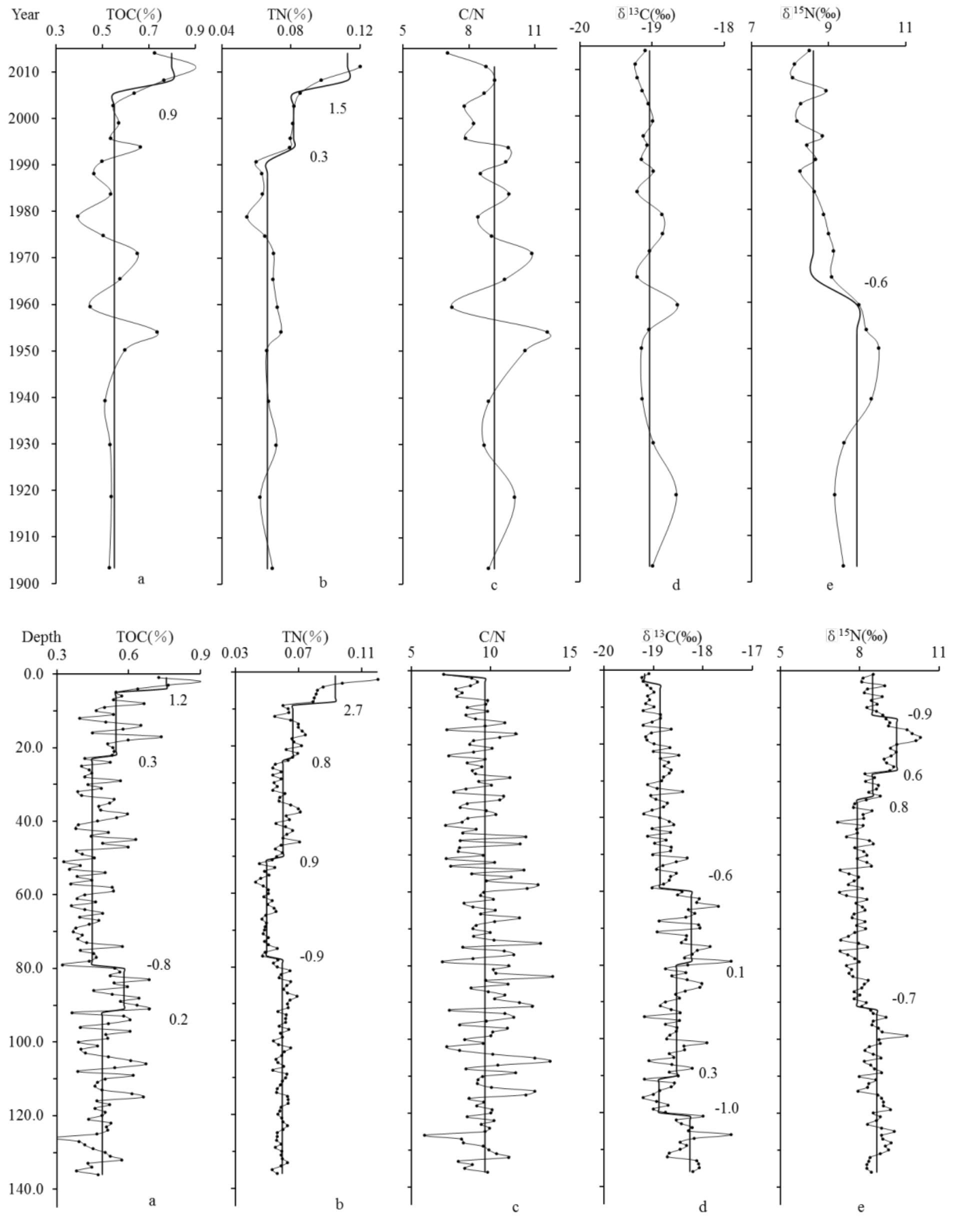

Figure 5.8. Profiles of geochemical parameters at Broome2 (a: TOC; b: TN; c: C/N; d: $\delta^{13}C$; e: $\delta^{15}N$;). Upper panels are shown against the aged section of the core and the lower panels are shown for the full depth range of the core.

6.2.4 Temperature proxies

Significant increases in temperature were detected in both cores from the mid-1990s (Figure 5.9), however the core from Broome 2 also shows a slight but significant reduction near the end of the 2000s.

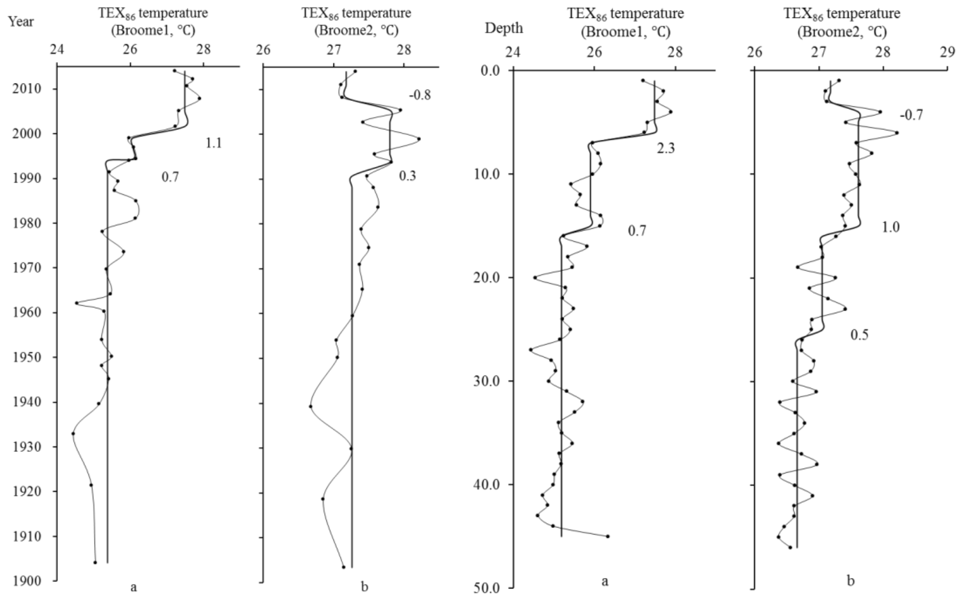

Figure 5.9. Profiles of TEX_{86}^{H} temperature at Broome1 (a) and Broome2 (b). The left two panels are shown against the aged section of the core and the two right panels are shown for the depth of the core the analyses were applied to.

6.2.5 Terrestrial influence proxies

Annual rainfall in Broome

The annual rainfall in Broome fluctuates from 132 to 1496 mm (Figure 5.4) and shows a slight increasing trend during 1941-2011. STARS detected a small shift after 1997, with an increase of approximately 40−50 mm per decade. From 1942 to 1997, Broome rainfall averaged 554 mm per year. From 1997 to 2016 this has increased 41 % to 780 mm. Long chain alkanes, which are derived from land plants and are an indicator of terrestrial input, increased in Both Broome 1 and 2 cores in the late 1990s.

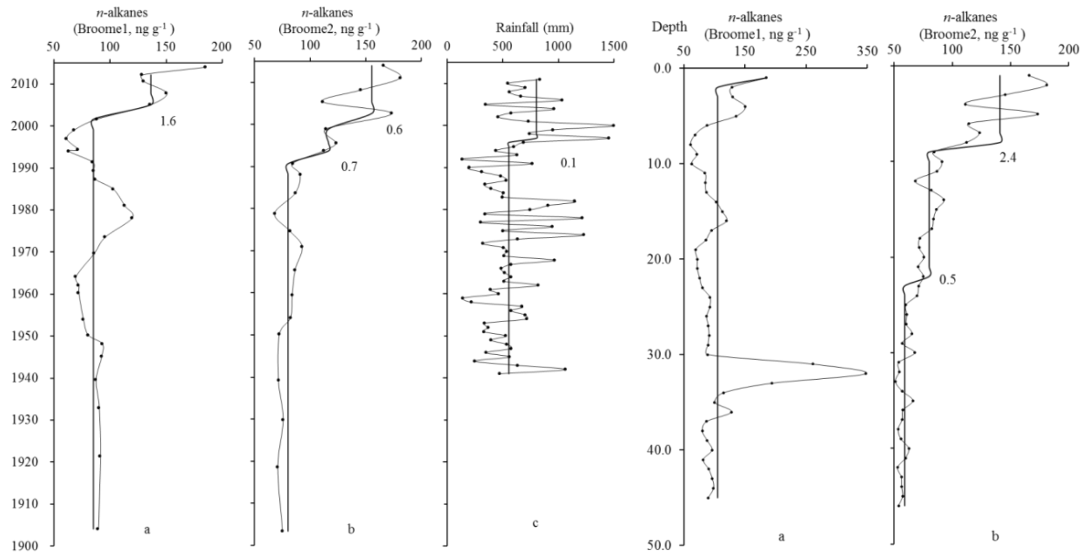

Figure 5.10. Profiles of terrestrial records: long chain *n*-alkanes contents at Broome1 (a) and at Broome2 (b). The left two panels are shown against the aged section of the core and the two right panels are shown for the depth of the core the analyses were applied to. Rainfall records for Broome airport (Bureau of Meteorology) are also shown with the lines showing shift changes assessed by STAR, and numbers showing regime shift index (RSI).

6.2.6 Phytoplankton proxies

Brassicasterol, dinosterol and alkenones are proxies for biomass of diatoms, dinoflagellates and haptophytes respectively. In the Broome 1 core all three biomarkers show an increasing trend from the late 1990s (Figure 5.11. Brassicasterol in particular shows an abrupt, significant increase from 1997. Both dinosterol and alkenones increased significantly after 2000 (Figure 5.11). In the core from Broome 2 all three biomarkers also increased significantly with brassicasterol and dinosterol increasing significantly in the early 1990s and then again in the mid-2000s.

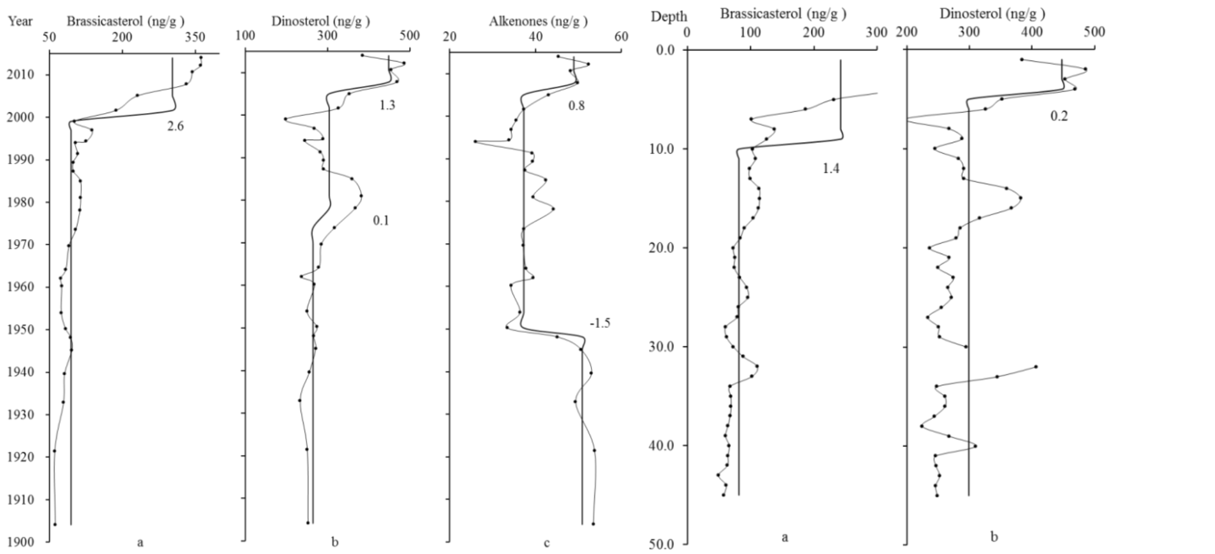

Figure 5.11. Profiles of (a) brassicasterol, (b) dinosterol, and, (c) alkenone at Broome1. The left three panels are shown against the aged section of the core and the two right panels are shown for the depth of the core the analyses were applied to.

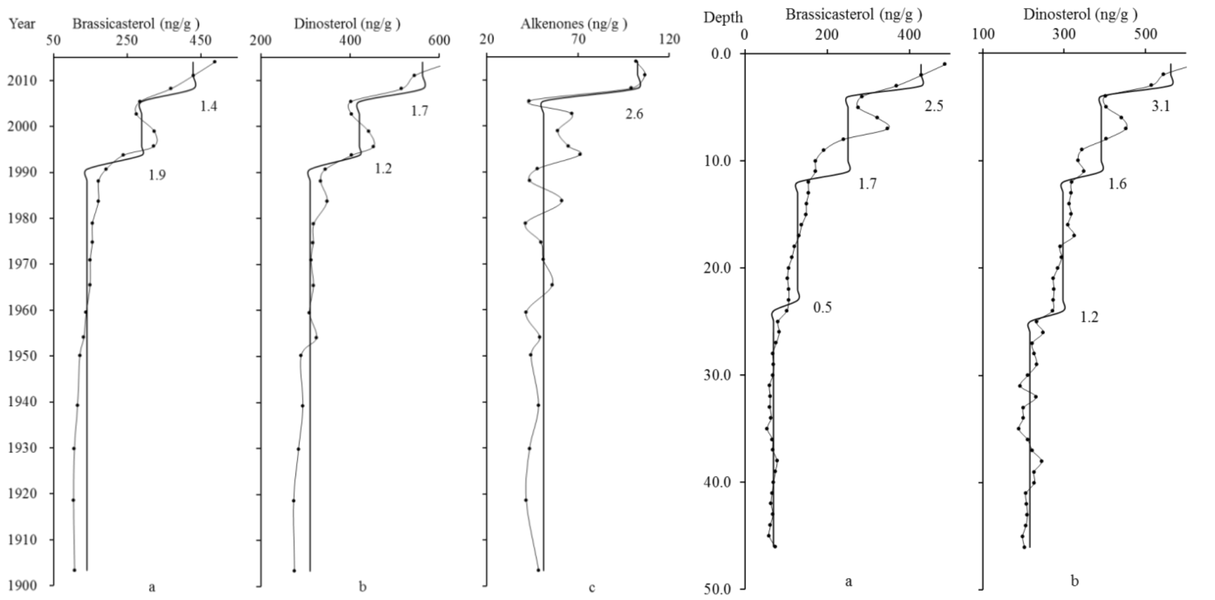

Figure 5.12. Profiles of (a) brassicasterol, (b) dinosterol, and, (c) alkenone at Broome2. The left two panels are shown against the aged section of the core and the two right panels are shown for the depth of the core the analyses were applied to.

6.3 Discussion

6.3.1 Impact of Broome city runoff and industrial discharges on coastal water quality and sediment characteristics

Broome is the largest population center in the Kimberley and in 2015 had a population of 17,000 people (Australian Bureau of Statistics) although during the tourist season this swells significantly. Issues of significance from a water quality point of view in Broome are the discharge from Dampier Creek which carries much of the runoff from the city, the Waste Water Treatment Plant (WWTP) and the golf course which are both close to the coast on the western side of the city. The annual flushing of Dampier creek each wet season (Late December or January to March carries a significant amount of nutrients into Roebuck Bay with the first 30% of runoff contributing 40-70 of total nutrient exports (Gunaratne et al. 2016). This means the majority of nutrients will discharge in January in most years. The WWTP (Figure 5.13) has been the source of controversy recently amid claims that sewage has been leaking from one or more of the bonds into Roebuck Bay (www.abc.net.au/news/2016-11-30/broome-marine-park-sewage-pollution-contested/8079620). The Broome golf course has used recycled wastewater from the WWTP for 20 years and there are concerns this has led to contaminated ground water (www.abc.net.au/news/2015-08-05/potential-groundwater-contamination-at-broome-golf-course/6674140?site=kimberley). This as well as unutilised nutrients from the irrigation are another potential sourced of nutrients entering Roebuck Bay. There was also a meatworks and abattoir which drained effluent into Roebuck Bay (Figure 5.1). The Derby Meat Processing Company and Demtel (from 1976) processed up to 50,000 head per year and operated between 1939 and 1983 when it closed due to the live cattle export trade (Source Heritage Council Government of WA inherit.stateheritage.wa.gov.au/Public/Inventory/Details/47cd2966-f06a-413b-bc35-fc7ebac727ae)

Levels of ^{15}Nitrogen an indicator of anthropogenic nitrogen increased gradually, but significantly at site Broome 1 from about 1960 (20 cm core depth, Figure 5.7) although it should be noted that the highest levels reached near the surface at about 2010 had occurred previously much deeper in the core (56-71 cm and 97-110 cm). Nevertheless, the trend of increasing ^{15}N since 1960 is very significant (Figure 5.7) and when compared with reference site (Broome 2) are highly suggestive of a real increase in anthropogenic nitrogen at Broome 1. Firstly, at both sites the total nitrogen increased significantly since about 1990 – 2000 while the ^{15}N at Broome 2 varied little over the period since 1960 (Figure 5.7). Secondly the ratio of ^{15}N at the two sites shows a significantly increasing linear trend at Broome 1 since 1959 (R^2=0.683, $p<0.0001$) and that since 1980 ^{15}N levels at site Broome 1 have been higher than at Broome 2 (Figure 5.14). Over the same period the relative proportion of Total Nitrogen was less at Broome 2 (Figure 5.14). Coprostanol, a biomarker of sewage was at levels close to detection in the samples and thus there was no evidence of significant sewage pollution detected in the cores.

Concerns of pollution affecting the ecology of Roebuck Bay have been highlighted since the annual (wet season) blooms of the blue green algae *Lyngbya cf. majuscula* began in 2005 (Estrella et al. 2011, Estrella 2013) and these authors also cite evidence of anthropogenic nitrogen levels were high enough to be detected in algae from Roebuck Bay. *Lyngbya* is not limited by nitrogen but is known to respond to phosphorus and iron enrichment. We did not measure these nutrients in our cores.

Cores taken within the intertidal area closer to Broome Town Beach may be more instructive as to both the time course of nutrient pollution and the history and spread of *Lyngbya* through the use of specific biomarkers for cyanobacteria such as zeaxanthin (Bianchi et al. 2000).

Figure 5.13. Broome Waste Water Treatment Plant (WWTP) as seen from Roebuck Bay. Broome city is to the right (east) of the picture. The golf course can be seen to the left (west) of the WWTP.

Source: www.abc.net.au/news/2016-11-30/broome-sewage-treatment/8079664

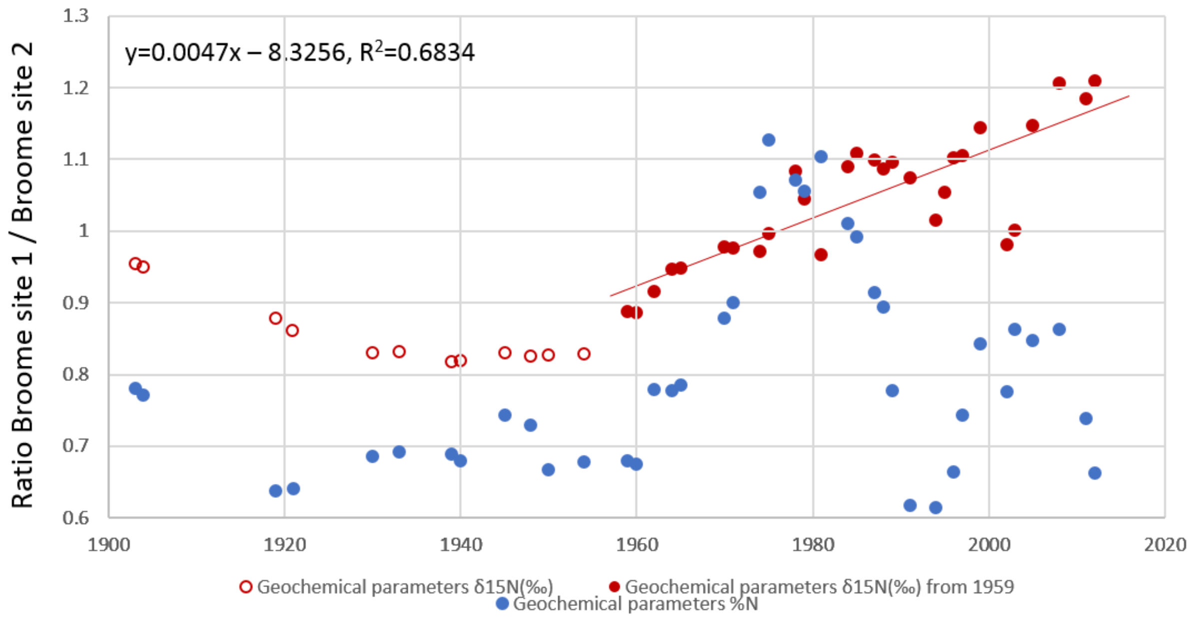

Figure 5.14. Ratio of Broome 1/ Broome 2 levels of Total Nitrogen and 15Nitrogen over 100 years.

6.3.2 Climate change impacts on terrestrial inputs and phytoplankton patterns

Climate change has had a significant impact on rainfall and temperature in the Kimberley (Shi et al. 2000, Zinke et al. 2015). Significantly increased rainfall in the Kimberley as a whole has occurred since the 1950s (Figure 5.15; Shi et al. 2000) and Broome rainfall shows a 41% increase since 1997 with average rainfall of 780 mm compared with 554 mm between 1940 and 1996 (Figure 5.16).

Ocean temperatures in the northwest of Australia have also risen especially in the last two decades with an increase in anomalous warm events superimposed on an overall trend of increasing water temperature. (Lough 2008, Zinke et al. 2015, Feng et al. 2015). Temperature reconstructed from the TEX_{86} biomarker is broadly consistent with this showing an increasing temperature trend over time with this being the clearest in the Broome 1 core with temperatures increasing from about 1974 and again after 1997 (Figures 5.9 and 5.18).

The coincidence of temperature and rainfall increases since the late 1990s make it difficult to determine which of these factors may have had the greatest influence on water quality indicators as represented in the sediment. In addition, Tropical Cyclone (TC) Rosita passed just 15 km south of Broome in April 2000 causing significant erosion and loss of coastal vegetation along the eastern side of Roebuck Bay and this may have also influenced our results. (Bennelongia 2009). Figure 5.19 shows that long chain alkanes, an indicator of land plant derived material, were elevated in Broome 1 core in years following increased rainfall between 1974 and 1982 and again in the late 1990s, albeit with a lag. The increase in alkanes at Broome 2 was more variable but also increased in the late 1990s. There was a significant correlation between alkanes and TEX_{86} temperature ($p<0.0001$) and alkanes and rainfall with a one-year lag ($p=0.003$) at Broome 1 and between alkanes and rainfall with a two-year lag ($p=0.016$) at Broome 2 (Table 5.1). The model which best predicted the alkane profile at Broome 1 combined TEX_{86} temperature and rainfall with a one-year lag explaining 52% of the variability ($p<0.0001$) although the model was not a significant improvement over using TEX_{86} alone as a predictor (Table 5.2), while no model combining temperature and rainfall was significant at Broome 2 (Table 5.2).

Figure 5.20 shows the profiles for biomarkers of diatoms (brassicasterol), dinoflagellates (dinosterol) and haptophytes (alkenones) along with Total Organic Carbon (TOC) and Total Nitrogen (TN) for both Broome cores with periods of significant rainfall periods around the late 1970s and 1990s shown on the graphs. At both Broome 1 and Broome 2, all parameters showed significant increases after the late 1990s coincident with both temperature and rainfall increases. At Broome 1 dinosterol, TOC and TN showed a possible response to significant rainfall events around the late 1970s, while at Broome 2 none of the parameters indicated such a response.

At Broome 1, all five parameters were significantly correlated with TEX_{86} temperature (Table 5.1, $p=0.008$ to <0.0001) and all were significantly correlated with Broome rainfall with a one-year lag (Table 5.1, $p=0.037$ to 0.001). At Broome 2, none of the parameters showed any significant correlation with rainfall or temperature (Table 5.1). Table 5.2 shows the results of multiple regression analyses on all five parameters and shows that no model which combined both TEX86 temperature and rainfall improved the prediction which could be obtained from using TEX86 temperature alone.

In summary, the results from the Broome cores indicate that while increased rainfall since the late 1990s and the passing of TC Rosita in 2000 is likely to have had an influence on the amount of land based plant material incorporated into sediments, that increased temperature rather than increased rainfall had the greatest influence on phytoplankton biomass, TOC and TN. Although the study was limited to two sites in Roebuck Bay, the consistency of this data with those from the Cygnet Bay and King George River sites suggest that it is likely that ocean warming in this region has had a significant increase in primary production in the region based on these results.

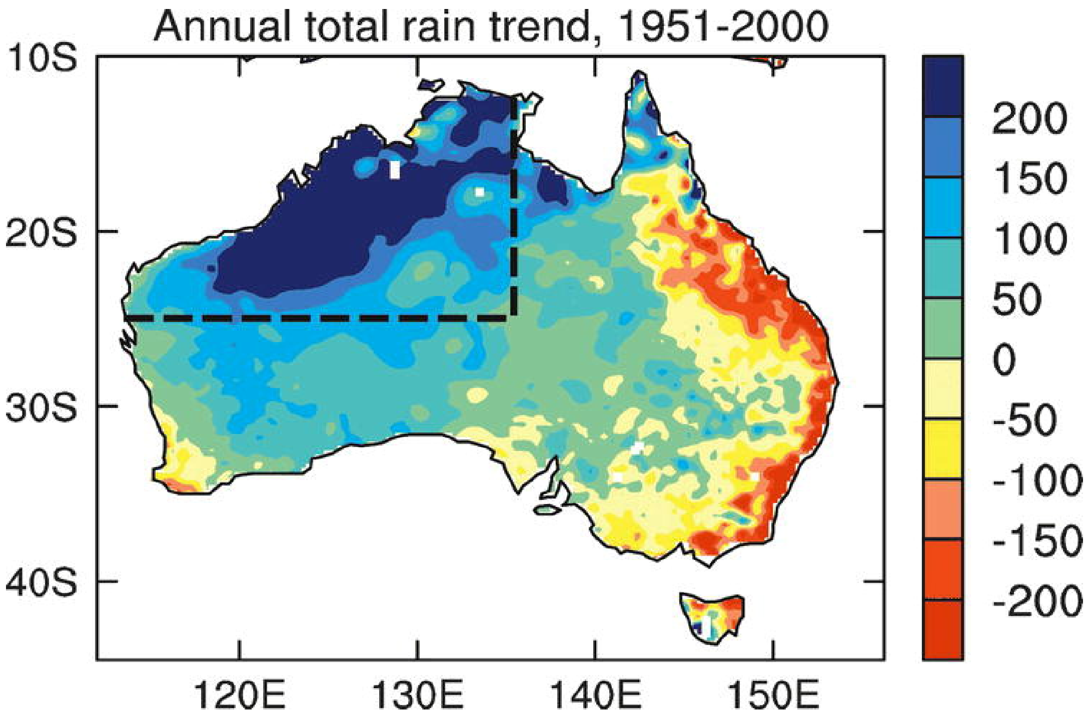

Figure 5.15. Observed annual total rainfall trend (mm) based on the BMRC rainfall data over 1951–2000. Blue colour shows rainfall increase and red indicates rainfall reduction. Source: Shi et al. 2000).

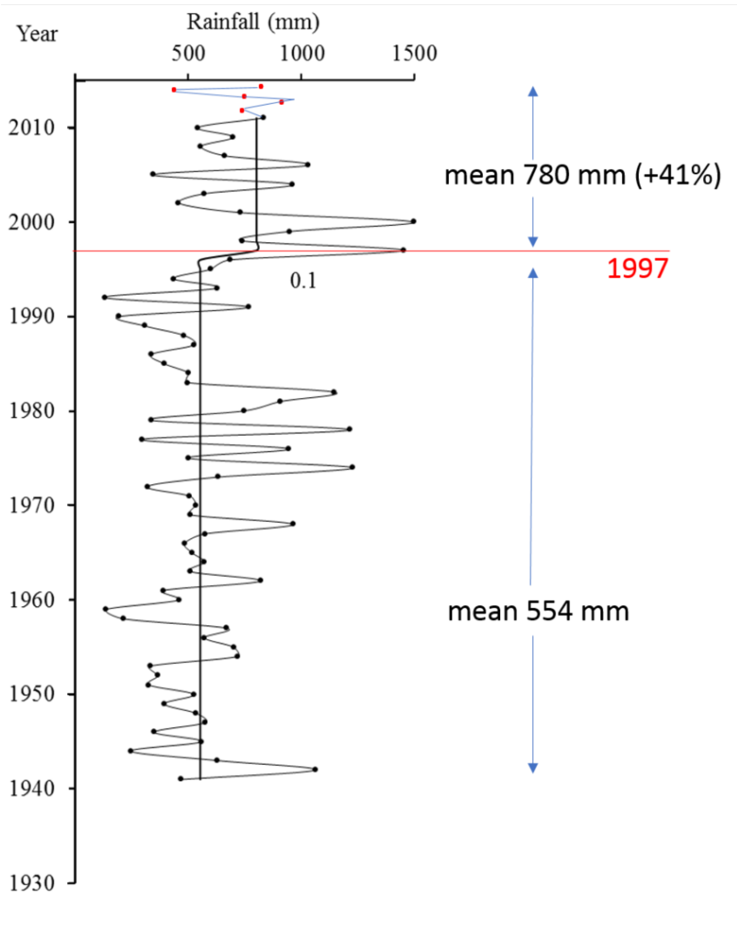

Figure 5. 16. Rainfall record for Broome. The solid lines show shift trends assessed by sequential *t*-test analysis of regime shift and numbers are regime shift index (RSI).

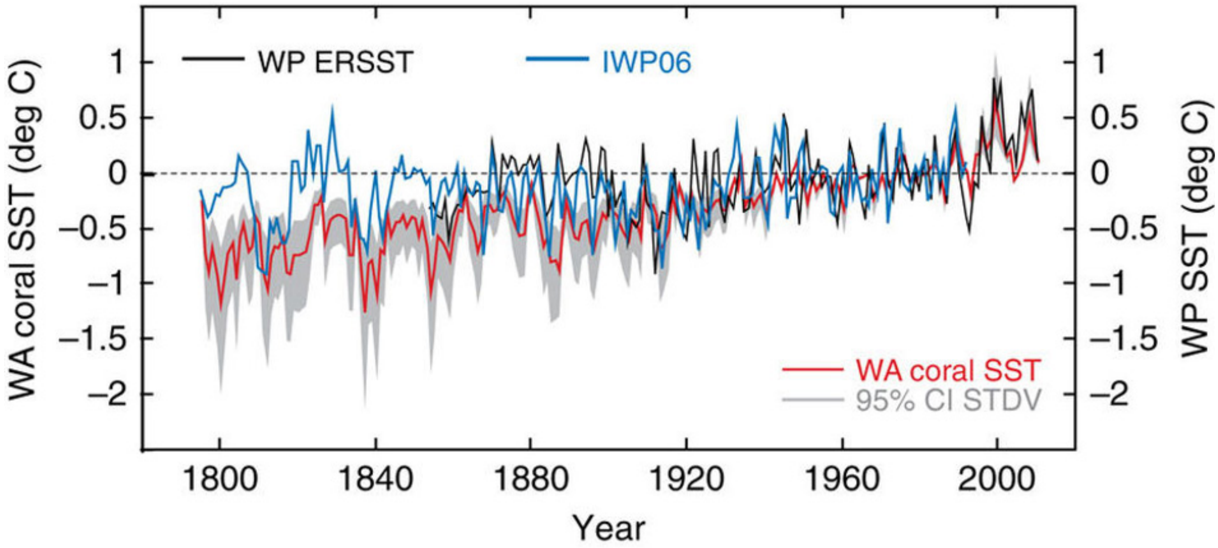

Figure 5.17. Reconstruction of SST anomaly (red) from coral core chronology with 95% confidence interval (grey shaded) based on the spread of both coral and ERSST standard deviations between 1961 and 1990 compared with Indonesian warm pool (IWP06; blue) and WP SST anomaly reconstructions (WP ERSST; black). SST anomalies are relative to 1961–1990 mean. Source: Zinke et al. 2015.

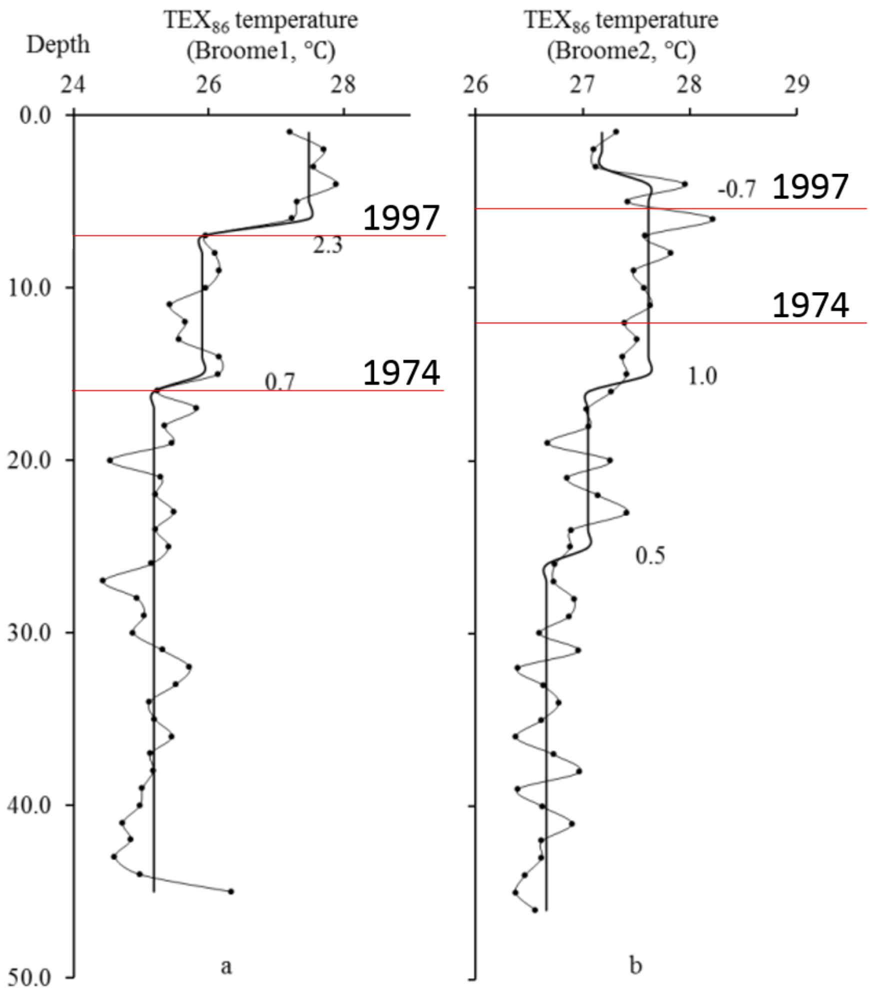

Figure 5.18. TEX_{86} temperature reconstruction for the two Broome sites. The solid lines show shift trends assessed by sequential *t*-test analysis of regime shift and numbers are regime shift index (RSI).

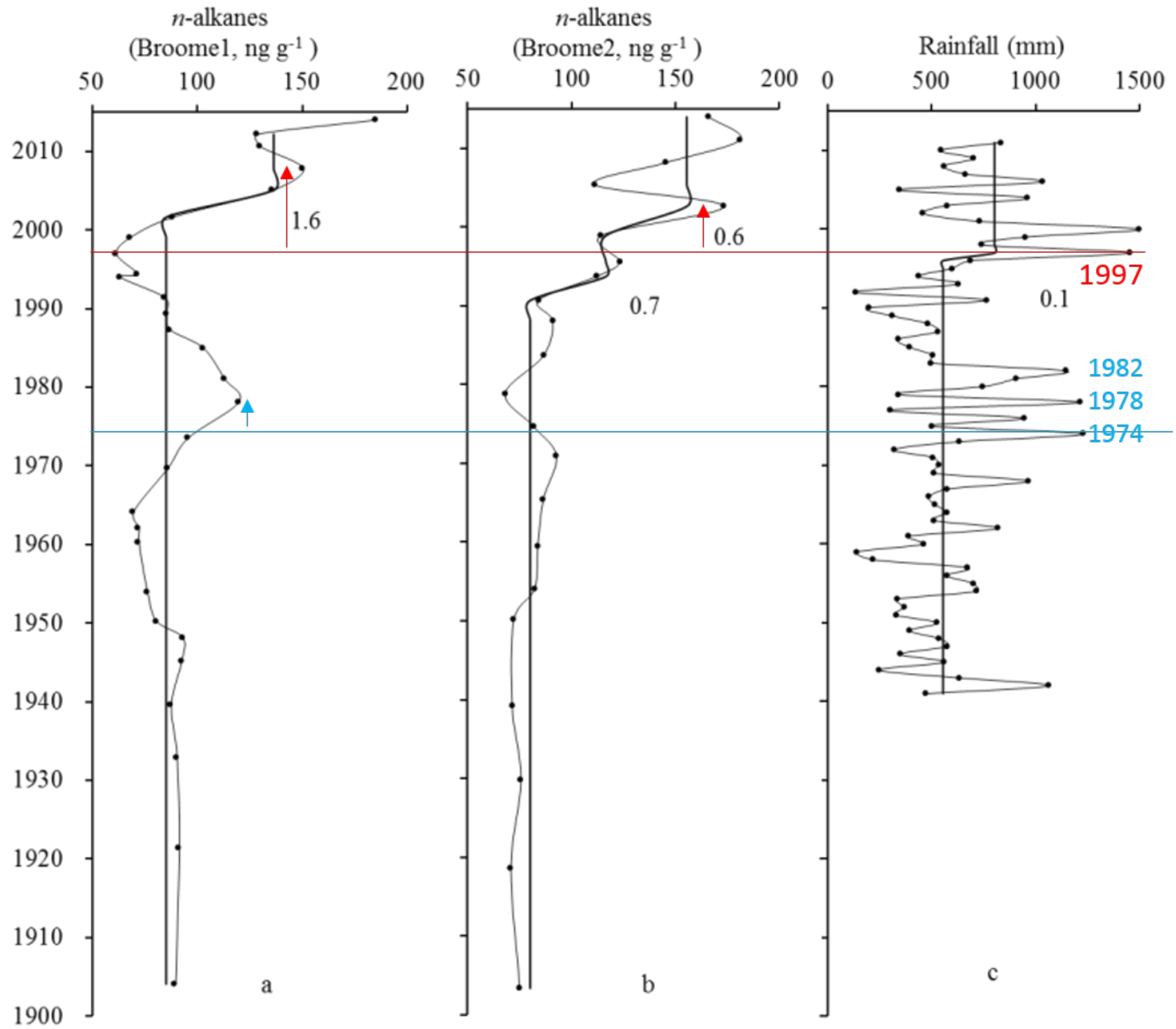

Figure 5.19. Long chain *n*-alkane (27+29+31) profiles at the two Broome core sites compared to Broome rainfall. The solid lines show shift trends assessed by sequential *t*-test analysis of regime shift and numbers are regime shift index (RSI).

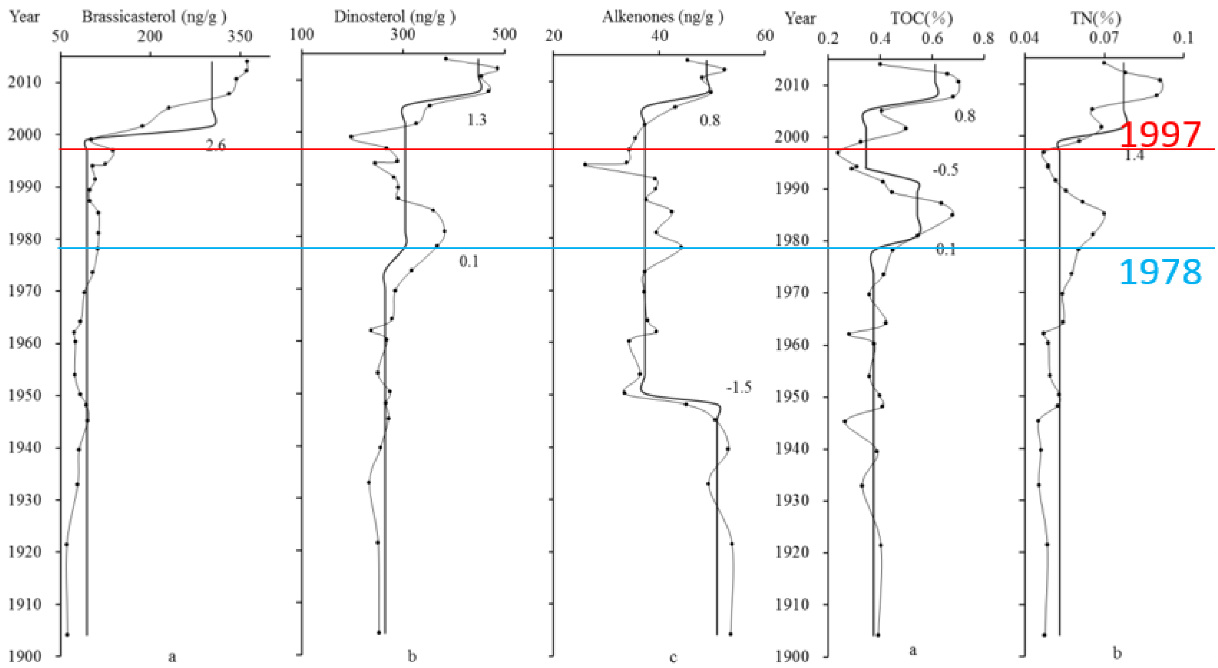

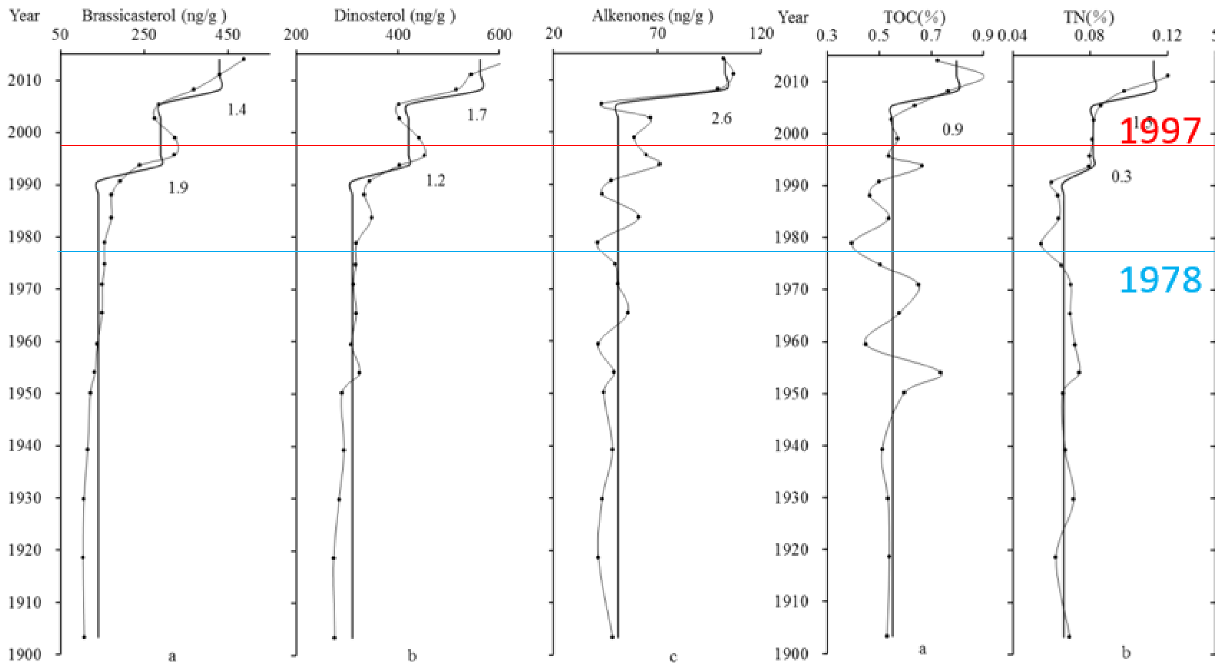

Figure 5.20. Biomarker profiles at the two Broome core sites (Broome 1 upper panel, Broome 2 lower panel) compared to dates of significant periods of increased rainfall at Broome. The solid lines show shift trends assessed by sequential *t*-test analysis of regime shift and numbers are regime shift index (RSI).

Table 5.1. Correlation matrix for biogeochemical and biomarker parameters against possible explanatory variables of temperature and rainfall using data from both cores back to 1945.

Broome Site 1

Variables	%N	δ15N (‰)	TOC(%)	δ13C (‰)	C/N	Brassi (ng/g)	Dino (ng/g)	Alkenone (ng/g)	long chain n-alkane (27+29+31) (ng/g)
Temp-TEX86	**< 0.0001**	**< 0.0001**	**0.002**	**0.008**	0.899	**< 0.0001**	**< 0.0001**	**0.001**	**< 0.0001**
rainfall (mm)	0.479	0.563	0.889	0.324	0.622	0.937	0.928	0.809	0.995
rainfall 1 y lag	**0.001**	0.063	**0.017**	**0.016**	0.446	**0.037**	**0.003**	**0.040**	**0.003**
rainfall 2 y lag	**0.019**	0.171	0.124	0.721	0.808	0.052	0.103	0.165	0.092

Broome Site 2

Variables	%N	δ15N (‰)	TOC(%)	δ13C (‰)	C/N	Brassi (ng/g)	Dino (ng/g)	Alkenone (ng/g)	long chain n-alkane (27+29+31) (ng/g)
Temp-TEX86	0.972	**< 0.0001**	0.118	0.748	**0.014**	0.089	0.274	0.872	0.319
rainfall (mm)	0.496	0.217	0.662	0.209	0.096	0.302	0.287	0.352	0.192
rainfall 1 y lag	0.324	**0.050**	0.834	0.997	0.069	0.075	0.077	0.158	0.118
rainfall 2 y lag	0.139	0.210	0.521	0.861	0.163	0.211	0.273	0.486	**0.016**

Table 5.2. Results of multiple regression modelling of biogeochemical and biomarker parameters against possible models combining temperature and rainfall as explanatory variables using data from both cores back to 1945. The R^2 value and probability is shown for the best model fit for each parameter unless no model explained a significant amount of the temporal variability. *denotes those models which were a better predictor than TEX86 temperature alone.

Broome Site 1	%N	δ15N (‰)	TOC(%)	δ13C (‰)	C/N	Brassi (ng/g)	Dino (ng/g)	Alkenone (ng/g)	long chain n-alkane (27+29+31) (ng/g)
R^2	0.719	0.478	0.309	0.265	0.027	0.826	0.594	0.302	0.518
F	38.451	13.753	6.705	5.397	0.422	71.094	21.989	6.481	16.127
Pr > F	< 0.0001	< 0.0001	0.004	0.010	0.660	< 0.0001	< 0.0001	0.005	< 0.0001
Temp-TEX86	46.646	24.078	6.003	3.685	0.263	142.152	24.864	7.407	16.142
	< 0.0001	< 0.0001	0.020	0.064	0.612	< 0.0001	< 0.0001	0.011	0.000
rainfall (mm)						1.692			
						0.203			
rainfall 1-year lag	3.836		1.892	2.426	0.828		3.063	0.863	3.430
	0.060		0.179	0.130	0.370		0.090	0.360	0.074
rainfall 2-year lag		0.299							
		0.589							

Broome Site 2	%N	δ15N(‰)	TOC(%)	δ13C(‰)	C/N	Brassi(ng/g)	Dino(ng/g)	Alkenone(ng/g)	long chain n-alkane (27+29+31) (ng/g)
R^2	0.089	0.498	0.091	0.058	0.255	0.171	0.130	0.089	0.223
F	1.513	15.383	1.559	0.950	5.295	3.201	2.320	1.511	4.439
Pr > F	0.236	< 0.0001	0.226	0.398	0.011	0.054	0.115	0.237	0.020
Temp-TEX86		23.656	2.675	0.294	6.449	2.813			
		< 0.0001	0.112	0.592	0.016	0.104			
rainfall (mm)				1.793			1.281	0.935	
				0.190			0.266	0.341	
rainfall 1-year lag	0.743	5.314			3.402	3.123	3.380	2.100	2.118
	0.395	0.028*			0.075	0.087	0.076	0.157	0.156
rainfall 2-year lag	1.992		0.570						5.909
	0.168		0.456						0.021

7 References

Abballe PA (2012) The origin and transport of terrestrial organic matter to two contrasting environments of the Australian continental shelf. PhD thesis. School of Earth and Environmental Sciences. University Wollongong, http://ro.uow.edu.au/theses/3561

Abbs D (2012) The impact of climate change on the climatology of tropical cyclones in the Australian region. Retrieved September, 5, 2014

Abelmann A, Gersonde R, Cortese G, Kuhn G, Smetacek V (2006) Extensive phytoplankton blooms in the Atlantic sector of the glacial Southern Ocean, Paleoceanography, 21, PA1013, doi:10.1029/2005PA001199

Abo K and Toda S (2001) Evaluation model of farming density of Japanese pearl oyster, *Pinctada fucatamartensii*, based on physiology and food environment. B J Jpn Soc Fish Oceanogr Tokyo 65: 4135–4144

Ajani PA, Allen AP, Ingleton T and Armand L (2014) A decadal decline in relative abundance and a shift in microphytoplankton composition at a long-term coastal station off southeast Australia. Limnol. Oceanogr, 59, 519-531

Amos KJ, Croke JC, Timmers H, Owens PN, Thompson C (2009) The application of caesium-137 measurements to investigate floodplain deposition in a large semi-arid catchment in Queensland, Australia: a low-fallout environment. Earth Surf Processes Landforms 34: 515–529

Andersen JH, Conley DJ, Hedal S (2004) Palaeoecology, reference conditions and classification of ecological status: the EU Water Framework Directive in practice. Mar Pollut Bull 49: 283−290

Andersen T, Carstensen J, Hernàndez-García E, Duarte CM (2009) Ecological thresholds and regime shifts: approaches to identification. Trends Ecol Evol 24: 49–57

Andréfouët S, Charpy L, Lo-Yat A, Lo C (2012) Recent research for pearl oyster aquaculture management in French Polynesia. Mar Pollut Bull 25: 407–414

Andrews JE, Greenaway AM, Dennis PF (1998) Combined carbon isotope and C/N ratios as indicators of source and fate of organic matter in a poorly flushed, tropical estuary: Hunts Bay, Kingston Harbour, Jamaica. Estuar Coast Shelf Sci 46: 743–756

Appleby PG (2001) Chronostratigraphic techniques in recent sediments. In: Last WM, Smol JP (ed) Tracking Environmental Change Using Lake Sediments. Volume 1: Basin Analysis, Coring, and Chronological Techniques. Kluwer Academic Publishers, Dordrecht, The Netherlands, p 171–203

Appleby PG and Oldfield F (1978) The calculation of lead-210 dates assuming a constant rate of supply of unsupported 210Pb to the sediment. Catena, 5, 1–8

Ajani PA, Allen AP, Ingleton T and Armand L (2014) A decadal decline in relative abundance and a shift in microphytoplankton composition at a long-term coastal station off southeast Australia. Limnology and Oceanography, 59, 519-531

Armbrecht LH, Thompson PA, Wright SW, Schaeffer A, Roughan M, Henderiks J and Armand LK (2015) Comparison of the cross-shelf phytoplankton distribution of two oceanographically distinct regions off Australia. Journal of Marine Systems, 148, 26-38

Barbosa AB, Domingues RB, Galvão HM (2010) Environmental forcing of phytoplankton in a Mediterranean Estuary (Guadiana Estuary, South-western Iberia): a decadal study of anthropogenic and climate influences. Estuar Coast 33: 324–341

Beaugrand G and Reid PC (2003) Long-term changes in phytoplankton, zooplankton and salmon related to climate. Glob Change Biol 9: 801–817

Behrenfeld MJ, O'Malley RT, Siegel DA, McClain CR, Sarmiento JL, Feldman GC, Milligan AJ, Falkowski PG, Letelier RM, Boss ES (2006) Climate-driven trends in contemporary ocean productivity. Nature, 444, 752-755

Behrenfeld MJ, Randerson JT, McClain CR, Feldman GC, Los SO, Tucker CJ, Falkowski PG, Field CB, Frouin R, Esaias WE (2001) Biospheric primary production during an ENSO transition. Science, 291, 2594-2597

Belkin IM (2009) Rapid warming of large marine ecosystems. Progress in Oceanography, 81, 207-213

Bennelongia (2009) Ecological Character Description for Roebuck Bay. Report to the Department of Environment and Conservation. Bennelongia Pty Ltd, Jolimont

Bertrand A, Segura M, Gutiérrez M, Vásquez L (2004) From small‐scale habitat loopholes to decadal cycles: a habitat‐based hypothesis explaining fluctuation in pelagic fish populations off Peru. Fish and fisheries, 5, 296-316

Berdalet E, Peters F, Koumandou VL, Roldan C, Guadayol O, Estrada M (2007) Species‐specific physiological response of dinoflagellates to quantified small‐scale turbulence. Journal of phycology, 43, 965-977

Bernárdez P, Prego R, Francés G, González-Álvarez R (2005) Opal content in the Ría de Vigo and Galician continental shelf: biogenic silica in the muddy fraction as an accurate paleoproductivity proxy. Cont Shelf Res 25: 1249–1264

Bianchi TS, Engelhaupt E, Westman P, Andren T, Rolff C, Elmgren R (2000) Cyanobacterial blooms in the Baltic Sea: Natural or human-induced?. Limnology and Oceanography, 45(3), 716-726

Boyce DG, Lewis MR, Worm B (2010) Global phytoplankton decline over the past century. Nature, 466, 591-596

Bratton JF, Colman SM, Seal RR (2003) Eutrophication and carbon sources in Chesapeake Bay over the last 2700yr: human impacts in context. Geochim Cosmochim Acta 67: 3385–3402

Brodie J and Waterhouse J (2012) A critical review of environmental management of the 'not so Great'Barrier Reef. Estuarine, Coastal and Shelf Science, 104, 1-22

Bureau of Meteorology (2014a) Australian climate average conditions—average conditions maps. http://www.bom.gov.au/climate/averages/maps.shtml

Bureau of Meteorology (2014b). Australian climate date online (Station: Broome Airport; Station number: 003003) http://www.bom.gov.au/climate/data/?ref=ftr

Burford MA, Alongi D, McKinnon A and Trott L (2008) Primary production and nutrients in a tropical macrotidal estuary, Darwin Harbour, Australia. Estuarine, Coastal and Shelf Science, 79, 440-448

Burford MA, Rothlisberg PC and Revill AT (2009) Sources of nutrients driving production in the Gulf of Carpentaria, Australia: a shallow tropical shelf system. Marine and Freshwater Research, 60, 1044-1053

Burford MA, Webster I, Revill A, Kenyon R, Whittle M and Curwen G (2012) Controls on phytoplankton productivity in a wet–dry tropical estuary. Estuarine, Coastal and Shelf Science, 113, 141-151

Burns KA, Volkman JK, Cavanagh JA and Brinkman D (2003) Lipids as biomarkers for carbon cycling on the Northwest Shelf of Australia: results from a sediment trap study. Marine chemistry, 80, 103-128

Cai W, Meyers G and Shi G (2005) Transmission of ENSO signal to the Indian Ocean. Geophysical research letters, 32

Cai W, Van Rensch P, Cowan T and Sullivan A (2010) Asymmetry in ENSO teleconnection with regional rainfall, its multidecadal variability, and impact. Journal of Climate, 23, 4944-4955

Cai W, Cowan T, Sullivan A, Ribbe J and Shi G (2011) Are anthropogenic aerosols responsible for the northwest Australia summer rainfall increase? A CMIP3 perspective and implications. Journal of Climate, 24, 2556-2564

Castañeda IS and Schouten S (2011) A review of molecular organic proxies for examining modern and ancient lacustrine environments. Quaternary Science Reviews, 30, 2851-2891

Callier MD, McKindsey CW, Desrosiers G (2008) Evaluation of indicators used to detect mussel farm influence on the benthos: Two case studies in the Magdalen Islands, Eastern Canada. Aquaculture 278: 77–88

Chavez F, Pennington J, Castro C, Ryan J, Michisaki R, Schlining B, Walz P, Buck K, McFadyen A, Collins C (2002) Biological and chemical consequences of the 1997–1998 El Niño in central California waters. Progress in Oceanography, 54, 205-232

Chavez F, Strutton P, Friederich G, Feely R, Feldman G, Foley D, McPhaden M (1999) Biological and chemical response of the equatorial Pacific Ocean to the 1997-98 El Niño. Science, 286, 2126-2131

Chavez FP, Messié M, Pennington JT (2011) Marine primary production in relation to climate variability and change. Annual Review of Marine Science, 3, 227-260

Chen W, Mohtadi M, Schefuß E, Mollenhauer G (2014) Organic-geochemical proxies of sea surface temperature in surface sediments of the tropical eastern Indian Ocean. Deep Sea Research Part I: Oceanographic Research Papers, 88, 17-29

CENRM, Centre of Excellence in Natural Resource Management (2010) Fitzroy River Catchment Management Plan. The University of Western Australia

Cheney DP, Haws MC, Ponia BE, Thomforde HW (1995) Ecological characterization and environmental monitoring in conjunction with pearl farming of the Tongareva Lagoon, Cook Islands. Aquaculture 95. Proceedings of the World Aquaculture Society Meeting, San Diego, California. February 1995 (abstract). i0730-8000-25-1-141–b4

Chong PL (2010) Archaebacterial bipolar tetraether lipids: physico-chemical and membrane properties. Chemistry and Physics of Lipids, 163, 253-265

Clarke AJ and Liu X (1994). Interannual sea level in the northern and eastern Indian Ocean. Journal of physical oceanography, 24, 1224-1235

Cloern JE, Jassby AD, Thompson JK, Hieb KA (2007) A cold phase of the East Pacific triggers new phytoplankton blooms in San Francisco Bay. Proceedings of the National Academy of Sciences, 104, 18561-18565

Cifuentes LA, Coffin RB, Solorzano L, Cardenas W, Espinoza J, Twilley RR (1996) Isotopic and elemental variation of carbon and nitrogen in a mangrove estuary. Estuar Coast Shelf Sci 43: 781–800

Condie S, Herzfeld M, Margvelashvili N, Andrewartha J (2009) Modeling the physical and biogeochemical response of a marine shelf system to a tropical cyclone. Geophysical research letters, 36

Condie SA (2011) Modeling seasonal circulation, upwelling and tidal mixing in the Arafura and Timor Seas. Continental Shelf Research, 31, 1427-1436

Crocker DE, Costa DP, Le Boeuf BJ, Webb PM, Houser DS (2006) Impact of El Niño on the foraging behavior of female northern elephant seals. Marine Ecology-Progress Series, 309

Cropp RA, Gabric AJ, Levasseur M, McTainsh GH, Bowie A, Hassler C, Law C, McGowan H, Tindale N, Rossel RV (2013) The likelihood of observing dust-stimulated phytoplankton growth in waters proximal to the Australian continent. Journal of Marine Systems, 117, 43-52

da Costa KG, Nalesso RC (2006) Effects of mussel farming on macrobenthic community structure in Southeastern Brazil. Aquaculture 258:655–663

D'Adamo N, Fandry C, Buchan S, Domingues C (2009) Northern sources of the Leeuwin current and the "Holloway Current" on the North West Shelf. Journal of the Royal Society of Western Australia, 92, 53-66

Dale B (2009) Eutrophication signals in the sedimentary record of dinoflagellate cysts in coastal waters. J Sea Res 61: 103–113

DeMaster DJ (2002) The accumulation and cycling of biogenic silica in the Southern Ocean: revisiting the marine silica budget. Deep Sea Res Part II 49: 3155–3167

DeMaster DJ, Nelson TM, Harden SL, Nittrouer CA (1991) The cycling and accumulation of biogenic silica and organic carbon in Antarctic deep-sea and continental margin environments. Mar Chem 35: 489–502

Deser C, Phillips AS, Hurrell JW (2004) Pacific interdecadal climate variability: Linkages between the tropics and the North Pacific during boreal winter since 1900. Journal of Climate, 17, 3109-3124

Dumbauld BR, Ruesink JL, Rumrill SS (2009) The ecological role of bivalve shellfish aquaculture in the estuarine environment: A review with application to oyster and clam culture in West Coast (USA) estuaries. Aquaculture 290:196–223

Doney SC (2006) Oceanography: Plankton in a warmer world. Nature, 444, 695-696

Egge JK and Aksnes DL (1992) Silicate as regulating nutrient in phytoplankton competition. Marine ecology progress series, 83, 281-289

Eglinton G & Hamilton RJ (1967) Leaf epicuticular waxes. Science, 156, 1322

Eglinton TI & Eglinton G (2008) Molecular proxies for paleoclimatology. Earth and Planetary Science Letters, 275, 1-16

Elling FJ, Könneke M, Lipp JS, Becker KW, Gagen EJ, Hinrichs KU (2014) Effects of growth phase on the membrane lipid composition of the thaumarchaeon Nitrosopumilus maritimus and their implications for archaeal lipid distributions in the marine environment. Geochimica et Cosmochimica Acta, 141, 579-597

Elling FJ, Könneke M, Mußmann M, Greve A, Hinrichs KU (2015) Influence of temperature, pH, and salinity on membrane lipid composition and TEX 86 of marine planktonic thaumarchaeal isolates. Geochimica et Cosmochimica Acta, 171, 238-255

Eppley RW (1972) Temperature and phytoplankton growth in the sea. Fish. Bull, 70, 1063-1085

Estrella SM (2013) Effects of nutrient enrichment and toxic Lyngbya blooms on benthic invertebrates-and migratory shorebird communities of Roebuck Bay Ramsar site. Final report to the NRM Office, WA. May 2013

Estrella SM, Storey AW, Pearson G, Piersma T (2011) Potential effects of Lyngbya majuscula blooms on benthic invertebrate diversity and shorebird foraging ecology at Roebuck Bay, Western Australia: preliminary results. Journal of the Royal Society of Western Australia, 94(2), 171-179

Folk RL, Andrews PB, Lewis DW (1970) Detrital sedimentary rock classification and nomenclature for use in New Zealand. N Z J Geol Geophys 13: 937–968

Fang Y, Chen Y, Tian C, Lin T, Hu L, Huang G, Tang J, Li J, Zhang G (2015) Flux and budget of BC in the continental shelf seas adjacent to Chinese high BC emission source regions, Global Biogeochem. Cycles, 29, 957–972, doi:10.1002/2014GB004985

Feng M, Böning C, Biastoch A, Behrens E, Weller E, Masumoto Y (2011) The reversal of the multi-decadal trends of the equatorial Pacific easterly winds, and the Indonesian Throughflow and Leeuwin Current transports, Geophys. Res. Lett., 38, L11604, doi:10.1029/2011GL047291

Feng M, Hendon HH, Xie SP, Marshall AG, Schiller A, Kosaka Y, Caputi N, Pearce A (2015) Decadal increase in Ningaloo Niño since the late 1990s, Geophys. Res. Lett., 42, 104-112, doi:10.1002/2014GL062509

Feng M, Colberg F, Slawinski D, Berry O, Babcock R. (2016) Ocean circulation drives heterogeneous recruitments and connectivity among coral populations on the North West Shelf of Australia. Journal of Marine Systems, 164, 1-12

Feng J, Li J, Xu H (2013) Increased summer rainfall in northwest Australia linked to southern Indian Ocean climate variability. Journal of Geophysical Research: Atmospheres, 118, 467-480

Field CB, Behrenfeld MJ, Randerson JT, Falkowski P (1998) Primary production of the biosphere: integrating terrestrial and oceanic components. Science, 281, 237-240

Fischer G and Wefer G (2012) Use of proxies in paleoceanography: examples from the South Atlantic. Springer Science & Business Media

Forrest BM, Keeley NB, Hopkins G, Webb SC, Clement DM (2009) Bivalve aquaculture in estuaries: Review and synthesis of oyster cultivation effects. Aquaculture 298: 1–15

Fry B and Sherr EB (1984) $\delta^{13}C$ measurements as indicators of carbon flow in marine and freshwater ecosystems. Mar Sci 27: 13–47

Folk R, Andrews PB, Lewis D (1970) Detrital sedimentary rock classification and nomenclature for use in New Zealand. New Zealand journal of geology and geophysics, 13, 937-968

Furnas M (2007) Intra-seasonal and inter-annual variations in phytoplankton biomass, primary production and bacterial production at North West Cape, Western Australia: Links to the 1997–1998 El Niño event. Continental Shelf Research, 27, 958-980

Furnas MJ and Carpenter EJ (2016) Primary production in the tropical continental shelf seas bordering northern Australia. Continental Shelf Research 129, 33-48

Gaertner-Mazouni N, Lacoste E, Bodoy A, Peacock L, Rodier M, Langlade M, Orempuller J, Charpy L (2012) Nutrient fluxes between water column and sediments: Potential influence of the pearl oyster culture. Mar Pollut Bull 65: 500–505

Gasiūnaitė Z, Cardoso A, Heiskanen A-S, Henriksen P, Kauppila P, Olenina I, Pilkaitytė R, Purina I, Razinkovas A, Sagert S (2005) Seasonality of coastal phytoplankton in the Baltic Sea: influence of salinity and eutrophication. Estuarine, Coastal and Shelf Science, 65, 239-252

Gifford S, Dunstan RH, O'Connor W, Roberts T, Toia R (2004) Pearl aquaculture-profitable environmental remediation?. Sci Total Environ 319: 27–37

Gliozzi A, Paoli G, De Rosa M, Gambacorta A (1983) Effect of isoprenoid cyclization on the transition temperature of lipids in thermophilic archaebacteria. Biochimica et Biophysica Acta, 735, 234-242

Godfrey J and Mansbridge J (2000) Ekman transports, tidal mixing, and the control of temperature structure in Australia's northwest waters. Journal of Geophysical Research: Oceans (1978–2012), 105, 24021-24044

Grosjean E, Logan G, Rollet N, Ryan G, Glenn K (2007) Geochemistry of shallow tropical marine sediments from the Arafura Sea, Australia. Organic Geochemistry, 38, 1953-1971

Gunaratne GL, Vogwill RI, Hipsey MR (2017) Effect of seasonal flushing on nutrient export characteristics of an urbanizing, remote, ungauged coastal catchment. Hydrological Sciences Journal, 62(5), 800-817

Gutiérrez D, Bouloubassi I, Sifeddine A, Purca S, Goubanova K, Graco M, Field D, Méjanelle L, Velazco F, Lorre A (2011) Coastal cooling and increased productivity in the main upwelling zone off Peru since the mid ‐ twentieth century. Geophysical Research Letters, 38

Hallegraeff GM, Jeffrey SW (1984) Tropical phytoplankton species and pigments of continental shelf waters of North and North-West Australia. Mar Ecol Prog Ser 20: 59–74

Halpern BS, Walbridge S, Selkoe KA, Kappel CV, Micheli F, D'Agrosa C, Bruno JF, Casey KS, Ebert C, Fox HE, (2008) A global map of human impact on marine ecosystems. Science, 319, 948-952

Han YM, Wei C, Bandowe BAM, Wilcke W, Cao JJ, Xu BQ, Gao SP, Tie XX, Li GH, Jin ZD, An ZS (2015) Elemental Carbon and Polycyclic Aromatic Compounds in a 150-Year Sediment Core from Lake Qinghai, Tibetan Plateau, China: Influence of Regional and Local Sources and Transport Pathways. Environ. Sci. Technol. 49 (7), 4176-4183

Hare SR and Mantua NJ (2000) Empirical evidence for North Pacific regime shifts in 1977 and 1989. Progress in Oceanography, 47, 103-145

Hargrave BT, Doucette LI, Cranford PJ, Law B, Milligan TG (2008) Influence of mussel aquaculture on sediment organic enrichment in a nutrient-rich coastal embayment. Mar Ecol Prog Ser 365: 137–149

Harley CD, Randall Hughes A, Hultgren KM, Miner BG, Sorte CJ, Thornber CS, Rodriguez LF, Tomanek L, Williams SL (2006) The impacts of climate change in coastal marine systems. Ecology letters, 9, 228-241

Hart A, Murphy D, Jones R (2013) Pearl oyster managed fishery status report. In: North coast bioregion, Status report of the fisheries and aquaculture resources of Western Australia 2013/14, p 213–218

Hartstein ND, Rowden AA (2004) Effect of biodeposits from mussel culture on macroinvertebrate assemblages at sites of different hydrodynamic regime. Mar Environ Res 57: 339–357

Hatcher A, Grant J, Schofield B (1994) Effects of suspended mussel culture (*Mytilus* spp.) on sedimentation, benthic respiration and sediment nutrient dynamics in a coastal bay. Mar Ecol Prog Ser 115: 219–235

Hassim ME and Walsh KJ (2008) Tropical cyclone trends in the Australian region. Geochemistry, Geophysics, Geosystems, 9, 1-17

Hertzberg JE, Schmidt MW, Bianchi TS, Smith RW, Shields MR, Marcantonio F (2016) Comparison of eastern tropical Pacific TEX 86 and Globigerinoides ruber Mg/Ca derived sea surface temperatures: Insights from the Holocene and Last Glacial Maximum. Earth and Planetary Science Letters, 434, 320-332

Hollins SE, Harrison JJ, Jones BG, Zawadzki A, Heijnis H, Hankin S (2011) Reconstructing recent sedimentation in two urbanised coastal lagoons (NSW, Australia) using radioisotopes and geochemistry. J Paleolimnol 46: 579–596

Holloway P (1983) Tides on the Australian North-west shelf. Marine and Freshwater Research, 34, 213-230

Holloway PE (1985) A comparison of semidiurnal internal tides from different bathymetric locations on the Australia North West Shelf. Journal of physical oceanography, 15, 240-251

Hopmans EC, Weijers JWH, Schefuß E, Herfort L, Sinninghe Damsté JS, Schouten S (2004) A novel proxy for terrestrial organic matter in sediments based on branched and isoprenoid tetraether lipids. Earth and Planetary Science Letters, 224, 107-116

Hu J, Zhang G, Li K, Peng PA, Chivas AR (2008) Increased eutrophication offshore Hong Kong, China during the past 75 years: evidence from high-resolution sedimentary records. Marine chemistry, 110, 7-17

Irwin AJ, Nelles AM, Finkel ZV (2012) Phytoplankton niches estimated from field data. Limnology and Oceanography, 57, 787-797

Irwin AJ, Finkel ZV, Müller-Karger FE, Troccoli GL (2015) Phytoplankton adapt to changing ocean environments. Proceedings of the National Academy of Sciences of the United States of America, 112, 5762-6

Jelbart JE, Schreider M, MacFarlane GR (2011) An investigation of benthic sediments and macrofauna within pearl farms of Western Australia. Aquaculture 319: 466–478

Jia G, Zhang J, Chen J, Peng P, Zhang C (2012) Archaeal tetraether lipids record subsurface water temperature in the South China Sea. Organic Geochemistry, 50, 68-77

Johannessen SC, Macdonald RW (2012) There is no 1954 in that core! Interpreting sedimentation rates and contaminant trends in marine sediment cores. Mar Pollut Bull 64: 675–678

Justić D, Rabalais NN, Turner RE (1995) Stoichiometric nutrient balance and origin of coastal eutrophication. Marine pollution bulletin, 30, 41-46

Kamatani A, Oku O (2000) Measuring biogenic silica in marine sediments. Mar Chem 68: 219–229

Katsumata K (2006) Tidal stirring and mixing on the Australian North West Shelf. Marine and Freshwater Research, 57, 243-254

Kennedy JJ (2014) A review of uncertainty in in situ measurements and data sets of sea surface temperature. Reviews of Geophysics, 52, 1-32

Keesing JK (2014) Marine biodiversity and ecosystem function in the King George River region of north-western Australia. Report to the Total Corporate Foundation. 145 pages. CSIRO, Australia

Kim J, Romero OE, Lohmann G, Donner B, Laepple T, Haam E, Sinninghe Damsté JS (2012) Pronounced subsurface cooling of North Atlantic waters off Northwest Africa during Dansgaard–Oeschger interstadials. Earth and Planetary Science Letters, 339, 95-102

Kim J, Van der Meer J, Schouten S, Helmke P, Willmott V, Sangiorgi F, Koç N, Hopmans EC, Damsté JSS (2010) New indices and calibrations derived from the distribution of crenarchaeal isoprenoid tetraether lipids: Implications for past sea surface temperature reconstructions. Geochimica et Cosmochimica Acta, 74, 4639-4654

Kishore P, Hunter J, Zeng C, Southgate PC (2014) The effects of different culture apparatuses and current velocities on byssus production by the black-lip pearl oyster, *Pinctada margaritifera*. Aquaculture 434: 74–77

Krause JW, Nelson DM, Brzezinski MA (2011) Biogenic silica production and the diatom contribution to primary production and nitrate uptake in the eastern equatorial Pacific Ocean. Deep Sea Res Part II 58: 434–448

Kong D, Tse Y-Y, Jia G, Wei G, Chen M-T, Zong Y, Liu Z (2015) Cooling trend over the past 4 centuries in northeastern Hong Kong waters as revealed by alkenone-derived SST records. Journal of Asian Earth Sciences, 114, 497-503

Kuchel RP, O' Connor WA, Raftos DA (2011) Environmental stress and disease in pearl oysters, focusing on the Akoya pearl oyster (*Pinctada fucata* Gould 1850). Reviews in Aquaculture 3: 138–154

Kuwae M, Yamaguchi H, Tsugeki NK, Miyasaka H, Fukumori K, Ikehara M, Genkai-Kato M, Omori K, Sugimoto T, Ishida S, Takeoka H (2006) Spatial distribution of organic and sulfur geochemical parameters of oxic to anoxic surface sediments in Beppu Bay in southwest Japan. Estuar Coast Shelf Sci 72: 1–11

Lamb AL, Wilson GP, Leng MJ (2006) A review of coastal palaeoclimate and relative sea-level reconstructions using $\delta^{13}C$ and C/N ratios in organic material. Earth Sci Rev 75: 29–57

Lees K, Pitois S, Scott C, Frid C, Mackinson S (2006) Characterizing regime shifts in the marine environment. Fish Fish 7: 104–127

Lehodey P, Bertignac M, Hampton J, Lewis A, Picaut J (1997) El Niño Southern Oscillation and tuna in the western Pacific. Nature, 389, 715-718

Leider A, Hinrichs KU, Mollenhauer G, Versteegh GJ (2010) Core-top calibration of the lipid-based and TEX86 temperature proxies on the southern Italian shelf (SW Adriatic Sea, Gulf of Taranto). Earth and Planetary Science Letters, 300, 112-124

Li D, Zhao M, Tian J, Li L (2013) Comparison and implication of TEX86 and U37K ' temperature records over the last 356 kyr of ODP Site 1147 from the northern South China Sea. Palaeogeography Palaeoclimatology Palaeoecology, 376, 213-223

Lima FP and Wethey DS (2012) Three decades of high-resolution coastal sea surface temperatures reveal more than warming. Nature communications, 3

Lin Z and Li Y (2012) Remote influence of the tropical Atlantic on the variability and trend in North West Australia summer rainfall. Journal of Climate, 25, 2408-2420

Litchman E, Klausmeier CA, Schofield OM, Falkowski PG (2007) The role of functional traits and trade ‐ offs in structuring phytoplankton communities: scaling from cellular to ecosystem level. Ecology letters, 10, 1170-1181

Liu D, Peng Y, Keesing JK, Wang Y, Richard P (2016) Paleo-ecological analyses to assess long-term environmental effects of pearl farming in Western Australia. Mar Ecol Prog Ser 552, 145-158

Liu D, Shen X, Di B, Shi Y, Keesing JK, Wang Y, Wang Y (2013) Palaeoecological analysis of phytoplankton regime shifts in response to coastal eutrophication. Mar Ecol Prog Ser 475: 1–14

Logan B, Taffs KH, Eyre BD, Zawadski A (2011) Assessing changes in nutrient status in the Richmond River estuary, Australia, using paleolimnological methods. J Paleolimnol 46: 597–611

Lough J (1998) Coastal climate of northwest Australia and comparisons with the Great Barrier Reef: 1960 to 1992. Coral Reefs, 17, 351-367

Lough J (2008) Shifting climate zones for Australia's tropical marine ecosystems. Geophysical research letters, 35

Lough JM and Hobday AJ (2011) Observed climate change in Australian marine and freshwater environments. Marine and Freshwater Research, 62, 984-999

Lü X, Yang H, Song J, Versteegh GJ, Li X, Yuan H, Li N, Yang C, Yang Y, Ding W (2014) Sources and distribution of isoprenoid glycerol dialkyl glycerol tetraethers (GDGTs) in sediments from the east coastal sea of China: Application of GDGT-based paleothermometry to a shallow marginal sea. Organic Geochemistry, 75, 24-35

McCallum B and Prince J (2009) Development of the scientific requirements of an Environmental Management System (EMS) for the pearling (*Pinctada maxima*) industry. Fisheries Research and Development Corporation, p 1–50

McClelland JW and Valiela I (1998) Linking nitrogen in estuarine producers to land derived sources. Limnol Oceanogr 43: 577–585

McGregor H, Dima M, Fischer HW, Mulitza S (2007) Rapid 20th-century increase in coastal upwelling off northwest Africa. Science, 315, 637-639

McQuatters-Gollop A, Raitsos DE, Edwards M, Pradhan Y, Mee LD, Lavender SJ, Attrill MJ (2007). A long‐term chlorophyll dataset reveals regime shift in North Sea phytoplankton biomass unconnected to nutrient levels. Limnology and Oceanography, 52, 635-648

Margalef R (1978) Life-forms of phytoplankton as survival alternatives in an unstable environment. Oceanologica Acta, 1, 493-509

Masqué P, Isla E, Sanchez-Cabeza JA, Palanques A, Bruach JM, Puig P, Guillén J (2002) Sediment accumulation rates and carbon fluxes to bottom sediments at the Western Bransfield Strait (Antarctica). Deep-Sea Research II, 921-933

Mesnage V, Ogier S, Bally G, Disnar J, Lottier N, Dedieu K, Rabouille C, Copard Y (2007) Nutrient dynamics at the sediment–water interface in a Mediterranean lagoon (Thau, France): influence of biodeposition by shellfish farming activities. Mar Environ Res 63: 257–277

Meyers PA (1994) Preservation of elemental and isotopic source identification of sedimentary organic matter. Chem Geol 114: 289–302

Meyers PA (1997) Organic geochemical proxies of paleoceanographic, paleolimnologic, and paleoclimatic processes. Org Geochem 27: 213–250

Meyers PA, Teranes JL (2001) Sediment organic matter. In: Last WM, Smol JP (ed) Tracking Environmental Change Using Lake sediments. Developments in Paleoenvironmental Research Volume 2: Physical and Geochemical Methods. Kluwer Academic Publishers, Dordrecht, The Netherlands, p 239–269

Meyers G (1996). Variation of Indonesian throughflow and the El Niño-Southern Oscillation. Journal of Geophysical Research: Oceans (1978–2012), 101, 12255-12263

Morgan GJ (Ed.) (1992) Survey of the Aquatic Fauna of the Kimberley Islands and Reefs, Western Australia: Report of the Western Australian Museum Kimberley Island and Reef Expedition, August 1991. Western Australian Museum

Mutshinda CM, Finkel ZV, Irwin AJ (2013) Which environmental factors control phytoplankton populations? A Bayesian variable selection approach. Ecological Modelling, 269, 1-8

Narayanasetti S, Swapna P, Ashok K, Jadhav J, Krishnan R (2016) Changes in biological productivity associated with Ningaloo Niño/Niña events in the southern subtropical Indian Oceanin recent decades. Scientific reports, 6, 27467

Ocean Studies Board (2010) Ecosystem Concepts for Sustainable Bivalve Mariculture. The National Academies Press, Washington DC, p 1–179

Ohman MD, Barbeau K, Franks PJ, Goericke R, Landry MR, Miller AJ (2013) Ecological transitions in a coastal upwelling ecosystem. Oceanography, 26, 210-219

Ong JJ, Rountrey AN, Zinke J, Meeuwig JJ, Grierson PF, O'Donnell AJ, Newman SJ, Lough JM, Trougan M, Meekan MG (2016) Evidence for climate‐driven synchrony of marine and terrestrial ecosystems in northwest Australia. Global Change Biology

Owens NJP (1988) Natural variations in ^{15}N in the marine environment. Adv Mar Biol 24: 389–451

Pancost RD, Boot CS (2004) The palaeoclimatic utility of terrestrial biomarkers in marine sediments. Mar Chem 92: 239–261

Pfitzner J, Brunskill G, Zagorskis I (2004) ^{137}Cs and excess ^{210}Pb deposition patterns in estuarine and marine sediment in the central region of the Great Barrier Reef Lagoon, north-eastern Australia. J Environ Radioact 76: 81–102

Plew DR, Stevens CL, Spigel RH, Hartstein ND (2005) Hydrodynamic implications of large offshore mussel farms. IEEE J Oceanic Eng 30: 95–108

Prins TC, Smaal AC (1994) The role of the blue mussel *Mytilus edulis* in the cycling of nutrients in the Oosterschelde estuary (The Netherlands). Hydrobiologia 282/283: 413–429

Power S, Casey T, Folland C, Colman A, Mehta V (1999) Inter-decadal modulation of the impact of ENSO on Australia. Climate Dynamics, 15, 319-324

Power SB and Kociuba G (2011) The impact of global warming on the Southern Oscillation Index. Climate Dynamics, 37, 1745-1754

Power SB and Smith IN (2007) Weakening of the Walker Circulation and apparent dominance of El Niño both reach record levels, but has ENSO really changed? Geophysical research letters, 34

Pusceddu A, Dell'Anno A, Fabiano M, Danovaro R (2009) Quantity and bioavailability of sediment organic matter as signatures of benthic trophic status. Mar Ecol Prog Ser 375: 41–52

QinW, Carlson LT, Armbrust EV, Devol AH, Moffett JW, Stahl DA, Ingalls AE (2015) Confounding effects of oxygen and temperature on the TEX86 signature of marine Thaumarchaeota. Proceedings of the National Academy of Sciences, 112(35), 10979-10984

Rampen SW, Abbas BA, Schouten S, Sinninghe Damste JS (2010) A comprehensive study of sterols in marine diatoms (Bacillariophyta): Implications for their use as tracers for diatom productivity. Limnology and Oceanography, 55, 91-105

Read P and Fernandes T (2003) Management of environmental impacts of marine aquaculture in Europe. Aquaculture 226: 139–163

Redfield AC, Ketehum BH, Richards EA (1963) The influence of organisms on the composition of seawater. In: Hill MN (ed) The sea. V2 Interscience, p 26– 77

Richard M, Archambault P, Thouzeau G, McKindsey CW, Desrosiers G (2007) Influence of suspended scallop cages and mussel lines on pelagic and benthic biogeochemical fluxes in Havre-aux-Maisons lagoon, Iles-de-la-Madelaine (Quebec, Canada). Can J Fish Aquat Sci 64: 1491–1505

Richardson AJ and Schoeman DS (2004) Climate impact on plankton ecosystems in the Northeast Atlantic. Science, 305, 1609-1612

Richey JN and Tierney JE (2016) GDGT and alkenone flux in the northern Gulf of Mexico: Implications for the TEX86 and UK'37 paleothermometers. Paleoceanography, *31*(12), 1547-1561

Ridgway KR (2007) Long‐term trend and decadal variability of the southward penetration of the East Australian Current. Geophysical research letters, 42, 188‐191

Rodionov S (2004) A sequential algorithm for testing climate regime shifts. Geophys Res Lett 31: 1–4

Rodionov S and Overland JE (2005) Application of a sequential regime shift detection method to the Bering Sea ecosystem. ICES J Mar Sci 62: 328–332

Rousseau L, Keraudren B, Pepe C, Laurent M, Blanc J (1995) Sterols as biogeochemical markers in Pliocene sediments and their potential application for the identification of marine facies. Quat Sci Rev 14: 605−608.

Ruiz-Fernández AC and Hillaire-Marcel C (2009) ^{210}Pb-derived ages for the reconstruction of terrestrial contaminant history into the Mexican Pacific coast: potential and limitations. Mar Pollut Bull 59: 134–145

Sanchez-Cabeza JA, Masqué P, Ani-Ragolta I (1998）。210Pb and 210Po analysis in sediments and soils by microwave acid digestion. Journal of Radioanalytical and Nuclear Chemistry, 227, 19–22

Sarà G, Lo Martire M, Sanfilippo M, Pulicanò G, Cortese G, Mazzola A, Manganaro A, Pusceddu A (2011) Impacts of marine aquaculture at large spatial scales: Evidence from N and P catchment loading and phytoplankton biomass. Mar Environ Res 71: 317–324

Savage C (2005) Tracing the influence of sewage nitrogen in a coastal ecosystem using stable nitrogen isotopes. AMBIO 34: 145–150

Schouten S, Hopmans EC, Schefuß E, Sinninghe Damsté JS (2002) Distributional variations in marine crenarchaeotal membrane lipids: a new tool for reconstructing ancient sea water temperatures? Earth and Planetary Science Letters, 204, 265-274

Schubert CJ, Villanueva J, Calvert SE, Cowie GL, Von Rad U, Schulz H, Berner U, Erlenkeuser H (1998) Stable phytoplankton community structure in the Arabian Sea over the past 200,000 years. Nature, 394, 563-566

Seki O, Kawamura K, Nakatsuka T, Ohnishi K, Ikehara M, Wakatsuchi M (2003) Sediment core profiles of long-chain n-alkanes in the Sea of Okhotsk: Enhanced transport of terrestrial organic matter from the last deglaciation to the early Holocene. Geophysical research letters, 30, 1-4

Shi G, Cai W, Cowan T, Ribbe J, Rotstayn L, Dix M (2008) Variability and trend of North West Australia rainfall: observations and coupled climate modeling. Journal of Climate, 21, 2938-2959

Semeniuk V (1981) Sedimentology and the stratigraphic sequence of a tropical tidal flat, north-western Australia. Sediment Geol 29: 195–221

Semeniuk V (2011) Stratigraphic patterns in coastal sediment sequences in the Kimberley region, Western Australia: products of coastal form, oceanographic setting, sedimentary suites, sediment supply, and biogenesis. J Roy Soc WA 94: 133–150

Semeniuk V ans Brocx M (2011) King Sound and the tide-dominated delta of the Fitzroy River: their geoheritage values. J Roy Soc WA 94: 151–160

Smith JN (2001) Why should we believe ^{210}Pb sediment geochronologies?. J Environ Radioact 55: 121–123

Smith M, De Deckker P, Rogers J, Brocks J, Hope J, Schmidt S, Lopes dos Santos R, Schouten S (2013) Comparison of U37K, TEX86H, and LDI temperature proxies for reconstruction of south-east Australian ocean temperatures. Organic Geochemistry, 64, 94-104

Smith TM, Reynolds RW, Peterson TC, Lawrimore J (2008) Improvements to NOAA's historical merged land-ocean surface temperature analysis (1880-2006). Journal of Climate, 21, 2283-2296

Smittenberg R, Pancost R, Hopmans E, Paetzel M, Damsté JS (2004) A 400-year record of environmental change in an euxinic fjord as revealed by the sedimentary biomarker record. Palaeogeography, Palaeoclimatology, Palaeoecology, 202, 331-351

Smol JP, Stoermer EF (2010) Applications and uses of diatoms: prologue. In: Smol JP, Stoermer EF (ed) The Diatoms: Applications for the Environmental and Earth Sciences. Cambridge University Press, New York, p 3–7

Strang TJ (2003) Nutrient regeneration under mussel farms: the environmental effects of mussel aquaculture in coastal bays. Thesis (MSc), Memorial University of Newfoundland, St. John's

Sun M-Y and Wakeham SG (1994) Molecular evidence for degradation and preservation of organic matter in the anoxic Black Sea Basin. Geochimica et Cosmochimica Acta, 58, 3395-3406

Taucher J and Oschlies A (2011) Can we predict the direction of marine primary production change under global warming? Geophysical research letters, 38

Thompson P, Baird M, Ingleton T, Doblin M (2009) Long-term changes in temperate Australian coastal waters: implications for phytoplankton. Marine ecology progress series, 394, 1-19

Thompson P and Bonham P (2011) New insights into the Kimberley phytoplankton and their ecology. J Roy Soc West Aust, 94, 161-170

Thompson PA, Bonham P, Thomson P, Rochester W, Doblin MA, Waite AM, Richardson A, Rousseaux CS (2015) Climate variability drives plankton community composition changes: the 2010–2011 El Niño to La Niña transition around Australia. Journal of Plankton Research, 37, 1-19

Tisdell C, Poirine B (2008) Economics of pearl farming. In: Southgate PC, Lucas JS (ed) The Pearl Oyster. The Boulevard, Langford Lane, Kidlington, Oxford OX5 1GB, UK, p 473–495

Turner RE, Rabalais NN, Fry B, Atilla N, Milan CS, Lee JM, Normandeau C, Oswald TA, Swenson EM, Tomasko DA (2006) Paleo-indicators and water quality change in the Charlotte Harbor estuary (Florida). Limnol Oceanogr 51: 518–533

Uda I, Sugai A, Itoh YH, Itoh T (2001) Variation in molecular species of polar lipids from Thermoplasma acidophilum depends on growth temperature. Lipids, 36, 103-105

Vecchi GA, Soden BJ, Wittenberg AT, Held IM, Leetmaa A, Harrison MJ (2006) Weakening of tropical Pacific atmospheric circulation due to anthropogenic forcing. Nature, 441, 73-76

Villanueva J, Grimalt JO, Cortijo E, Vidal L, Labeyriez L (1997) A biomarker approach to the organic matter deposited in the North Atlantic during the last climatic cycle. Geochimica et Cosmochimica Acta, 61, 4633-4646

Volkman JK (1986) A review of sterol markers for marine and terrigenous organic matter. Organic geochemistry, 9, 83-99

Volkman JK (2003) Sterols in microorganisms. Applied Microbiology and Biotechnology, 60, 495-506

Volkman JK, Barrett SM, Blackburn SI, Mansour MP, Sikes EL, Gelin F (1998) Microalgal biomarkers: a review of recent research developments. Organic geochemistry, 29, 1163-1179

Volkman , , Revill AT, Bonham PI, Clementson LA (2007) Sources of organic matter in sediments from the Ord River in tropical northern Australia. Organic Geochemistry, 38, 1039-1060

Wainwright L, Meyers G, Wijffels S, Pigot L (2008) Change in the Indonesian Throughflow with the climatic shift of 1976/77. Geophysical research letters, 35

Wernberg T, Bennett S, Babcock RC, de Bettignies T, Cure K, Depczynski M, Dufois F, Fromont J, Fulton CJ, Hovey RK (2016) Climate-driven regime shift of a temperate marine ecosystem. Science, 353, 169-172

Wernberg T, Smale DA, Tuya F, Thomsen MS, Langlois TJ, De Bettignies T, Bennett S, Rousseaux CS (2013) An extreme climatic event alters marine ecosystem structure in a global biodiversity hotspot. Nature Climate Change, 3, 78-82

Wells FE and Jernakoff P (2006) An assessment of the environmental impact of wild harvest pearl aquaculture (*Pinctada maxima*) in Western Australia. J Shellfish Res 25: 141–150

Weijers JWH, Schouten S, Spaargaren OC, Sinninghe Damsté JS (2006) Occurrence and distribution of tetraether membrane lipids in soils: Implications for the use of the TEX86 proxy and the BIT index. Organic geochemistry, 37, 1680-1693

Wolanski E and Spagnol S (2003) Dynamics of the turbidity maximum in King Sound, tropical Western Australia. Estuar Coast Shelf Sci 56: 877–890

Woodruff SD, Worley SJ, Lubker SJ, Ji Z, Eric Freeman J, Berry DI, Brohan P, Kent EC, Reynolds RW, Smith SR (2011) ICOADS Release 2.5: extensions and enhancements to the surface marine meteorological archive. International Journal of Climatology, 31, 951-967

Yokoyama H (2002) Impact of fish and pearl farming on the benthic environments in Gokasho Bay: Evaluation from seasonal fluctuations of the macrobenthos. Fisheries Sci 68: 258–268

Yokoyama H, Abo K, Ishihi Y (2006) Quantifying aquaculture-derived organic matter in the sediment in and around a coastal fish farm using stable carbon and nitrogen isotope ratios. Aquaculture 254: 411–425

Xing L, Zhao M, Zhang T, Yu M, Duan S, Zhang R, Huh C-A, Liao W-H, Feng X (2016) Ecosystem responses to anthropogenic and natural forcing over the last 100 years in the coastal areas of the East China Sea. The Holocene, 26, 1-9

Yuan Z, Xing L, Li L, Zhang H, Xiang R, Zhao M (2013) Biomarker records of phytoplankton productivity and community structure changes during the last 14000 years in the mud area southwest off Cheju Island, East China Sea. Journal of Ocean University of China, 12, 611-618

Zhang Y, Wallace JM, Battisti DS (1997) ENSO-like interdecadal variability: 1900-93. Journal of Climate, 10, 1004-1020

Zhang YG, Zhang CL, Liu XL, Li L, Hinrichs KU, Noakes JE (2011) Methane Index: A tetraether archaeal lipid biomarker indicator for detecting the instability of marine gas hydrates. Earth and Planetary Science Letters, *307*(3), 525-534

Zhang YG, Pagani M, Liu Z (2014) A 12-million-year temperature history of the tropical Pacific Ocean. Science, 344, 84-87

Zhao J, Feng X, Shi X, Bai Y, Yu X, Shi X, Zhang W, Zhang R (2015) Sedimentary organic and inorganic records of eutrophication and hypoxia in and off the Changjiang Estuary over the last century. Marine pollution bulletin, 99, 76-84

Zhao ML, Mercer J, Eglinton GJ, Higginson M, Huang CY (2006) Comparative molecular biomarker assessment of phytoplankton paleoproductivity for the last 160 kyr off Cap Blanc,NW Africa. Organic Geochemistry, 37, 72-97

Zhu C, Weijers JW, Wagner T, Pan JM, Chen JF, Pancost RD (2011) Sources and distributions of tetraether lipids in surface sediments across a large river-dominated continental margin. Organic Geochemistry, *42*(4), 376-386

Zimmerman AR and Canuel EA (2000) A geochemical record of eutrophication and anoxia in Chesapeake Bay sediments: anthropogenic influence on organic matter composition. Marine chemistry, 69, 117-137

Zinke J, Hoell A, Lough J, Feng M, Kuret A, Clarke H, Ricca V, Rankenburg K, McCulloch M (2015) Coral record of southeast Indian Ocean marine heatwaves with intensified Western Pacific temperature gradient. Nature Communications, 6, 8562

8 Communication

8.1 Students and Postdocs supported

Dr Yajun Peng completed her PhD on the data from the Cygnet Bay study and Dr Zineng Yuan carried out postdoctoral research contributing the biomarker analyses for the project.

8.2 Journal publications

Yuan Z, Liu D, Keesing, J K, Zhao M, Guo S, Peng Y, Zhang H (2018*)* Paleoecological evidence for decadal increase in phytoplankton biomass off northwestern Australia in response to climate change**.** Ecology and Evolution doi:10.1002/ece3.3836

Liu D, Peng Y, Keesing JK, Wang Y, Richard P. (2016) Paleo-ecological analyses to assess long-term environmental effects of pearl farming in Western Australia. Marine Ecology Progress Series, 552, 145-158

8.3 Proceedings/Technical Reports

Nil

8.4 Presentations

- Keesing J. Historical reconstructions of water quality in the Kimberley using sediment records. WAMSI Research Conference 2017 (audio) Presentation slides
- Australian Marine Sciences Association annual conference, Geelong, 2014
- WAMSI Research Conference 2015 (1st April 2015):

  www.wamsi.org.au/sites/wamsi.org.au/files/files/John%20Keesing_1005.mp3
- Prof Dongyan Liu (Chinese Collaborator) presented at the Coastal & Estuarine Research Foundation Conference (Portland Oregan, 12 Nov 15) - focus of presentation was on the pearl oyster sample results

8.5 Other communications achievements

- DPAW Parks and Wildlife Lunchtime Presentation (27th July 2017) – John Keesing:

  Historical reconstructions of water quality in the Kimberley using sediment records: www.wamsi.org.au/research-site/sediment-record
- KRMP Project 2.2.9 Summary:

  indd.adobe.com/view/1e6dd742-6a9d-45d5-83dd-b4b3a326a809
- WAMSI Bulletin – November 2015

  us9.campaign-archive.com/?u=b7d174444ce3e7dbc753f6b28&id=d5c9c3c2d2

9 Appendices

Appendix 1.

This project directly addresses the following questions outlined in the Kimberley Marine Research Program Science Plan and in the project Agreement.

Key Question Informed Response
Have there been changes in water quality that may be associated with pollution, with particular types of use or with climate variability? The only suggestion of water quality deterioration found in this study was in Roebuck Bay at Broome. The results of this study (section 5.3) are consistent with other studies which have found anthropogenic nitrogen inputs from Broome into Roebuck Bay. We did not find any evidence of sewage contamination of sediments.
NEW QUESTIONS POSED BY MANAGERS
Would it be possible to get and analyse samples from Cambridge Gulf? and/or Roebuck Bay? We did analyse cores from Roebuck Bay. Cambridge Gulf would be an ideal place to take cores given the large catchment and protection from the ocean offered by Cape Domett, Cape Dussejour and Lacrosse Island. In addition, there have been other studies done there is the past on surface sediments, making our work easier to interpret.
What man made substances might have been laid down over the last 100 years in Roebuck Bay? Our focus in this study was to look at things like nutrients, especially nitrogen, as well as phytoplankton which responds to anthropogenically derived nitrogen sources like sewage. We did find anthropogenic nitrogen indicators in Roebuck Bay and that they had increased over time. The indicator of sewage pollution, Coprostanol was however close to detection limits (very low). So, while our focus was on nutrients, it is possible to detect metals and permanent organic pollutants in sediments.
How will this apply to characterization of sand vs silt habitat and how they are laid down? We analyse sediment grain size composition and so can see whether areas are sandier or siltier and if they have changed over time. However, where possible it is best to take cores from silty habitats as the age preservation and preservation of organic derived matter is better is silty habitats.
Crocs in Ord have highest levels of DDT in their bones. Will/can this project test for DDT? It would be possible to test core samples for permanent organic pollutants. We have not done that on our cores. We do not have cores from the Ord catchment, but they could be collected.

Appendix 2

Published paper: Liu D, Peng Y, Keesing JK, Wang Y & Richard P (2016). Paleo-ecological analyses to assess long-term environmental effects of pearl farming in Western Australia. Marine Ecology Progress Series, 552, 145-158. **doi:10.3354/meps11740** **(PDF provided separately)**

Appendix 3

Published paper: Yuan Z, Liu D, Keesing, J K, Zhao M, Guo S, Peng Y, Zhang H (2018*)* Paleoecological evidence for decadal increase in phytoplankton biomass off northwestern Australia in response to climate change**.** Ecology and Evolution doi:10.1002/ece3.383**6** **(PDF provided separately)**